

Build and operation of a custom 3D, multicolor, single-molecule localization microscope

Rory M. Power¹✉, Aline Tschanz², Timo Zimmermann^{1,2} & Jonas Ries^{1,2,3,4,5}✉

Abstract

Single-molecule localization microscopy (SMLM) enables imaging scientists to visualize biological structures with unprecedented resolution. Particularly powerful implementations of SMLM are capable of three-dimensional, multicolor and high-throughput imaging and can yield key biological insights. However, widespread access to these technologies is limited, primarily by the cost of commercial options and complexity of de novo development of custom systems. Here we provide a comprehensive guide for interested researchers who wish to establish a high-end, custom-built SMLM setup in their laboratories. We detail the initial configuration and subsequent assembly of the SMLM, including the instructions for the alignment of all the optical pathways, the software and hardware integration, and the operation of the instrument. We describe the validation steps, including the preparation and imaging of test and biological samples with structures of well-defined geometries, and assist the user in troubleshooting and benchmarking the system's performance. Additionally, we provide a walkthrough of the reconstruction of a super-resolved dataset from acquired raw images using the Super-resolution Microscopy Analysis Platform. Depending on the instrument configuration, the cost of the components is in the range US\$95,000–180,000, similar to other open-source advanced SMLMs, and substantially lower than the cost of a commercial instrument. A builder with some experience of optical systems is expected to require 4–8 months from the start of the system construction to attain high-quality three-dimensional and multicolor biological images.

Key points

- The authors describe the complete configuration and assembly of a custom-built single-molecule localization microscope, including optical alignment, software and hardware integration, validation steps and benchmarking of the system's performance.
- The microscope is optimized for ultra-stable three-dimensional imaging performance and multichannel functionalities, while remaining substantially less expensive than similar commercial systems.

Key references

- Li, Y. et al. *Nat. Methods* **15**, 367–369 (2018): <https://doi.org/10.1038/nmeth.4661>
- Diekmann, R. et al. *Nat. Methods* **17**, 909–912 (2020): <https://doi.org/10.1038/s41592-020-0918-5>
- Deschamps, J. et al. *HardwareX* **13**, e00407 (2023): <https://doi.org/10.1016/j.ohx.2023.e00407>
- Thevathasan, J. V. et al. *Nat. Methods* **16**, 1045–1053 (2019): <https://doi.org/10.1038/s41592-019-0574-9>
- Wu, Y.-L. et al. *Nat. Methods* **20**, 139–148 (2023): <https://doi.org/10.1038/s41592-022-01676-z>

¹EMBL Imaging Centre, EMBL Heidelberg, Heidelberg, Germany. ²Cell Biology and Biophysics Unit, EMBL Heidelberg, Heidelberg, Germany. ³Max Perutz Labs, Vienna Biocenter Campus, Vienna, Austria. ⁴University of Vienna, Center for Molecular Biology, Department of Structural and Computational Biology, Vienna, Austria. ⁵University of Vienna, Faculty of Physics, Vienna, Austria. ✉e-mail: rory.power@embl.de; Jonas.ries@univie.ac.at

Introduction

Single-molecule localization microscopy (SMLM) is a super-resolution fluorescence microscopy technique based on the precise two-/three-dimensional (2D/3D) localization of individual fluorophores. Unambiguous localization relies on spatial sparsity of the single-molecule emitters. Following many rounds of imaging, each comprising a small fraction of all fluorophores, their positions are determined with a precision in the single-nanometer range (under ideal conditions) and used to reconstruct a super-resolution image. The sparsity of fluorophores may be regulated through photochemical on/off switching of the fluorophores, for example, in (fluorescence) photoactivation localization microscopy, ((f)PALM)^{1,2} or (direct) stochastic optical reconstruction microscopy ((d)STORM)^{3,4}. On–off binding of fluorophores provides an alternative route, for example, in DNA-based point accumulation in nanoscale topology microscopy (DNA-PAINT)⁵ target structures are tagged with short single-stranded DNA, and fluorescently labeled complementary strands stochastically bind and detach to elicit a blinking effect.

Engineering laboratories operating optimized custom-built microscopes have driven the development of SMLM, with their creations typically outperforming commercially available variants in terms of image quality, stability and robustness. Furthermore, the custom-build approach provides agency in the design process, freedom from reliance on service technicians to maintain advanced imaging devices and ability to upgrade hardware freely. The efforts of many to democratize SMLM technology have centered largely on developing particularly low-cost systems^{6–11}. While this is a worthwhile pursuit, such systems often omit powerful features, lack the convenience and feature set of turnkey systems and generally do not reflect the current state of the art. For more advanced implementations, the technical challenge associated with replicating a system with limited documentation and instruction limits the widespread application of the associated advances. Nevertheless, the benefits of the custom-build approach make dissemination of these devices of crucial importance for biological imaging.

Development of the protocol

In this protocol, we seek to bridge the gap between entry-level open-source projects and costly, though not necessarily more capable, commercial systems by providing a detailed and complete guide to allow nonspecialist laboratories to establish SMLM with state-of-the-art performance and advanced features and apply it to their biological studies. We note at this juncture that the main article includes only the necessary steps to set up the base version of the microscope to meet the need for brevity. We nevertheless present additional sections in the Supplementary Information, where we comprehensively explain how to expand the functional palette available and guide the builder on the construction and alignment of the SMLM, as well as a wealth of other details to expand the scope of the proposed SMLM activities. The information given in this protocol enables the builder to complete the build and use of an SMLM in a timely manner. To encourage builders to configure the instrument as they wish, the microscope presented is modular and customizable in design. The scheme outlined includes the necessary resources to construct and use an advanced SMLM system. All necessary validation steps, processes for acquiring benchmark images and their subsequent analysis are similarly included.

Our laboratories benefit from over a decade of experience in SMLM development and optimization of the desirable features of the microscope itself. While many technical developments from ourselves and others have expanded the capabilities of SMLM, there is clearly a balance to be sought between cost/complexity versus performance/usability. In this regard, we believe that the following features are suitable to cover most applications and user needs spanning (d)STORM, DNA-PAINT and PALM workflows, and are well suited to a multifunctional system covering many such applications.

The first feature is the design of an inverted microscope body. To deliver a spatial resolution at least one order of magnitude better than that of standard widefield epi-fluorescence microscopy, mechanical disturbances such as drift and vibration must be minimized.

A custom-machined body can provide a substantial improvement over a commercial inverted microscope stand in this regard because extraneous features, which often contribute to instability, can be eliminated and the feature set tuned to this single-use case. We included long-range (several mm) refocusing to accommodate different sample types, hot-swappable optics (e.g., dichroic mirrors), transmission illumination and the controlled heating of the microscope for live-cell imaging under physiological conditions. These features are often missing in custom microscopes, yet have proven useful across the developmental lifetime of the microscope reported herein. We also include a focus lock system to minimize axial drift. While real-time lateral drift correction schemes have been reported¹², such schemes required fiducial markers, placing constraint on the sample preparation so we correct lateral drift in postprocessing.

From an illumination perspective, homogeneity is a primary concern but so too is the possibility for high-quality total internal reflection fluorescence (TIRF) illumination. Although schemes effectively demonstrating both exist^{13–16}, they have only recently been transferred to open-source systems with multiple laser lines¹⁷. Achieving suitable irradiance of the sample in often power-hungry applications is of similar concern. Even when sufficient laser power and minimally lossy schemes are available, statically sized illumination fields do not allow for optimization of the intensity with respect to the background generated nor avoid damage to expensive objective lenses where high-power lasers are used to illuminate an unnecessarily large field of view. Particularly in multi-user settings, such field-adjustable illumination, which maintains homogeneity and TIRF compatibility, is invaluable. Note, intensity is used here to refer to power per unit area, more rigorously termed irradiance in radiometry. We use the term intensity throughout as this is a more common convention in microscopy.

On the emission side, multicolor imaging is, of course, desirable and can be achieved serially. However, many powerful methods such as (d)STORM and single-molecule Förster resonance energy transfer require the synchronous acquisition of multiple color channels to discriminate as many as four spectrally overlapping far-red fluorophores¹⁸ and elucidate close contacts between Förster resonance energy transfer pairs, respectively^{19,20}. Given the resolution of modern scientific complementary metal-oxide semiconductor (sCMOS) cameras, image splitters forming a pair of images on a single camera provide such capabilities and offer a doubling of imaging speed even for applications where serial acquisition is tolerable. Given the inherently 3D nature of biological samples, the ability to discriminate emitters based on depth information is critical to many SMLM applications and the related point spread function (PSF) engineering approaches to do so have been among the most impactful extensions of the technology^{21,22}.

Advanced microscopes require suitable control systems in the form of software with an intuitive interface and powerful acquisition engine, electronics and hardware synchronization. Moreover, SMLM acquisitions are typically long, requiring tens of thousands of images to reconstruct a single super-resolution view of the sample. As such, and given the need for statistical significance and perturbations in biological studies, automation of SMLM plays a key role in its success. The supplied control systems and associated hardware must therefore be capable of unsupervised imaging, not only moving from point to point in a predetermined manner, but also performing quality checks and, where appropriate, modulating photoactivation parameters in line with on-the-fly (i.e., during the acquisition with a small time delay) detected emitter density. Naturally, the data and metadata structures should streamline the subsequent analysis by being fully integrated with freely available analysis software.

The capabilities of various open-source SMLM projects have been well summarized as they relate to a recent implementation, the NanoPro 1.0 (ref. 23). We do not replicate this discussion but extend the analysis of these systems in Supplementary Table 1^{6,7,9–11,16,17,23–25}. As can be seen from the feature list, the 3D-SMLM system reported herein delivers all desired features highlighted in Danial et al.²³, including several additional criteria including fully integrated 3D capability. We note that while many aspects of this project could be applied to other open-source systems, a given functionality is not merely the result of its inclusion as a hardware

option but also the availability of detailed instructions for deployment of said functionality. For example, high-quality 3D imaging is a multifaceted aspect of SMLM, requiring adjustment of hardware as well as protocols for quality control and analysis. Ultimately, our microscope has been designed to optimize performance and functionality while maintaining sensitivity to pricing such that the instrument represents a substantial saving compared to similar commercial systems. Laboratories wishing for an entry-level SMLM system without many features described are advised to seek out many of the excellent open-source SMLM projects, some of which are optimized for low cost^{7–9,11} and ease of construction⁶.

The instrument detailed herein, which, to differentiate from other 3D-SMLM microscopes, we refer to as EMBL-SMLM represents the sixth generation refinement of our SMLM developments across more than a decade of development and features improvements to the optical, mechanical, electronic and computational designs reported previously^{26–32}. These microscopes were instrumental for key biological discoveries^{33–36}. Microscopes constructed from this scheme are currently in use in research and service settings at the European Molecular Biology Laboratory (EMBL), while implementation of previous generations has been carried out in several labs worldwide. We note that the most recent generation of the microscope has been developed at the EMBL Imaging Centre, as part of efforts to develop custom imaging technologies in partnership with EMBL developer laboratories. The particular challenges inherent in the deployment of such technologies in a multi-user environment for advanced service provision require a greater flexibility of approach than would be the case for a single research laboratory with a narrower research focus. The aspects developed to serve the range of needs encountered are fully represented in the instrument described herein accordingly.

Successful implementation of the protocol is contingent on some familiarity with the construction of optical systems and a working understanding of SMLM. We expect a full-time builder would require 8 months to successfully implement the protocol described, culminating in the reconstruction of exemplary super-resolution images, while an expert builder may require as little as 4 months. A full list of materials including parts list (Supplementary Table 2 and Supplementary Information Note 1), computer-aided design (CAD) models and associated toleranced drawings, software and electronic schematics can be found on GitHub (<https://github.com/ries-lab/3DSMLM>). CAD models are included in SolidWorks (Dassault Systèmes) assembly and part file format for those wishing to modify the design. For those wishing to follow the protocol as written, the CAD assemblies are also provided in eDrawing format, which can be viewed using a freely available eDrawing viewer (<https://www.edrawingsviewer.com/download-edrawings>). The viewer also allows suppression of components, configuration of the assemblies and cut away views, all of which are helpful to follow the protocol. Toleranced drawings for the custom mechanical parts are provided as SolidWorks drawings for manufacture by a workshop with precision computer numerical control milling capabilities. We advise that laboratories wishing to replicate the system first familiarize themselves with the assemblies and contact the EMBL mechanical and electronic workshops (mw@embl.de/ew@embl.de) to discuss appropriate sourcing of parts and to seek direct correspondence with the authors before embarking on the protocol to clarify uncertainties and check for forthcoming updates.

We note that the parts provided at the time of publication are by no means final as the system undergoes continuous improvements and the online resources noted will be maintained accordingly. Furthermore, we encourage builders to engage in this effort by modifying or otherwise suggesting modifications of part files to further improve their functionality or suggest desirable features that could be developed.

Overview of the automated 3D multicolor single-molecule localization microscope

A CAD rendering of the microscope is shown in Fig. 1. In essence, the EMBL-SMLM comprises an inverted epi-fluorescence microscope constructed around a robust, yet flexible, custom microscope body. The body incorporates xy stages, a z-focusing piezo and long-range travel platform for the objective lens/piezo as well as switchable kinematic mounts for dichroics, housing for a tube lens and optional filters and, if specified, the capacity to operate at elevated temperatures suitable to mammalian systems. Samples mounted on coverslips are subject to

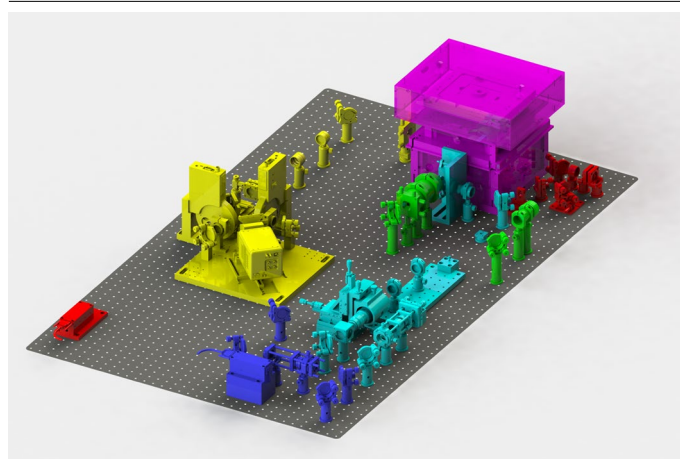


Fig. 1 | A full rendering of the EMBL-SMLM. The system features a custom microscope body (magenta), emission path with 3D and synchronous multichannel/color imaging capabilities (yellow) and focus lock path (red). Multiple illumination sources are available: a single-mode illumination path with fiber-coupled laser engine source (cyan) and a single-mode booster laser (blue), multimode illumination path (green). The configuration shown includes all optional modules. For scale, the underlying optical breadboard measures 1.5×0.9 m.

widefield laser illumination via an objective lens, which collects fluorescence and separates the emitted light from the excitation source on a dichroic mirror. The emission path further comprises a tube lens and additional optics for spectral discrimination and image relaying to produce two synchronously captured color channels on a sCMOS camera. For example, ratiometric imaging with two spectrally distinct channels may be employed to separate multiple spectrally overlapping far-red dyes suitable for dSTORM imaging. For 3D imaging, a distortion-free and tunable astigmatism module allows fine control over the extension of the PSF in two orthogonal axes either side of the native focus. As such, one may attain localization precisions as high as 2 nm in xy and 8 nm in z under idealized conditions²⁹ using a calibrated spline model of the PSF²⁷. Excitation can be provided by single- or multimode laser sources, depending on specific requirements to yield a uniform illumination field using various homogenization schemes. The laser excitation can be centered/offset at the back focal plane of the imaging objective lens via a motorized mirror to provide epi-/highly inclined and laminated optical sheet (HILO)/TIRF illumination. A focus lock system is included, comprising a near infrared (NIR) laser at 808 nm under total internal reflection (TIR) from the coverslip and subsequent height sensitive detection using a position-sensitive detector with feedback to the piezo-coupled objective lens. Sample throughput presents a challenge to SMLM since large numbers of camera frames are required to reconstruct a single image and constant user input may be required during the experiments. We note that while high-throughput applications are not specifically included in the protocol, we have performed unsupervised high-throughput imaging of thousands of sites in previous studies using the microscope^{34,36}. Various aspects of the microscope control allow such studies to be realized. For example, most functionalities are motorised including the Bertrand lens used for back focal plane imaging to check for bubbles in the immersion oil, which may become apparent and problematic when moving between positions. Likewise, the 3D astigmatic module and epi-/HILO/TIRF illumination are motorized while switching to brightfield mode can also be achieved without manual intervention. Where single- and multimode sources are provided in tandem, switching between the two is similarly automated. Furthermore, during acquisition the emitter density is computed, compared with a user-supplied target and the pulse length of the 405 nm laser (commonly used for photoactivation) is automatically adjusted. Likewise, the imaging of a given position can be terminated when the vast majority of emitters are activated (determined by reaching a maximum pulse length). During imaging, many quality control parameters are logged, such as the position of the objective-mounting piezo flexure stage, the measured laser power and, as desired, back focal plane/brightfield images. Furthermore, we developed the super-resolution microscopy analysis platform (SMAP) software³⁰ and use it to check for consistency across measurements. For example, deteriorating buffers can be detected in a change of photon counts, background and fluorophore on times. Paired with a powerful

acquisition engine, the user can perform complex unsupervised multiposition experiments including all aforementioned quality checks as well as 2D/3D localization, z-stack and time-lapse experiments each with epi-/HILO/TIRF illumination. The builder may even assign additional hardware functions beyond those described herein to automatable user interface controls.

The microscope comprises four optomechanical subsystems (Fig. 1): the body, and the excitation, emission and focus lock paths, described in more detail in Supplementary Information Note 2. The beam paths are shown in Fig. 2. Since the configuration of spectrally discriminative optics (dichroic mirrors and spectral filters) will be dependent on the intended application, we have refrained from specifying these components absolutely. We provide a guide to their selection in Supplementary Information Note 3 and include therein the choices of components required to follow the protocol as intended. We expect that this configuration will be suitable for a large number of potential use cases.

The microscope's subsystems are themselves comprised of a large number of custom mechanical parts as well as many commercially available components. To assist prospective builder, discussions of component procurement is provided in Supplementary Information Note 4. Under typical procurement conditions, 4 months is sufficient to acquire the necessary materials. Where certain components are not immediately available or facing undue delays, it is possible to reorganize some of the protocol or otherwise to begin sections before completing earlier ones. There is some flexibility in the system to tune the configuration to the end-user's needs, budget and proficiencies in optical system construction. The optomechanical configuration must be determined before sourcing commercial and custom parts. For selection of costly hardware elements such as objective lenses, lasers, stages and cameras, refer to Supplementary Information Notes 5–8. The CAD assembly files provided are configurable allowing the builder to construct the appropriate system *in silico* before proceeding. The parts list is similarly structured to allow easy identification of components required for different configurations. Supplementary Table 3 is provided to estimate the final cost for the system. Control of the microscope including previewing and acquisition functions is carried out using the open-source μ Manager software³⁷ with a custom high-throughput SMLM²⁸ (htSMLM) graphical user interface (GUI). In particular, builders wishing to make use of the extensive automation functionality should refer to the htSMLM documentation (<https://github.com/jdeschamps/htSMLM/tree/main/guide>). Figure 3 shows the μ Manager and htSMLM GUIs (also see Supplementary Fig. 4). The microscope makes use of the open-source microFPGA (FPGA: field-programmable gate arrays) project for synchronization of hardware components³⁸. A full list of software controllable hardware elements used in the microscope is provided in Supplementary Table 4. A more complete discussion of the control software and electronics aspects is given in Supplementary Information Note 9 and sourcing of the electronic components is discussed in Supplementary Information Note 10.

Applications

The relative benefits of SMLM with regard to other super-resolution microscopies have been covered in detail elsewhere^{39–42}. In general, applications requiring spatial resolution beyond that which can typically be achieved by stimulated emission depletion⁴³, structured illumination⁴⁴ or image-scanning microscopy⁴⁵ may be ideally suited to the use of EMBL-SMLM. Using oil or silicone oil objectives as well as TIRF/HILO/epi-illumination, one may image structures close to the coverslip boundary or as far as 50 μ m beyond. The microscope acquisition workflow is flexible enough to allow for multiple SMLM imaging modalities including (f)PALM^{1,2}, (d)STORM^{3,4} and DNA-PAINT⁵. We describe a few applications that have used various generations of the microscope in Supplementary Information Note 11.

Comparisons with other methods and limitations

Regarding the specific EMBL-SMLM implementation presented here, we consider this to be the most complete and detailed description of implementation of not only the hardware aspects but also biological validation and analysis. Nevertheless, we consider the associated limitations relative to other SMLM setups and more widely in the context of other super-resolution microscopies in Supplementary Information Note 12.

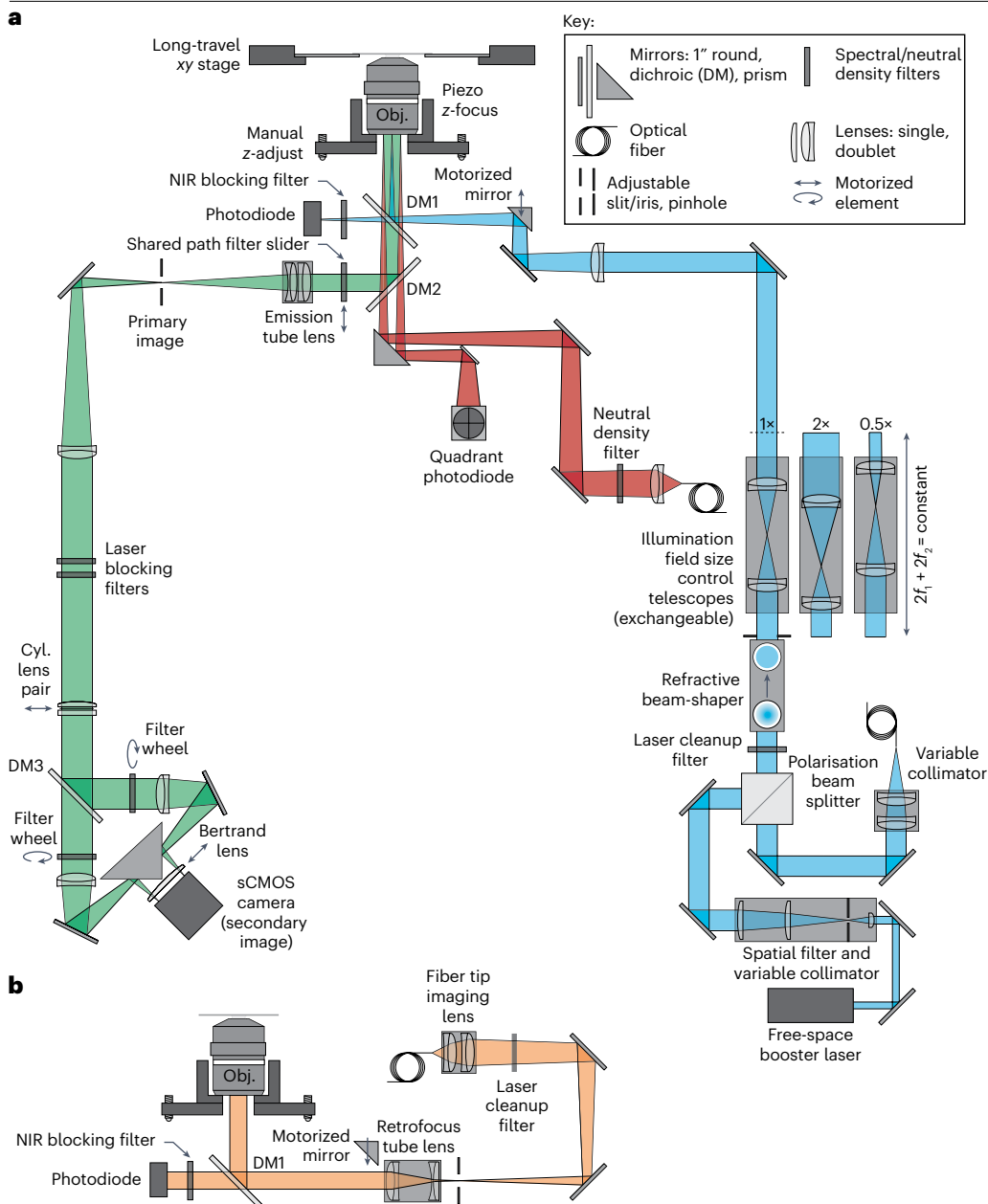


Fig. 2 | Schematic of the optical and motion control aspects of the EMBL-SMLM. a, The single-mode illumination path(s) (blue): the single-mode laser(s) are spatially filtered, expanded and homogenized. The resulting flat-top intensity profile is further expanded by exchangeable telescopes to control the size of the illumination field. Setting the angle for TIRF/HILO illumination is accomplished by positioning of a motorized mirror. The laser power is monitored in real-time (i.e., with negligible delay) by measuring the ~1% transmission of the laser lines at the illumination dichroic mirror (DM1). The emission path (green): Fluorescence is reflected by the emission dichroic (DM2) and a primary image is produced by a tube lens. The image is restricted in spatial extent by a slit, filtered by laser line blocking filters and relayed in a 4f configuration via a spectrally discriminative image splitter (dichroic, DM3) to form two secondary images on an sCMOS camera. A variable astigmatic lens (cylindrical lens pair) can be removed/inserted for 2D/3D imaging, while a Bertrand lens allows viewing of the objective back focal plane. The focus lock path (red): the focus lock laser is separated from emitted fluorescence by DM2, focused to the objective back focal plane and launched obliquely to return under the TIR condition allowing axial drift of the coverslip relative to the objective lens (Obj.) to be measured via a quadrant photodiode and corrected via the control loop of the piezo flexure stage mounting the objective. **b,** For clarity the multimode laser illumination path (orange) has been shown separately but all modules are compatible. A magnified image of the tip of a square core multimode fiber (coupled to a multimode laser engine) is produced and re-imaged onto the sample via a tube lens in a retrofocus arrangement and the objective lens. The multimode laser is coupled into the microscope by translation of the motorized mirror (HILO/TIRF) fully out of the beam path.

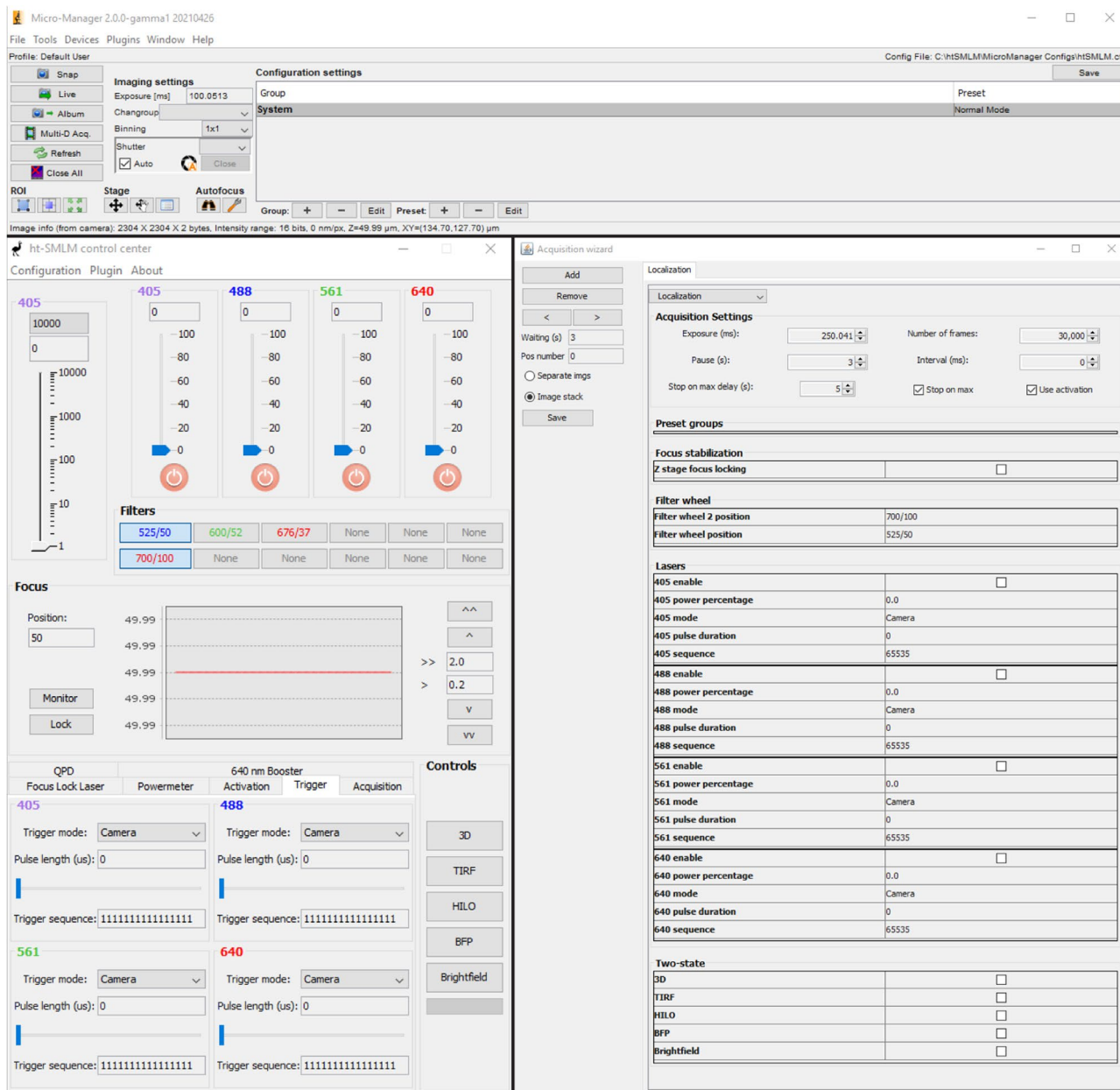


Fig. 3 | The μ Manager and htSMLM GUIs. Top: the μ Manager user interface, which is primarily used to configure the microscope devices, to control the camera, define stage positions for multisite imaging and to carry out simple image acquisitions. Bottom/left: the htSMLM control center, which provides the majority of microscope control including lasers, filters, focus locking and on/off control of various user assignable functions (e.g., HILO/TIRF illumination,

2D/3D imaging). The Trigger tab is shown, where laser trigger modes and complex interleaved experiments can be set up. Additional tabs are shown and described in Supplementary Fig. 4. Bottom/right: the htSMLM Acquisition Wizard, which allows complex experiments with quality checks to be set up for unsupervised imaging.

Experimental design

Personnel

For successful completion of the protocol including planning, procurement of commercial and custom parts, construction/alignment and validation, one full-time scientist or engineer is required. Preferably this person would have some familiarity with optical systems although such experience is not strictly required. The responsible individual should familiarize themselves

Protocol

with the laser safety measures discussed in Supplementary Information Note 13. Alternatively, it may be desirable to split certain tasks over more specialized or suitable individuals. For example, samples may be prepared by life-science technicians. From the point where all required hardware is available, we assert that the protocol may be completed in 4–8 months.

Laboratory environment

The microscope should be housed in a suitable laboratory space that meets the requirements of temperature and vibration stability, size and ability to achieve the laser safety measures, and are detailed in Supplementary Information Note 14.

Computational infrastructure

The microscope requires a range of computational infrastructure to be available for microscope control and data writing/storage/analysis. The specifics of how this infrastructure is configured is somewhat flexible with regard to the locally available resources and a general guide to suggested practices is given in Supplementary Information Notes 15 and 16.

Data analysis and rendering

During data acquisition, the raw camera frames and metadata describing the state of the microscope are saved by μ Manager. These data require extensive analysis steps to yield biological insights: fitting of single-molecule positions, postprocessing such as filtering and drift correction, rendering as a super-resolution image and quantitative evaluation. We use SMAP³⁰ and here detail the analysis steps using this solution, but there are numerous other software, notably Picasso⁴⁶ and ThunderStorm⁴⁷ that can be equally used. For an overview of the performance of different localization algorithms, we recommend that users study the results of the SMLM software challenge⁴⁸.

To analyze 3D or multicolor data in SMAP, first the PSF of the microscope and/or channel transformation are calibrated from image stacks of fluorescent beads. Then SMAP identifies possible single-molecule events in the raw camera frames and determines their position with subpixel precision by maximum likelihood estimation. Localizations with low accuracy can be filtered out, before residual drift is corrected and a super-resolution image is rendered. These steps can be performed in on-the-fly during data acquisition. SMAP provides numerous plugins to segment and quantitatively analyze cellular structures based on the coordinates of the detected fluorophores.

Biological validation

To validate the microscope performance, we use a well-characterized and homogeneous biological structure that can serve as a reference standard. The nuclear pore complex (NPC), responsible for transfer of molecules across the nuclear membrane, has been thoroughly studied with complementary methods including cryogenic electron microscopy⁴⁹. It comprises ~30 proteins, of which Nup96 is our preferred candidate for benchmarking. This protein is present in 32 copies within the NPC, and distributed symmetrically across the structure, with 16 copies forming the cytoplasmic ring and 16 copies forming the nucleoplasmic ring. Each ring contains 8 corners formed by two Nup96 proteins. Two Nup96 proteins in one corner are 12 nm apart, two corners are 42 nm apart, the entire ring has a diameter of 107 nm and the two rings are separated by 50 nm. This eightfold symmetrical distribution of Nup96 makes it an ideal candidate to estimate the resolving power of the setup, and resulting images and downstream computational analyses allow for the identification of potential issues and more targeted troubleshooting⁵⁰.

Materials

Reagents

▲ **CAUTION** All reagents present potential hazards and should be handled correctly by personnel trained in general laboratory safety and materials handling. Specific hazards are

noted below with the respective reagent. Note that the further preparation of reagents from the stock list provided below is described in Supplementary Information Note 17.

- β -Mercaptoethanol (Sigma-Aldrich, cat. no. M6250)
▲ CAUTION Handle with care. β -Mercaptoethanol is toxic, corrosive and a strong irritant that poses risks to human health upon contact, inhalation or ingestion, potentially causing skin, eye and respiratory irritation, as well as sensitization and allergic reactions.
- SNAP-Surface BG-AF647 (New England Biolabs, cat. no. S9136S)
- Bovine serum albumin (Sigma-Aldrich, cat. no. A7030)
- Catalase (Sigma-Aldrich, cat. no. C3155)
- Isopropanol (Merck, cat. no. 67-63-0)
▲ CAUTION Handle with care. Isopropanol is a highly flammable liquid and vapor, causes serious eye irritation and may cause drowsiness or dizziness.
- Petrol ether (Carl Roth GmbH, cat. no. 3295)
▲ CAUTION Handle with care. Highly flammable liquid and vapor, may be fatal if swallowed and enters airways, causes skin irritation, may cause drowsiness or dizziness and is toxic to aquatic life with long lasting effects.
- Coverslips 12 \times 12 mm (Marienfeld Superior, cat. no. 0101000)
- Coverslips no. 1.5H \varnothing 24 mm (Marienfeld Superior, cat. no. 0117640)
- Dulbecco's Modified Eagle Medium (DMEM) (Gibco, cat. no. 11880-02)
- Dithiothreitol (DTT, Biomol, cat. no. 04010.10)
▲ CAUTION DTT is a reducing agent that can cause eye and skin irritation upon contact, and may lead to respiratory irritation or allergic reactions when inhaled or ingested in substantial amounts.
- Fetal bovine serum (Gibco, cat. no. 10270-106)
- 2-Deoxy-D-glucose (Sigma-Aldrich, cat. no. D3179)
- Glucose oxidase (Sigma-Aldrich, cat. no. 49180)
- GlutaMAX (Gibco, cat. no. 35050-038)
- Glycerol (Merck, cat. no. 1.04094)
- Hydrochloric acid, HCl (Sigma-Aldrich, cat. no. 7647-01-0)
- Immersion oil (Olympus, cat. no. IMMOIL-F30CC)
- Silicone immersion oil (Olympus, cat. no. SIL300CS-30CC)
- Minimum Essential Medium Nonessential Amino Acids (MEM NEAA) (Gibco, cat. no. 11140-035)
- Methanol (Sigma-Aldrich, cat. no. 67-56-1)
- Millex-GP filters, 0.22 μ m (Merck, cat. no. SLGP033RS)
- Sodium chloride (NaCl, Merck, cat. no. 7647-14-5)
- Ammonium chloride (NH₄Cl, Merck, cat. no. 12125-02-9)
▲ CAUTION Handle with care. Ammonium chloride may cause skin, eye and respiratory irritation upon contact, inhalation or ingestion, with potential for more severe effects following prolonged exposure.
- Parafilm (Thermo Fisher, cat. no. HS234526B)
- Phosphate buffered saline (PBS), 1 \times , 2 \times
- Paraformaldehyde, 16% (Electron Microscopy Sciences, cat. no. 15710)
▲ CAUTION Handle with care. Paraformaldehyde is flammable, harmful if swallowed or inhaled, causes skin irritation, may cause an allergic skin reaction, causes serious eye damage, may cause respiratory irritation, is suspected of causing genetic defects if exposed and may cause cancer if exposed.
- TetraSpeck fluorescent beads (100 nm) (Thermo Fisher, cat. No. T7279)
- Tris-HCl, pH8, 1 M
- Triton X-100 (Sigma Aldrich, cat. no. X100)
▲ CAUTION Handle with care. Triton X-100 is harmful if swallowed, can cause skin irritation and serious eye damage. Very toxic to aquatic life with long lasting effects.
- TrypLe (Gibco, cat. no. 12604013)
- Anhydrous, deoxygenated dimethylsulfoxide (Sigma-Aldrich, cat. no. 900645-4X2ML)
- WGA-CF680 (Biotium, cat. no. 29029-1)

Sample preparation

▲ **CAUTION** All samples should be prepared following the instructions provided in Supplementary Information Note 18 by personnel trained in biological safety and materials handling. The following samples are used in the protocol. All samples are prepared on #1.5 precision ø24 mm coverslips (170 ± 5 µm thickness).

- TetraSpeck fluorescent beads (100 nm)
- Fluorescent dye sandwiched between coverslips
- Fixed and stained U2OS cells (https://scicrunch.org/resolver/RRID:CVCL_B7FL)

Equipment

A full list of parts shared between all configurations is provided in Supplementary Table 2. The parts list is correct at the time of publication; however, improvements and additions to the design are ongoing. An up-to-date parts list can be downloaded from: <https://github.com/ries-lab/3DSMLM>, where the associated CAD files are also hosted.

Software

The following software is required to set up the microscope, acquire data and perform image analysis.

Software for hardware setup

To test and configure the various hardware elements before full integration with µManager, it is necessary to install the following software that is either provided with the hardware or freely available from the manufacturer.

- Hamamatsu DCAM API (<https://dcam-api.com>)
- Hamamatsu HCLImage Live
- Toptica, TOPAS for iBeam smart laser(s)
- Toptica, TOPAS for iChrome MLE laser engine
- Thorlabs, Elliptec, ELLO software (https://www.thorlabs.com/software_pages/ViewSoftwarePage.cfm?Code=ELL)
- Thorlabs, FWxC filter wheel software
- Physik Instrumente, PIMikroMove
- Smaract, SCUConfigure, SCUFirmwareUploader
- Beam profiling camera software (e.g., Coherent BeamView)
- Infinite conjugate viewing camera software (e.g., FLIR Spinnaker SDK/SpinView)
- Alchitry, AlchitryLabs (<https://alchitry.com/alchitry-labs>)

Software for microscope control

The following software is required to control the microscope. Additional device adapters and a GUI will be added to the base µManager installation during the protocol.

- µManager 2.0.1 latest nightly build (https://micro-manager.org/Download_Micro-Manager_Latest_Release)
- ImageJ (installed as part of µManager)

Software for image analysis

SMAP³⁰ provides the basis for super-resolution image reconstruction in the protocol. SMAP may be installed with MATLAB offering greater extensibility or as a standalone version requiring only the MATLAB runtime engine, which is freely available. Consult the SMAP documentation (<https://www.embl.de/download/ries/Documentation/>) for installation notes and for tutorials to get accustomed with the data analysis workflow:

- SMAP latest official release for MATLAB (<https://github.com/jries/SMAP>)
- MATLAB 2022a or newer with toolboxes: optimization, image processing, curve fitting, statistics and machine learning
or
- SMAP standalone version, latest release (installs the MATLAB runtime). (<https://www.embl.de/download/ries/SMAPCompiled/>)

- μ Manager 1.4 latest official release. This is a legacy version μ Manager required to load images into SMAP. (https://micro-manager.org/Download_Micro-Manager_Latest_Release)
- ImageJ (installed as part of μ Manager)
- Nvidia graphics drivers, studio version (<https://www.nvidia.de/Download/index.aspx?>)
- Nvidia CUDA toolkit and graphics driver, version 10.1 or newer (for GeForce products 471.41 or later) (<https://developer.nvidia.com/cuda-downloads>)

Tools

Completion of the protocol requires several tools, including screwdrivers, balldrivers/hex keys (L-shaped). These are assumed to be available and not included in the parts list. In addition, several tools that are less commonplace are included in the parts list. Furthermore, there are several assembled tools including alignment jigs/fixtures/optical references that are included in the parts list and as individual CAD assemblies (Supplementary Table 2). A description of many of the tools specified and their use is provided in Supplementary Information Note 19.

Equipment setup

Before commencement of the protocol itself, ensure that all parts listed in the parts list (Supplementary Table 2) are available. For custom-made parts, check all toleranced dimensions with calipers, tapped holes with their respective threaded component and dowel pin holes with correctly toleranced dowel pins. Dowel pin holes may become undersized during the anodizing process. If this occurs, the holes should be remachined to the required tolerances. We note a few general points regarding conventions, mechanical/electrical assembly, optical alignment and best working practices in Supplementary Notes 20–23. The builder is assumed to have familiarized themselves sufficiently with the recommendations before proceeding.

Throughout the protocol, a multitude of instructions will be given requiring interaction with software to control hardware and acquire data. The builder is expected to familiarize themselves with the software and controls before continuing with the protocol. For brevity, specific instructions regarding how to achieve a given command are provided. For example, the instruction: image fluorescent beads, assumes that the user is familiar with previewing and acquiring images using the μ Manager GUI. Similarly, it is assumed that the user can set laser power, region of interest (ROI) and exposure time or select filters appropriately to achieve a desired temporal resolution and image signal to noise or exposure level.

Procedure

Microscope body buildup

● TIMING 4 d

▲ **CRITICAL** The microscope body provides the core of the microscope around which the illumination, emission and focus lock optical pathways are constructed. A CAD rendering of the completed body is shown in Fig. 4. The microscope body is handed: in the base configuration, illumination is provided from the back side, while emission and focus lock paths are from the right/left respectively. Back/front and left/right are defined from the normal user viewing orientation at the short edge of the optical table and are inscribed onto the body lower plate (3D-SMLM-FAB-000001). For a guide to configuration of the microscope body including discussion of achieving a differently handed layout on the optical table, see Supplementary Information Note 24. In the base configuration, shown in Fig. 1, access (for example, to mount samples on the microscope) is primarily from the front of the microscope along the shorter optical table edge. Secondary access is provided from the left side (Supplementary Information Note 14).

1. (Optional) Install the heating foil and/or temperature sensor in the central recess of the body middle plate (FAB-EMBL-000007). The temperature sensor can still provide a useful readout of temperature in the absence of the heating foil. Route the heating foil and/or temperature sensor cables along the cable channel to the slotted recess on the outside edge of the plate.

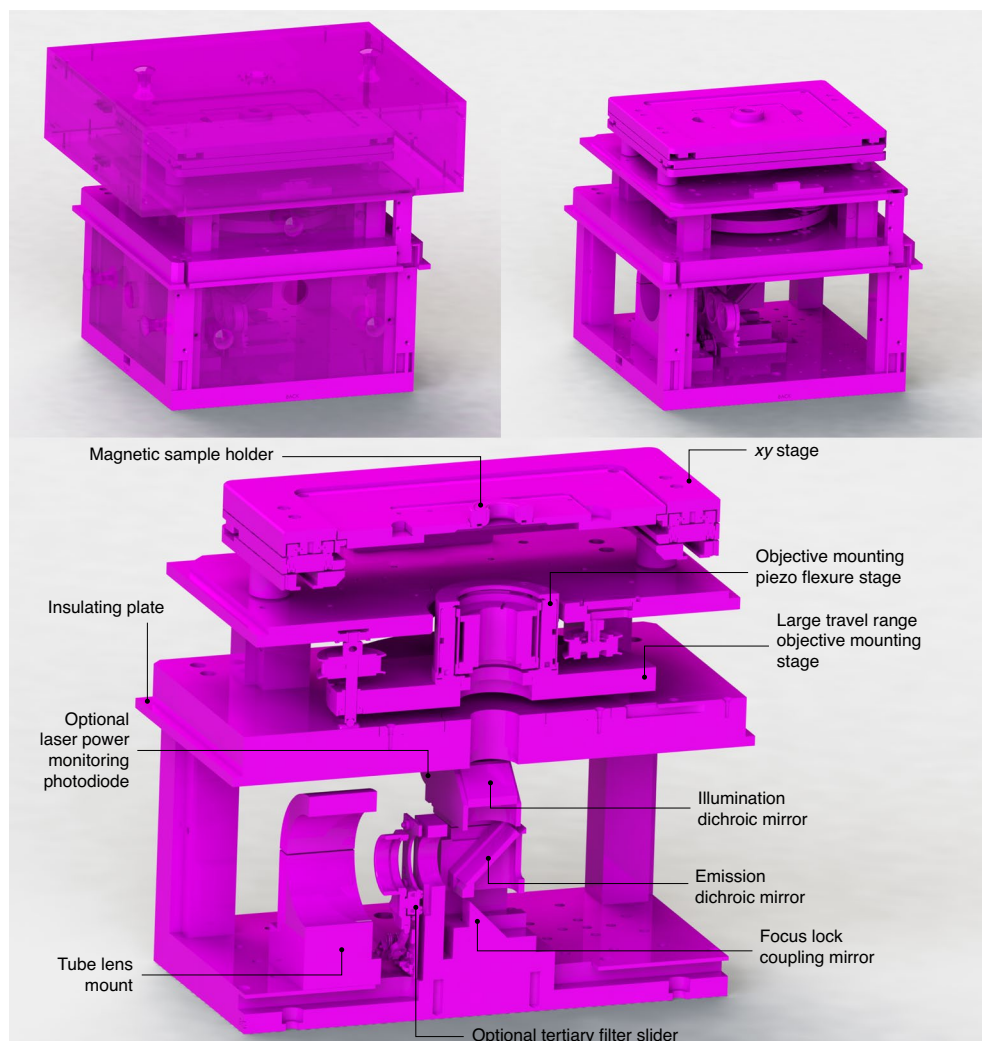


Fig. 4 | The fully assembled inverted microscope body. Top/left: the microscope body with covers installed for laser safety and to aid thermal stability. Top/right: the microscope body with covers removed. Bottom: a cut-away view of the microscope body showing its various motion control, optical and optomechanical aspects. The various optical components including high numerical aperture (NA) objective lens (omitted, mount shown) and dichroic mirrors for coupling the optical paths/in/out are situated below an xy stage. An optional filter slider can be included in the infinity space before a tube lens (omitted, mount shown) produces a primary image outside of the microscope body.

2. (Optional) Cover the channels with their respective covers (FAB-EMBL-000051/52) and secure in place with 7× M2.5×6 mm countersunk screws.
3. (Optional) Secure the heating foil cover (FAB-EMBL-000041) in place with 7× M2.5×8 mm countersunk screws.
4. Install the threaded bushings (COTS-F6MSSA1) in the objective piezo platform (FAB-EMBL-000038) using a drill press.
5. Install the 6× dowel pins (COTS-91585A437) into the body middle plate (FAB-EMBL-000007) using a drill press.
6. Install the 4 mm ball bearings (COTS-9292K37) into the hollow end of the 3× actuators (FAB-EMBL-000039) using epoxy glue. Ensure that the epoxy has hardened fully before proceeding.
7. Use a small quantity of vacuum grease to lubricate the threaded section of the 3× actuators (FAB-EMBL-000039).

8. Install the 3× timing pulleys (COTS-HTPT48S2M060-A-P6.35) onto the 3× actuators and secure in place with the set screws contacting the flat surface.
9. Install the 3× actuators into the threaded bushings (COTS-F6MSSA1). Screw the actuator in just until the ball tips protrude ~1 mm from the bushing.
▲ CAUTION Take care of the orientation of the actuator in the bushing, if the bushing and actuator are incorrectly oriented, use of the actuator may act to remove the bushing from the objective piezo platform (FAB-EMBL-000038).
10. Install the objective thread adapter (FAB-EMBL-000043) into the objective piezo flexure stage (COTS-P-726.1CD) using an adjustable spanner wrench (COTS-SPW801) to securely tighten it.
11. Install the objective piezo flexure stage onto the objective piezo platform (FAB-EMBL-000038).
12. Rest the three ball tips of the actuators (FAB-EMBL-000039) on the three sets of pins installed on the body middle plate (FAB-EMBL-000007), orient the platform on the pins such that the cable of the objective piezo flexure stage (COTS-P-726.1CD) can be easily routed to the underlying cable channel of the body middle plate.
13. Remove the objective piezo flexure stage (COTS-P-726.1CD).
14. Install the 6× hooked springs (COTS-RZ-099I) with 6× retaining pins (COTS-91585A371) in the objective piezo platform (FAB-EMBL-000038) such that the springs pass through the clearance holes in the body middle plate (FAB-EMBL-000007).
15. Use a spring pulling hook to pull the springs fully through the body middle plate (FAB-EMBL-000007) and install the 6× retaining pins (COTS-91585A371) such that objective piezo platform (FAB-EMBL-000038) and body middle plate are held together under spring tension.
16. Screw in the 3× actuators (FAB-EMBL-000039) such that the separation between the objective piezo platform and body middle plate is large enough to just permit 1× 7 mm optical post spacer (COTS-RS7M) to pass freely between the two components around the circumference of the objective piezo platform (FAB-EMBL-000038).
17. Insert 3× 7 mm optical post spacers (COTS-RS7M) between the objective piezo platform (FAB-EMBL-000038) and the body middle plate (FAB-EMBL-000007) close to the circumference of the objective piezo platform with approximately even spacing.
18. Lower the platform using the 3× actuators FAB-EMBL-000039 until the objective piezo platform (FAB-EMBL-000038) is supported by the 3× 7 mm optical post spacers (COTS-RS7M). One should feel the resistance to turning the actuator decrease at the point of touching. Note, it may be necessary to perform this adjustment iteratively to ensure flatness.
19. Raise the platform using the 3× actuators (FAB-EMBL-000039) just enough that the 3× 7 mm optical post spacers (COTS-RS7M) can be removed. Check that the spacing between the objective piezo platform (FAB-EMBL-000038) and body middle plate (FAB-EMBL-000007) is 7 mm throughout by moving the post spacers around the circumference.
▲ CAUTION If the actuators are not adjusted correctly, they will not mate correctly with other components later in assembly and the objective lens will be tilted relative to the xy stage assembly.
20. Loop the timing belt (COTS-60S2M494) around the 3× timing pulleys (COTS-HTPT48S2M060-A-P6.35). Note, at this stage the belt will not be under tension and so will not hold on the pulleys. The assembly should now appear as shown in Supplementary Fig. 8 (timing belt omitted).
21. Install the body upper standoffs (FAB-EMBL-000008/09/10/11) on the body middle plate (FAB-EMBL-000007) using 8× M4×16 mm dowel pins and 8× M4×20 mm socket head screws.
▲ CAUTION Ensure that the parts are installed with the correct orientation to form 4× pairs of recesses for magnets on the four sides of the microscope.
22. Affix the illumination dichroic mount (FAB-EMBL-000026) to the top plate of its kinematic mount (COTS-KB25-M) using 1× M4×6 mm socket head screw, ensuring that the plate is situated flush with the sides of the recess marked by the corner clearance hole.
23. (Optional) If wishing to make use of the laser power monitoring photodiode. Install the color balance filter (COTS-FGT200) and focus lock laser blocking filter (COTS-FESH0650)

- in a lens tube (COTS-SM1L03) with the caret pointing away from the externally threaded section. Secure the filters in place by threading the SM1 threaded photodiode (COTS-SM1PD1A) into the lens tube. Install the lens tube in the illumination dichroic mount (FAB-EMBL-000026). Note, the choice of filters is somewhat application specific (Supplementary Information Note 23). The recommendations provided efficiently remove any contribution from the focus lock laser and correct for the stronger spectral response of the photodiode at longer wavelengths.
24. Install the emission and illumination dichroic mirrors (COTS-25.5x36x3MM-DICHROIC-EM/ COTS-25.5x36x3MM-DICHROIC-ILL) into their mounts (FAB-EMBL-000025/26 respectively) following the instructions in Supplementary Note 23. Note, if using 5 mm thick dichroics and/or a mirrored configuration of the body, install the mirrors into the respective mounts. Consult the CAD assemblies for respective part numbers and adjust the following instructions accordingly. Supplementary Information Note 3.
 25. Install the prism mirror (COTS-MRA20-E03) into the prism mirror mount (FAB-EMBL-000024). Take care that the mirror sits flush with the two sides of the recess sharing the corner clearance hole.
 26. Install the prism mirror mount (FAB-EMBL-000024) on the optic pillar base plate (FAB-EMBL-000022) using 2× M3×16 mm socket head screws and 2× M3×10 mm dowel pins.
 27. Install the optic pillar (FAB-EMBL-000023) onto the optic pillar base plate (FAB-EMBL-000022) using 2× M4×12 mm socket head screws and 2× M4×10 mm dowel pins.
 28. Affix the emission dichroic mount (FAB-EMBL-000025) to the optic pillar (FAB-EMBL-000023) using 2× M3×12 mm dowel pins and 2× M3×30 mm socket head screws.
 29. Install the lower mounting plate of the illumination dichroic kinematic mount (COTS-KB25-M) onto the optic pillar (FAB-EMBL-000023) using 1× M4×6 mm socket head screw taking care that the magnets, balls and three sets of locating pins line up correctly with the upper mounting plate of COTS-KB25-M (affixed to FAB-EMBL-000026), in the correct orientation. Ensure that the lower mounting plate sits flush with the sides indicated by the corner clearance hole.
 30. (Optional) If wishing to make use of the four-position shared-path filter slider (COTS-ELL9) inside the body, install the filters (COTS-25MM-HOUSED-FILTER) individually mounted in lens tubes (COTS-SM1L03) into the corresponding SM1 thread on the filter slider. Supplementary Information Note 3.
▲ CAUTION Ensure filters are correctly oriented with the caret pointed as indicated by the filter manufacturer.
 31. (Optional) Install four-position shared-path filter slider (COTS-ELL9) on its mounting plate (FAB-EMBL-000027) via 4× #4-40 hex standoffs (3D-SMLM-COTS-91075A873) using 4× #4-40x3/8" socket head screws.
 32. (Optional) Install the mounting plate (FAB-EMBL-000027) onto the optic pillar base plate (FAB-EMBL-000022) using 1× M4×12 mm socket head screw and 2× M4×10 mm dowel pins. Note, whenever using the alignment laser (3D-SMLM-EMBL-007) for alignment of the emission path, switch the filter slider to an open position.
 33. Install the body lower standoffs (FAB-EMBL-000002/3/4/5) onto the body lower plate (FAB-EMBL-000001) using 8× M4×20 mm socket head screws and 8× M4×12 mm dowel pins. Take care that the standoffs are oriented correctly and installed on the correct corner of the body lower plate.
 34. Install the optic pillar base plate (FAB-EMBL-000022) on the body lower plate (FAB-EMBL-000001) using 4× M6×10 mm socket head screws and 2× M4×12 mm dowel pins.
 35. Install the body lower plate (FAB-EMBL-000001) on the optical table (COTS-M-VIS3660-PG4-325A) using 2× M6×10 mm and 2× M6×20 mm socket head screws. Note, the shorter screws should be used to secure the plate through the counterbores in the cable channels.
▲ CAUTION The location of this plate will determine the respective location of all other components of the microscope relative to the optical table. Ensure that it is installed at the correct position, allowing space on the table for the optical pathways.
 36. (Optional) Route the four-position shared-path filter slider (COTS-ELL9) ribbon cable out of the body and secure with its cover (FAB-EMBL-000050) and 4× M2.5×6 mm countersunk screws.

37. Install the tube lens mount (FAB-EMBL-000035) onto the tube lens base (FAB-EMBL-000034), securing with 4× M6×16 mm socket head screws.
38. Loosely install the tube lens retaining cap (FAB-EMBL-000036) onto the tube lens mount (FAB-EMBL-000035) using 2× M4×10 mm socket head screws.
39. Install the tube lens base (FAB-EMBL-000034) onto the body lower plate (FAB-EMBL-000001), in an approximate nominal position securing with 3× M6×20 mm socket head screws and 3× M6 washers.
40. Install the mounted illumination dichroic (COTS-25.5x36x3MM-DICHROIC-ILL, FAB-EMBL-000026) by reuniting the two halves of the kinematic mount (COTS-KB25-M).
41. Install 8× M4×20 mm dowel pins into the protruding end of the body lower standoffs (FAB-EMBL-000002/3/4/5). The assembly should now appear as shown in Supplementary Fig. 9 (dowel pins omitted).
42. Place the insulator plate (FAB-EMBL-000006) onto the body lower standoffs (FAB-EMBL-000002/3/4/5) such that the dowel pins pass through the clearance holes. Ensure that the plate is oriented correctly with respect to the standoffs and the body lower plate (FAB-EMBL-000001).
43. Install the body middle plate FAB-EMBL-000007 on the insulator plate (FAB-EMBL-000006), taking care to orient correctly with respect to the lower portion of the body. Secure in place with 8× M4×25 mm socket head screws.
44. Install the objective piezo flexure stage (COTS-P-726.1CD) onto the objective piezo platform (FAB-EMBL-000038).
45. Route the objective piezo flexure stage cable out of the body using the channels in the body middle plate (FAB-EMBL-000007), securing in place with the channel covers (FAB-EMBL-000054/55) and 5× M2.5×6 mm countersunk screws. The assembly should appear as shown in Supplementary Fig. 10.
46. Insert the 8× magnets (COTS-S-08-05-N) into their recesses in the body upper standoffs (FAB-EMBL-000008/09/10/11) and 4× covers (FAB-EMBL-000018), ensuring that the magnets are oriented correctly to attract and allow for interchange of the identical covers (FAB-EMBL-000018) between the four sides. Remove the covers afterward.
47. Glue the magnets in place using a two-part epoxy adhesive (COTS-JB-WELD) once the correct orientation is confirmed.
48. Use a drill press to install the three flanged bearings (COTS-SFL625ZZ) into the body upper plate (FAB-EMBL-000012).
49. Use a drill press to install the idler (COTS-SFD11-25) onto its mounting pin (FAB-EMBL-000064).
50. Loosely install the idler and mounting pin onto the underside of the body upper plate (FAB-EMBL-000012) using an M4×10 mm socket head screw such that the screw and pin can be translated along the slot. Note, that there are three possible recessed slots for the screw, allowing for placement of the idler as desired. However, the recommended position is indicated by the CAD files and shown in Supplementary Fig. 11.
51. Install 8× M4×12 dowel pins into top of the body upper standoffs (FAB-EMBL-000008/09/10/11).
52. Carefully lower FAB-EMBL-000012 onto the 8× protruding pins and bosses of the 3× actuators (FAB-EMBL-000039), which mate with the bearings (COTS-SFL625ZZ) while capturing the outer flat side of the timing belt (COTS-60S2M494) between the two flanges of the idler (COTS-SFD11-25).
- ◆ **TROUBLESHOOTING**
53. Secure the body upper plate (FAB-EMBL-000012) to the body upper standoffs (FAB-EMBL-000008/09/10/11) using 8× M4×12 mm socket head screws.
54. Ensure that the timing belt (COTS-60S2M494) is now looped correctly around the 3× timing pulleys (COTS-HTPT48S2M060-A-P6.35, inside the belt) and the idler (COTS-SFD11-25, outside the belt).
55. Tension the timing belt (COTS-60S2M494) by sliding the idler pin (FAB-EMBL-000064) along the slotted recess in the body upper plate (FAB-EMBL-000012) and tightly secure the M4 socket head screw when an appropriate tension is achieved.

56. Check that the objective piezo platform (FAB-EMBL-000038) can be moved up and down by rotating any of the timing pulleys (COTS-HTPT48S2M060-A-P6.35). Return the platform to the nominal 7 mm spacing using 1× optical post 7 mm spacer (COTS-RS7M) placed between the body middle plate (FAB-EMBL-000007) and objective piezo platform (FAB-EMBL-000038).

◆ TROUBLESHOOTING

57. Install the *xy* stage (COTS-SOM-12090) onto the body upper plate (FAB-EMBL-000012) via the 4× stage standoffs (FAB-EMBL-0000047) using 4× M6×30 mm socket head screws. Note, it is necessary to move the stages from their central position to access the counterbored holes. The assembly should now appear as shown in Supplementary Fig. 12.
58. Install the sample holder support (FAB-EMBL-000044) onto the *xy* stage (COTS-SOM-12090) using 4× M2.5×6 mm socket head screws.
59. Install the cable channel (COTS-EMBL-000059) between the body middle and upper plates (COTS-EMBL-000007/12), securing with 1× M2.5×6 mm socket head screw and 2× M2.5×6 mm countersunk screws.
60. Route the *xy* stage (COTS-SOM-12090) cables out of the body using the channels on the body upper plate (FAB-EMBL-000012), cable channel (FAB-EMBL-000059) and body lower standoff (FAB-EMBL-000003) securing in place with the respective channel covers (FAB-EMBL-000056/57/58) and 7× M2.5×6 mm countersunk screws while additionally capturing the objective piezo flexure stage (COTS-P-726.1CD) cable with channel cover (FAB-EMBL-000058).
61. (Optional) Install the channel cover (FAB-EMBL-000053) on body lower standoff (FAB-EMBL-000059), capturing the heating foil and temperature sensor cables, as appropriate, using 2× M2.5×6 mm countersunk screws. The assembly should now appear as shown in Supplementary Fig. 13.
62. Assemble the microscope cover by affixing 2× back/front cover (FAB-EMBL-000019, 2× left/right cover (FAB-EMBL-000020), 1× upper cover FAB-EMBL-000021 and 1× lower clearance cover (FAB-EMBL-000066) using 24× M2.5×10 mm countersunk screws. Note, matching side panels should oppose each other.
63. Install the ring light-emitting diode (LED) FAB-EMBL-000037 in the top plate of the upper cover (FAB-EMBL-000021) using 4× M3×6 mm hex standoffs (COTS-98952A104) and 4× M3×5 mm socket head screws.
64. Install the 2× strain relievers (FAB-EMBL-000017) capturing the LED cable and tightening it to the left/right cover (FAB-EMBL-000020), as determined by the LED placement.
65. Install 12× panel knob (COTS-24540.0021) to the covers (FAB-EMBL-000013/14/15/16, 4× FAB-EMBL-000018, FAB-EMBL-000021) using 12× M5×10 mm countersunk screws.
66. Install all covers (FAB-EMBL-000013/14/15/16, 4× FAB-EMBL-000018, FAB-EMBL-000019/20/21/66) on the microscope checking for fit and appropriate routing of the LED cable.
▲ **CAUTION** certain covers (FAB-EMBL-000013/14/15/16/18) can be installed in two orientations. For FAB-EMBL-000013/14/16, which have apertures at specific heights for the various optical pathways, ensure that the panels are installed the correct way round. The assembly should now appear as shown in Supplementary Fig. 14.

(Optional) Assembly of the microFPGA

● TIMING 4 d

▲ **CRITICAL** Prospective builders are advised to directly source the assembled microFPGA from EMBL/EMBLEM (Supplementary Information Note 10). For those wishing to build up the microFPGA themselves instructions are provided (Supplementary Protocol 1).

Configuration of the microFPGA

● TIMING 2 h

▲ **CRITICAL** Before the microFPGA can be used, it must be configured by uploading a configuration file to the device.

67. Install AlchitryLabs from <https://alchitry.com/alchitry-labs>.
68. Download the FPGA configuration binary (.bin) for the Alchitry Au from the release page of the microFPGA repository: <https://github.com/mufpga/MicroFPGA/releases>.

69. Connect the FPGA to the host PC.
70. Upload the configuration to the FPGA target using AlchitryLoader (installed as part of Alchitry labs).

Setup and configuration of software and hardware for acquisition

● TIMING 7 d

▲ **CRITICAL** Certain hardware elements require nonfactory configuration for operation. For example, the piezo flexure stage controller needs to be configured in its host software such that it provides appropriate positional feedback on the basis of the analog signal provided by the focus lock system quadrant photodiode (QPD). The various piezo resonant stages used for illumination control (epi-/HILO/TIRF), back focal plane viewing and astigmatic lens positioning also require that a unique address is established for each in their host software. μ Manager, which ultimately provides the basis for hardware control must be installed. Communication with the various hardware devices from μ Manager requires that a hardware configuration is established, whereby communication with each device is defined via its device adapter (e.g., COM port etc. for serial devices). All required device adapters for the hardware elements described are available in μ Manager with one exception, the objective lens piezo flexure stage uses a modified version of the PI_ZStage device adapter, PI_FocusLock, a precompiled version of which is available on our GitHub. The htSMLM GUI is provided as a configuration for μ Manager's Easier Micro-manager User interface (EMU)) plugin. A precompiled version is subsequently installed and its various controls and indicators are associated with relevant hardware properties.

71. Install all manufacturer supplied software and drivers listed under: software for software/hardware setup. Connect all hardware devices to the host PC, except for the piezo resonant stages and associated controller/distributor boards, as appropriate for the specific hardware device.
72. Test all connected hardware devices in their host software for general functionality. Return defective devices to the manufacturer for replacement.
73. Email firmware@smaract.com with the model and serial number of the COTS-HCU-3D stage controller to obtain firmware for ASCII communication with the device. Use SCUFirmwareUploader to upload the supplied firmware for the xy stage (COTS-SOM-12090) to allow the device to be controlled via serial commands. Connect the xy and QPD stage (COTS-2445-L) stages to the controller such that the xy stage corresponds to channels A/B and the QPD stage to channel C. Set step sizes as desired (5 μ m A/B and 50 μ m C step size provides sufficiently fine control of sample positioning and focusing during focus lock operation, respectively). Under MENU/CONTROL MODES, set all stages to 'CL' (closed loop). Note, you may prefer to use the inverted axes configuration of the stage controller (COTS-HCU-3D) depending on personal preference. This can be carried out at any point during the protocol (MENU/KNOB CONFIG).
74. Crimp suitable length cables for the three to four piezo resonant stages using the connectors (COTS-90327-0308) and ribbon cables (COTS-AWG 28-08G 3M) following the manufacturer guidelines. Typically, 1 m length is sufficient to position the distributor board centrally on the optical table while reaching all devices.
75. Mount the piezo resonant stage control board (COTS-ELLC2) to its base mount (FAB-EMBL-000095) using 8 \times M3 \times 12 mm hex standoffs (COTS-93655A099) (4 \times standoffs, then the board, then 4 \times standoffs on top). Mount the bus distributor board (COTS-ELLB) on top of the exposed standoff another 4 \times M3 \times 12 mm hex standoffs. Secure the base to an appropriately centralized location on the optical table. Note, the boards will be covered later allowing the assembly to be located on the optical table without potential interference from the LEDs on the boards.
76. Connect the piezo resonant stage control board (COTS-ELLC2) and the bus distributor board (COTS-ELLB) via a short ribbon cable. Provide power to the distributor board before connecting the control board to the PC via USB.
77. (Optional) Connect the four-position shared-path filter slider (COTS-ELL9) to the bus distributor (COTS-ELLB). Use the host software (Thorlabs, ELLO) to assign the device to address 3.

78. Connect the piezo resonant stages one at a time to the bus distributor (COTS-ELLB) and assign the following addresses: 0: COTS-ELL17-M, 1: COTS-ELL20-M, 2: COTS-ELL6. Note, COTS-ELL17-M should be connected last to be automatically assigned the address 0.
79. Test the piezo resonant stages in ELLO for general functionality. Return defective devices to the manufacturer for replacement.
80. Install the board cover (FAB-EMBL-000096) on the protruding 4×M3×12 mm hex standoffs from the bus distributor board (COTS-ELLB), ensuring that the cut-outs for the various cables line up correctly and secure it in place.
81. In PIMikroMove set the parameters for the P-709.CRG controller given in Supplementary Table 7. See the manufacturer documentation for a description of these parameters, using an analog input to control the stage position and how to write/save parameters correctly in PIMikroMove.
82. Using Windows Device Manager or other means, identify the relevant communication port for each hardware element, which will use a serial protocol for communication with μ Manager. This includes the controller for the objective piezo focusing device (COTS-P-726.1CD), piezo resonant stages (COTS-ELL6/ELL9/ELL17-M/ELL20-M), lasers (COTS-ICHROME-MLE, COTS-IBEAM), filter wheels (COTS-FW102C), microFPGA (COTS-AU-FPGA) and xy stage (COTS-SOM-12090).
83. Ensure all software used for communication with the devices is closed.
84. Install the most recent nightly build of μ Manager 2.0.1 as necessary from https://micro-manager.org/Download_Micro-Manager_Latest_Release.
85. Download the precompiled PI_FocusLock device adapter from <https://github.com/ries-lab/3DSMLM>. Put the device adapter in the root μ Manager directory (e.g., C:\Program Files\micro-manager 2.0).
▲ CAUTION During operation, the device adapter will set some internal parameter values in the associated Physik Instrumente E-709.CRG controller.
86. Configure and save a hardware configuration in μ Manager including all hardware elements. For notes on each device including communications settings and device adapter name, see Supplementary Table 4.
◆ TROUBLESHOOTING
87. Establish several μ Manager configuration presets following Supplementary Table 8.
88. Turn on metadata generation by μ Manager by navigating to Tools from the ribbon menu, then Options and ensure 'Create metadata.txt file with Image Stack Files' is ticked.
89. Download the precompiled htSMLM GUI from <https://github.com/ries-lab/3DSMLM> and place the .jar file in the EMU folder in the root μ Manager directory (e.g., C:\Program Files\micro-manager 2.0\EMU).
90. Open μ Manager and load the saved hardware configuration file. Ensure that all hardware devices are detected correctly.
91. Launch the htSMLM GUI by navigating to Plugins/Interface/EMU and then selecting the compiled htSMLM UI (.jar file).
92. In the htSMLM EMU plugin, configure the GUI using the configuration wizard (Configuration/Modify configuration) as described in Supplementary Table 9. Subsequently, associate the GUI controls and indicators with the respective device property as given in Supplementary Table 10. In the case of a system using both the multimode and single-mode laser engines, created individually configured htSMLM configurations for each with the corresponding parameters.
93. See <https://github.com/jdeschamps/htSMLM/tree/main/guide> for a guide to the various panels of the EMU htSMLM GUI and their functions.

(Optional) Testing of the microFPGA

● TIMING 1 d

▲ CRITICAL Prospective builders are advised to directly source the assembled microFPGA from EMBL/EMBLEM (Supplementary Information Note 10). For those who have built the microFPGA themselves instructions for testing are provided (Supplementary Protocol 2).

Making electrical connections to hardware

● TIMING 1 d

▲ **CRITICAL** Proper control of the various hardware elements by the microFPGA requires that the appropriate connections are made between its I/O and those on the associated hardware including the camera, lasers/laser engine and laser power monitoring photodiode. Connection to the QPD amplifier is omitted at this stage and follows later in the protocol, when it is required.

94. For active camera synchronization, connect the camera timing 1 output subminiature version A (SMA) connector to the DI:CAM:EX SMB connector on the microFPGA.
95. For passive camera synchronization, connect the camera trigger input SMA connector (Ext. Trig.) to TTL4 on panel 2 of the microFPGA.
96. Connect the laser engine 'enable' SMB connectors (DO:L0-3:EN) to their equivalent SMB connector on the Toptica iChrome MLE laser engine (if present in the system). Note that the laser engine defines the laser lines in reverse order of wavelength. For example, for the standard 405/488/561/640 nm configuration, 640 nm is laser 0 and 405 nm is laser 3.
97. Connect the D-SUB9 connector of the laser engine panel of the microFPGA to the multimode laser engine control box as appropriate. The D-SUB9 connector duplicates the signals DO:L0-3:EN and DO:L0-3:POW).
98. (Optional) If wishing to make use of the laser power monitoring photodiode, connect the photodiode Bayonet Neill–Concelman (BNC) output connector to the SMB AI:PD connector on the microFPGA. Route the cable out of the body using an unused cable channel in the body lower plate (FAB-EMBL-000001).

Setup of the infinite conjugate viewing camera and infinite conjugate transmission target

● TIMING 1 d

▲ **CRITICAL** The camera and lens must be spaced appropriately to provide a reference to an object viewed at infinite distance. To do so, the camera and lens assembly should be taken to an appropriate location and focused to image a distant object. Once the infinite conjugate viewing camera is setup correctly, it can be unified with the infinite conjugate transmission target, which is then brought into focus on the camera by varying the distance between the target and its lens. Since the camera is setup to image an infinite conjugate object, this ensures that the lens is positioned to produce an image of the target at infinity.

99. Assemble the infinite conjugate viewing camera and infinite conjugate transmission target (3D-SMLM-EMBL-004), omitting the $\varnothing 24$ mm round coverslip (Supplementary Fig. 20).
100. Uncouple the infinite conjugate viewing camera from the infinite conjugate transmission target by removing the lens tube coupler (COTS-SM1S10).
101. Take the infinite conjugate viewing camera to an appropriate location to image an object > 350 m away. Typically, a window of a building or a remote location is required. The rationale for choosing this distance is described in Supplementary Information Note 25.
102. Loosen a lock ring (COTS-SM1NT) of the lens tube coupler (COTS-SM1T10, CAD configuration: infinity camera) and focus the camera on the distant object by threading the adjoining lens tube (COTS-SM1L30, on either side of the coupler) inward or outward. Once a maximally sharp image has been produced, lock the position using the lock ring(s). Check the image sharpness again after securing.
103. Produce a transmission target by taking a $\varnothing 24$ mm round coverslip and repeatedly flicking the tip of a permanent marker in close proximity to the coverslip such that a spray of fine ink particles is produced thereupon.
104. Install the coverslip transmission target in the lens tube (COTS-SM1L03) of the infinite conjugate viewing target, securing it in place with 2× retaining rings (COTS-SM1RR).
105. Reunify the infinite conjugate viewing camera and the infinite conjugate transmission target by reinstalling the lens tube coupler (COTS-SM1S10).
106. Backlight the target with a white light source.
107. Loosen the lock ring (COTS-SM1NT) of the lens tube coupler (COTS-SM1T10, on the infinite conjugate transmission target side) and focus the image of the target on the camera by threading the adjoining lens tube (COTS-SM1L15 or COTS-SM1M15) inward or outward.

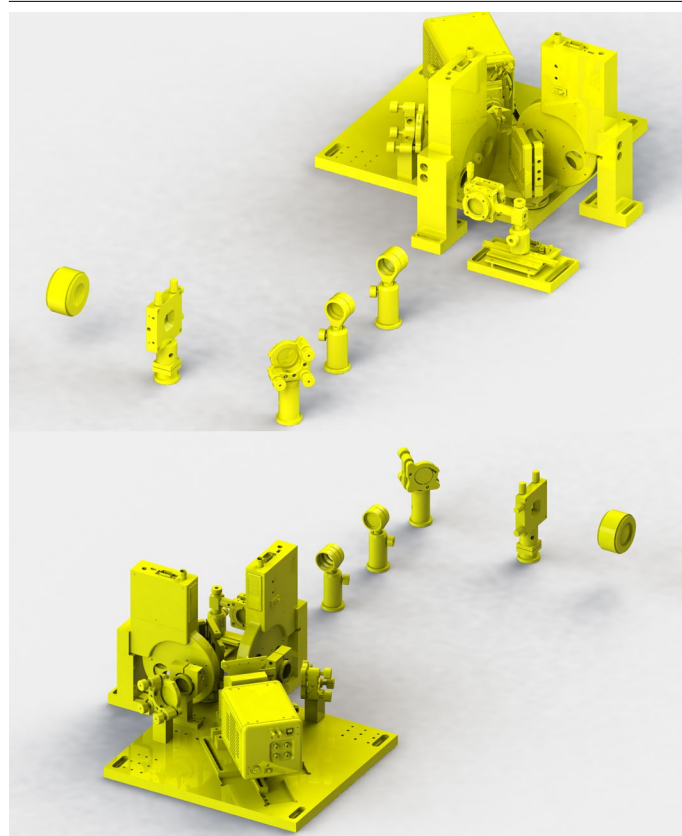


Fig. 5 | The fully assembled multicolor, 3D imaging capable emission path. Top: as viewed from the front/right of the microscope. From left-right: the tube lens, field aperture, first steering mirror, first relay lens, laser blocking filters, astigmatic lens and filter wheels either side of the image splitter dichroic mirror. Bottom: as viewed from the back/left of the microscope highlighting the image splitter platform. Following the filter wheel, the transmitted and reflected paths each comprise a second relay lens and steering mirror before the images are recombined by a knife-edge mirror (occluded in figure) and imaged onto an sCMOS camera.

Once a maximally sharp image has been produced, lock the position using the lock ring(s). Check the image sharpness again after securing.

108. Uncouple the infinite conjugate viewing camera from the infinite conjugate transmission target by unthreading the lens tube coupler (COTS-SM1S10) on the camera side.

Emission path beam routing

● TIMING 6 d

▲ **CRITICAL** Refer to a CAD rendering of the completed emission path (Fig. 5). To establish the route of the emission path, an alignment laser is aligned to the objective lens port to indicate the optical axis of the emission path. The image splitter platform and a pair of pinned alignment targets are first used as a guide to ensure proper reflection of light out of the microscope body. The image splitter platform is subsequently installed in place for imaging operation and the beam split by a dichroic mirror. The two beamlets are subsequently steered to route the corresponding image channels onto the camera with appropriate spatial separation using an alignment tool. This tool provides a reference position where the two beams from the reflected and transmitted pathway should cross each other owing to a small tilt of the two images with respect to the camera. The displacement of the image planes from the camera chip is small with respect to the depth of focus and so does not affect the optical performance across the field of view.

109. Remove all covers (FAB-EMBL-000013/14/15/16, 4× FAB-EMBL-000018, FAB-EMBL-000019/20/21/66) from the microscope.
110. Install the pre-aligned 532 nm alignment laser assembly (3D-SMLM-EMBL-007) in the RMS (Royal Microscopical Society) thread of the objective port (FAB-EMBL-000043).
111. Introduce the image splitter platform (FAB-EMBL-000077) (omitting all mounted components) as indicated in Supplementary Fig. 21. Ensure that the side facing the right side of the microscope body sits flush against the body lower plate (FAB-EMBL-000001).

112. Install two alignment targets (FAB-EMBL-000081) with two irises (COTS-SM1D12D) at positions spaced as far apart as possible along the emission path axis (the alignment targets should be placed in the transmitted pathway of the image splitter as shown in Supplementary Fig. 21).
113. Using the alignment laser as a guide, translate the image splitter platform (FAB-EMBL-000077) along the edge of the body lower plate (FAB-EMBL-000001) such that the beam reflected by the emission path dichroic mirror (COTS-25.5x36x3MM-DICHROIC-EM) aligns laterally with the distal iris before securing the platform in position.
114. Check whether the alignment laser passes the proximal iris in the lateral direction.
◆ **TROUBLESHOOTING**
115. Check that the laser passes correctly through the proximal and distal irises in the vertical direction repositioning the splitter platform as described above as necessary.
◆ **TROUBLESHOOTING**
116. Remove the image splitter platform (FAB-EMBL-000077) but leave the alignment targets in place.
117. Install the lower section of the kinematic magnetic mount (COTS-SB1-M) on the image splitter platform (FAB-EMBL-000077). Note, the rotational orientation should be set such that when the upper section is installed, its release lever should be accessible so check the resulting orientation of the upper section and secure the lower section accordingly.
118. Install the knife-edge mirror (COTS-MRAK25-P01) secured with the clamp (COTS-PM3-M) on its pedestal (FAB-EMBL-000075) as well as the camera image alignment target (FAB-EMBL-000093, COTS-SM1D12D, COTS-SM1L10) and the steering mirror pedestals FAB-EMBL-000079/FAB-EMBL-000080) on the image splitter platform (FAB-EMBL-000077).
119. Install the image splitter platform (FAB-EMBL-000077) on the optical table as shown in Supplementary Fig. 22.
120. Place the first emission path steering mirror (COTS-RS2P4M, COTS-RS5M, COTS-POLARIS-K1, COTS-BB1-E02) such that the alignment laser beam is centered on the mirror. Position and steer the mirror such that the beam remains centered on the mirror and passes the two alignment targets (FAB-EMBL-000081) on the image splitter platform (FAB-EMBL-000077) through the irises (COTS-SM1D12D). Secure the mirror in place using a pedestal post clamp (COTS-PS-F).
121. Preconfigure the actuators of the two steering mirror mounts (COTS-POLARIS-K1) for the transmitted and reflected paths to nominal positions using a 1/8" post height spacer (3D-SMLM-PS-0.125) inserted between the steerable and mounting sections of the steering mirror mount and adjusting each actuator in an iterative manner. This ensures that the mirrors are centered with regard to the system optical axis when installed later. Note, the later addition of the splitting dichroic (COTS-25.5x36x3MM-DICHROIC-SP) elicits an ~1 mm optical axis shift (for a 3-mm-thick dichroic) resulting in only a minor path length difference between the two arms, which is adjusted for by later alignment of the steering mirror in the transmitted path.
122. Remove the alignment targets (FAB-EMBL-000081) and install the steering mirror for the transmitted path (COTS-POLARIS-K1, COTS-BB1-E02) on its pedestal (FAB-EMBL-000080, Supplementary Fig. 23). The beam should reflect from the mounted mirror onto the subsequent knife-edge mirror. Steer the mirror such that the reflected beam passes the camera image alignment target (FAB-EMBL-000093) through the iris (COTS-SM1D12D).
123. Glue the splitting dichroic mirror (COTS-25.5x36x3MM-DICHROIC-SP) into its mount (FAB-EMBL-000069) as described previously and install the mount into the steerable kinematic mount (COTS-KM200S). Supplementary Information Note 3.
124. Replace the 2× pre-installed actuators of the steerable kinematic mount (COTS-KM200S) with the alternative 2× hex-drive actuators (COTS-F25SS050).
125. Install the two alignment targets (FAB-EMBL-000081) with irises (COTS-SM1D12D) as far apart as possible in two available positions of the reflected (angled) pathway of the image splitter platform (FAB-EMBL-000077).

126. Install the upper section of the kinematic magnetic mount (COTS-SB1-M) and place the mounting plate for the image splitter dichroic kinematic mount (FAB-EMBL-000068) on the top. Since the orientation of the mounting plate will determine the initial orientation of the splitter dichroic, secure the mounting plate loosely such that the upper plate can be rotated by hand on the magnetic mount under light pressure.
127. Use a suitable machined flat component as a guide to orient the mounting plate for the splitter dichroic kinematic mount (FAB-EMBL-000068) relative to the underlying image splitter platform (FAB-EMBL-000077). When correctly positioned the sides of the mounting plate and splitter platform facing away from the reflected pathway (closest to the optical table edge) should be flush with each other. Secure in place when a correct orientation is achieved.
128. Install the steerable kinematic mount (COTS-KM200S) housing the dichroic (COTS-25.5x36x3MM-DICHOIC-SP)/FAB-EMBL-000069 onto the mounting plate for the image splitter dichroic kinematic mount (FAB-EMBL-000068) ensuring that the rear side of the mount is flush with the locating surface.
129. Use the hex adjustment screws of the steerable mirror mount (COTS-F25SS050, COTS-KM200S) to reflect the incident beam through the irises (COTS-SM1D12D) of the two alignment targets (FAB-EMBL-000081), optimizing preferentially for the distal target. The beam should pass the proximal iris to within ± 0.5 mm. The assembly should now look as shown in Supplementary Fig. 24.
130. Remove the alignment targets (FAB-EMBL-000081) and install the steering mirror (COTS-POLARIS-K1, COTS-BB1-E02) for the reflected path on its pedestal (FAB-EMBL-000079) following the process for the transmitted path. Use the steering mirror adjusters to align the beam to the camera image alignment target (FAB-EMBL-000093) as previously described (Supplementary Fig. 25).

Emission path alignment

● TIMING 7 d

▲ **CRITICAL** Having routed the beam through the emission path, the tube lens and relay lens pair must be positioned to produce primary and secondary images of the objective focal plane (the design focal plane for which the objective produces a conjugate image at infinity). The tube lens mount is aligned to the optical axis using an alignment assembly and positioned for telecentricity by passing the alignment laser through the tube lens (to produce a focus at the back focal plane) and subsequently collimating the beam with the objective lens. The objective and tube lens thus provide a 4f imaging system yielding an $\sim 92\times$ magnification primary image. Spacing and alignment of the first relay lens is similarly achieved by using the tube lens to generate a focus from an infinite conjugate source and collimating with the relay lens accordingly. To aid alignment, the second relay lenses of the reflected and transmitted paths of the image splitter feature mounts with circumscribed degrees of freedom: a dowel pin slot and a pair of dowel pins in the base allow lateral translation but not reorientation of the mount. The tube lens is removed from its base adapter to produce a focus from the first relay lens thus again presenting the longitudinal positioning of the second relay lens as a collimation operation. Once correctly positioned, the emission path and image splitter are set up to produce two secondary images on the camera with $\sim 61\times$ magnification. The addition of blocking filters for the laser lines used for illumination/focus lock and various emission filters allows for fluorescence images to be collected in subsequent steps. Initially, the camera is installed in a nominal position and then focused using a reference to an infinite conjugate object.

131. Remove the upper section of the kinematic magnetic mount (COTS-SB1-M) with dichroic mirror and associated components (COTS-25.5x36x3MM-DICHOIC-SP, COTS-KM200S, FAB-EMBL-000068/69). Install one alignment target with iris (FAB-EMBL-000081, COTS-SM1D12D) as shown in Supplementary Fig. 26. The alignment laser should be aligned to the target.

◆ TROUBLESHOOTING

132. Install the tube lens alignment target (3D-SMLM-EMBL-002) in the tube lens mount (FAB-EMBL-000035), securing it with the retaining cap (FAB-EMBL-000036) as shown in Supplementary Fig. 27.
133. Position the tube lens mount on its base (FAB-EMBL-000034/35/36) such that the laser passes through the ground-glass alignment target and subsequent iris. Note, the base (FAB-EMBL-000034) should remain loosely affixed to the body lower plate (FAB-EMBL-000001) during this operation. Firmly secure the base in place.
134. Remove the tube lens alignment target (3D-SMLM-EMBL-002) and install the tube lens (COTS-TTL165-A) at an arbitrary position along the axis of the mount (FAB-EMBL-000035) without securing the retaining cap (FAB-EMBL-000036) such that the lens may be moved back and forth.
 - ▲ **CAUTION** The tube lens has a correct orientation with the infinite conjugate (objective lens) side indicated by the arrow on the housing.
 - ▲ **CAUTION** Take care not to touch optical surfaces of the tube lens.
135. Check that the beam still passes the iris target on the image splitter platform within an allowable margin of ± 0.5 mm.
 - ◆ **TROUBLESHOOTING**
136. Remove the alignment laser assembly (3D-SMLM-EMBL-002) from the objective port (FAB-EMBL-000043) and replace it with the objective port alignment target assembly (3D-SMLM-EMBL-006) with the beam profiling camera installed on the distal end.
137. Use the pitch/yaw (COTS-KAD11F) and xy (COTS-CXY1) mounts of the alignment laser assembly to align through the two irises (COTS-SM1D12D) before removing the 2× slotted lens tubes (SM1L30C), 2× irises (COTS-SM1D12D), lens tube (COTS-SM1S10) and thread adapter (COTS-SM1A4). Install the thread adapter (COTS-SM1A2) into the exposed SM1 port of the xy mount and install the assembly onto the tube lens (COTS-TTL165-A) via the SM2 internal thread of the thread adapter (Supplementary Fig. 28).
138. Use the pitch/yaw (COTS-KAD11F) and xy (COTS-CXY1) mounts of the alignment laser assembly to roughly align through the two irises (COTS-SM1D12D) of the objective port alignment target assembly (3D-SMLM-EMBL-006).
139. Remove the objective port alignment target assembly (3D-SMLM-EMBL-006) and replace it with the objective lens.
 - ▲ **CAUTION** When illuminating the tube lens with the alignment laser, a small and divergent beam will exit the objective lens and even small misalignments may result in a strong deviation from the optical axis and constitute a laser safety hazard accordingly. Wear laser safety eyewear whenever assessing alignment through the objective lens. If the laser is launched substantially off-axis, use the pitch/yaw (COTS-KAD11F) and xy (COTS-CXY1) mounts of the alignment laser assembly to approximately center the output with respect to the objective lens such that the beam emerges approximately on axis.
140. Move the tube lens (COTS-TTL165-A) along the axis of its mount to collimate the beam by minimizing the laser spot size on the ceiling or optical table enclosure.
141. Secure the tube lens in place with the retaining cap (FAB-EMBL-000036).
142. Remove the alignment laser assembly (3D-SMLM-EMBL-002) from the tube lens and the objective lens from the objective port (FAB-EMBL-000043). Reinstall the 2× slotted lens tubes (SM1L30C), 2× irises (COTS-SM1D12D), lens tube (COTS-SM1S10) and thread adapter (COTS-SM1A4) of the alignment laser assembly.
143. Install the four covers (FAB-EMBL-000013/14/15/16) on the body lower standoffs (FAB-EMBL-000002/3/4/5) using 8× M4×6 mm socket head screws. Take care to install the correct cover on each side of the microscope body. The covers on the side of the body where the illumination, emission, and focus lock paths are coupled in/out should have their aperture centers at 110.4, 80 and 48.4 mm from the table surface, respectively.
144. Reinstall the alignment laser assembly (3D-SMLM-EMBL-002) in the objective port (FAB-EMBL-000043) and realign through the two irises.
145. Adjust for minor beam walk-off resulting from installation of the tube lens by using the first steering mirror (COTS-POLARIS-K1/COTS-BB1-E02) of the emission path to align the

- beam to the alignment target (FAB-EMBL-00081) installed in the transmitted path of the image splitter platform (FAB-EMBL-000077).
146. Set up the shear plate (3D-SMLM-EMBL-005) just upstream of the image splitter platform (FAB-EMBL-000077) such that the diverging alignment laser is incident on it.
 147. Introduce and align the first relay lens (COTS-AC254-300-A-ML, COTS-LMR1-M, COTS-PH50E-M, COTS-TRA30-M) to collimate the alignment laser focused by the tube lens using the back reflection method (see Supplementary Information Note 23) with the installed alignment target (FAB-EMBL-000081, COTS-SM1D12D) as the downstream target and an additional target placed upstream of the lens (e.g., 3D-SMLM-EMBL-003, adjusted to the correct beam height). The relay lens has a correct orientation with the infinite conjugate (collimated) side indicated by the arrow on the housing. If the alignment is performed correctly, the associated walk off should be negligible for the two pathways. It will be necessary to move the shear plate (3D-SMLM-EMBL-005) in and out of the beam path to assess collimation and alignment individually.
 148. Remove the shear plate assembly (3D-SMLM-EMBL-005).
 149. To adjust for minor walk-off, use the second steering mirror for the transmitted path (COTS-POLARIS-K1/COTS-BB1-E02) to align the beam to the camera alignment target (FAB-EMBL-000093).
 150. Replace the upper section of the kinematic magnetic mount (COTS-SB1-M) with its dichroic mirror and associated components (COTS-25.5x36x3MM-DICHROIC-SP, COTS-KM200S, FAB-EMBL-000068/69).
 151. Remove the alignment target with iris (FAB-EMBL-000081, COTS-SM1D12D) from the transmitted pathway of the image splitter platform (FAB-EMBL-000077) and reinstall as far downstream as possible in the reflected pathway.
 152. Adjust the alignment of the reflected alignment laser to the alignment target (FAB-EMBL-000081, COTS-SM1D12D) on the image splitter platform (FAB-EMBL-000077) using the steerable kinematic mount for the image splitter dichroic mirror mount (COTS-KM200S) and the second steering mirror (COTS-POLARIS-K1/COTS-BB1-E02) to align the beam to the camera alignment target (FAB-EMBL-000093).
 153. Remove the alignment target with iris (FAB-EMBL-000081, COTS-SM1D12D) from the reflected pathway of the image splitter platform (FAB-EMBL-000077) and reinstall it as far downstream as possible in the transmitted pathway.
 154. Install the second relay lens mounts (FAB-EMBL-000078) in the transmitted and reflected pathways. Loosely secure with the screws just enough that the mount can still be translated along the axis of the dowel pin slot.
 155. Install the second relay lenses (COTS-AC254-200-A) approximately half way down the length of their lens tubes (COTS-SM1M10) using the two retaining rings (COTS-SM1RR) to secure them place.

▲ **CAUTION** The relay lenses have a correct orientation with the finite conjugate side (toward the camera) facing the side of least curvature (flattest). Indicate the orientation on the lens tube with a permanent marker with an arrow pointing away from the side of least curvature (toward the infinite conjugate).
 156. Insert the second relay lenses mounted in lens tubes (COTS-AC254-200-A, COTS-SM1M10) into the second relay lens mounts (FAB-EMBL-000078) in the reflected and transmitted paths with the arrow pointing toward the image splitter dichroic assembly. Secure the lens tubes in an arbitrary longitudinal position by gently closing the split clamp of the respective second relay lens mount.

▲ **CAUTION** Too much pressure could deform the lens tube and the lens contained therein. Tighten just enough to prevent motion of the lens. Ensure that the lens tube is correctly centered in the mount with three points of contact. The assembly should now appear as shown in Supplementary Fig. 29.
 157. Laterally translate the mounted lens in the reflected path to align the beam to the iris of the camera image alignment target (FAB-EMBL-000093/COTS-SM1D12D) and secure in place. Depending on previous alignment steps, some vertical walk-off is possible. This will be corrected when viewing the beam foci on the camera.

158. Repeat the alignment process (Step 157) for the transmitted path lens. Alignment of the transmitted path is more challenging since only a fraction of a percent of the laser power will be transmitted by the long pass image splitter dichroic mirror (COTS-25.5x36x3MM-DICHOIC-SP). Nevertheless, it should be possible to translate and align the lens as above.
▲ CAUTION Do not remove the dichroic to increase the visibility of the alignment laser before attempting alignment since replacement of the dichroic will shift the beam.
159. Remove the camera image alignment target (FAB-EMBL-000093) and release the second relay lens tubes (COTS-SM1L10) by opening the split clamp on the second relay lens mount (FAB-EMBL-000078).
160. Remove the mounted emission tube lens (FAB-EMBL-000035/36, COTS-TTL165-A) from its base adapter as a single piece.
▲ CAUTION Do not remove the base (FAB-EMBL-000034) that is affixed to the microscope body lower plate (FAB-EMBL-000001) nor the tube lens retaining cap (FAB-EMBL-000036) from the tube lens mount (FAB-EMBL-000035). Removing the tube lens assembly correctly will allow it to be replaced later without requiring realignment. The collimated beam from the alignment laser should now be focused by the first relay lens and approximately collimated by the second relay lens of the transmitted path.
161. Set up the shear plate (3D-SMLM-EMBL-005) to assess the beam collimation for the transmitted pathway by placing the assembly downstream of the knife-edge mirror. Slide the lens tube housing of the second relay lens of the reflected path (COTS-AC254-200-A, COTS-SM1L10) to collimate the beam.
◆ TROUBLESHOOTING
162. Repeat the process of collimating the beam using the second relay lens (COTS-AC254-200-A, COTS-SM1L10) for the transmitted path. Note, if the beam is too dim to judge collimation, remove the upper section of the kinematic magnetic mount (COTS-SB1-M) with its dichroic mirror and associated components (COTS-25.5x36x3MM-DICHOIC-SP, COTS-KM200S, FAB-EMBL-000068/69) and replace them once collimation has been achieved.
163. Install the Bertrand lens assembly (COTS-#32-963, COTS-SM1AD20) in its piezo resonant slider (COTS-ELL6).
164. Install the Bertrand lens piezo resonant slider (COTS-ELL6) on the Bertrand lens piezo resonant slider mount (FAB-EMBL-000074) and in turn install that on the camera base plate (FAB-EMBL-000077).
165. Adjust the longitudinal position of the Bertrand lens (COTS-#32-963, COTS-SM1AD20) approximately to the nominal position and lightly secure the lens in place with the locking ring (COTS-SMINT).
166. Switch the Bertrand lens piezo resonant slider (COTS-ELL6) to the open position.
167. Mount the sCMOS camera (COTS-C15440-20UP) to the camera mounting plate (FAB-EMBL-000071) via the camera c-mount fastener (FAB-EMBL-000073).
168. Install the mounted sCMOS camera (COTS-C15440-20UP) onto the camera base plate (FAB-EMBL-000074). The assembly should appear as shown in Supplementary Fig. 30.
169. Rotate the camera such that its upper side faces up by loosening the camera c-mount fastener (FAB-EMBL-000073) and tightening once the desired orientation has been achieved. With the camera base plate (FAB-EMBL-000074) secured to the optical table, the camera can be rotated to a precise orientation using a bubble level (COTS-LVL01) placed on top. The rationale for choosing this orientation is discussed in Supplementary Information Note 26.
170. Remove the alignment laser assembly (3D-SMLM-EMBL-002) from the objective port (FAB-EMBL-000043) and replace it with the infinite conjugate transmission target (3D-SMLM-EMBL-004) using an RMS to SM1 thread adapter (COTS-SM1A4) to couple the lens tube (COTS-SM1S10) to the port (Supplementary Fig. 31).
171. Install the sCMOS camera/Bertrand lens assembly to the nominal position on the image splitter platform (FAB-EMBL-000077) and secure it in place as shown in Supplementary Fig. 32. The camera base plate (FAB-EMBL-000074) should sit flush against one edge of the image splitter platform. Consult the CAD assembly for guidance.

172. Backlight the target with a white light source and image the target on the sCMOS camera, adjusting exposure time appropriately for the supplied light source to not saturate the camera. Note, that the magnification from the target to the camera is 1.1 \times , thus delivering a view of the central $\sim 13.6 \times 13.6$ mm of the target (for the specified Hamamatsu Orca Fusion BT camera).
173. Loosen the screws securing the camera base plate (FAB-EMBL-000074) to the image splitter platform (FAB-EMBL-000077).
174. Observe the target on the camera and focus the camera by translating the camera base plate (FAB-EMBL-000074) against its linear guiding surface of the image splitter platform (FAB-EMBL-000077, see CAD assemblies) such that the target appears maximally in focus. Fine adjustment can be performed by installing a ball-tipped kinematic adjuster (COTS-KL02L) on the image splitter platform as needed. Secure the camera base plate in place once a fine focus has been achieved. The camera is now positioned to sharply focus the infinite conjugate image produced by the objective lens.
175. Install an effective ND 6 filter (e.g., COTS-NE20A-A, COTS-NE40A-A) onto the accessible internal SM1 thread of the first relay lens (COTS-AC254-300-A-ML) to near-fully attenuate the alignment laser beam.
176. Remove the infinite conjugate transmission target (3D-SMLM-EMBL-004) from the objective port (FAB-EMBL-000043) and replace it with the alignment laser assembly (3D-SMLM-EMBL-002).
177. Preview the image from the sCMOS camera (1 ms exposure time) and decrease the total neutral density until the laser spot can be seen on the camera for the reflected path (the transmitted beam will be dimmer).
178. Use the image display and the second steering mirror (COTS-POLARIS-K1, COTS-BB1-E02) of the reflected path to steer the beam center to the x,y pixel positions given in Supplementary Table 11.
179. Appropriately block the reflected path using a laser safety screen (COTS-TPSM1-M).
180. Decrease the neutral density further until the laser spot can be seen on the camera image for the transmitted path.
181. Use the second steering mirror (COTS-POLARIS-K1, COTS-BB1-E02) of the transmitted path to steer the beam center to the x,y pixel positions given in Supplementary Table 11.
182. Remove the alignment laser assembly (3D-SMLM-EMBL-002) from the objective port (FAB-EMBL-000043) and replace it with the objective lens.
183. Install the blocking filters for the excitation and focus lock lasers (2 \times COTS-25MM-HOUSED-FILTER, COTS-SM1L03, 1 \times COTS-LMR1-M, COTS-PH50E-M, COTS-TRA30-M) just downstream of the first relay lens (AC254-300-A-ML), avoiding locations that will block later installation of other components and secure using a pedestal post clamp (COTS-PS-F) as shown in Supplementary Fig. 33. Supplementary Information Note 3.
184. Install all filters in the transmitted and reflected path filter wheels (COTS-FW102C), ensuring that each is installed in the correct positions for the GUI control bindings (or amend these bindings appropriately). Ensure that the filters are correctly oriented when the filter wheels (check with the filter manufacturer for the correct orientation of the arrow/caret relative to the direction of light propagation). Supplementary Information Note 3.
185. Install the filter wheels (COTS-FW102C) in their mounts (FAB-EMBL-000076/000111) and install the mounted filter wheels in position ensuring that the correct wheel is placed in each path. The assembly should now appear as shown in Supplementary Fig. 34.

◆ TROUBLESHOOTING

Basic epi-illumination alignment

● TIMING 6 d

▲ **CRITICAL** To aid initial focusing and quality control of the microscope in the following section, the illumination path is set up first for simple basic epi-illumination without the additional advanced features of homogenization/TIRF/HILO/variable field size that will follow.

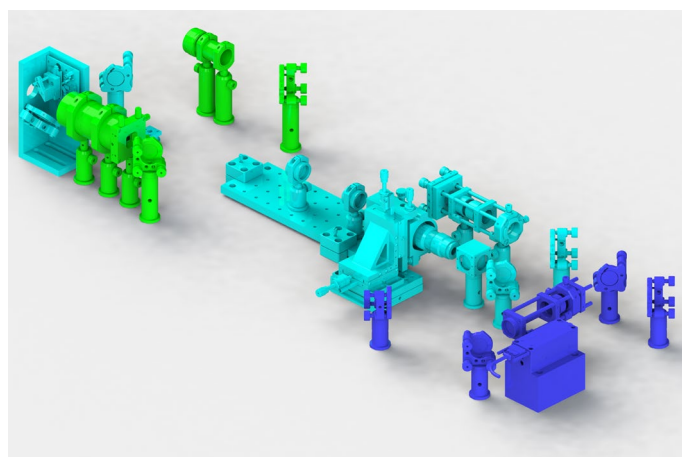


Fig. 6 | The fully assembled illumination paths showing the different optional modules. Cyan: single-mode laser engine path. Blue: single-mode booster laser path. Green: multimode laser engine path. The modules are compatible with each other allowing for the expanded set of capabilities offered by each and allowing for easy expansion of the system as desired.

Nevertheless, it is necessary to consider some aspects of these features en route. For example, to ensure proper operation of the refractive beam shaper, the beam(s) from the single-mode sources need to be carefully expanded to a diameter of 6 mm and subsequently routed through the illumination path to the objective port using various alignment targets. The illumination tube lens is subsequently aligned to the illumination path optical axis and focused to achieve a collimated output from the objective lens. A CAD rendering of the fully assembled illumination path including optional components (e.g., booster laser, multimode laser path and associated parts) and those that will be installed in later sections is shown in Fig. 6.

186. Pre-adjust all three actuator steering mirror mounts (COTS-POLARIS-K1, COTS-POLARIS-K1E3) for the illumination path to nominal spacing using a 1/8" post height spacer (3D-SMLM-PS-0.125).
187. Build up the single-mode beam launch assembly (3D-SMLM-EMBL-001-003-001) for the single-mode laser engine omitting the two collimating lenses (COTS-AC254-075-A-ML) as shown in Supplementary Fig. 35. Secure the assembly on the optical table using 2× pedestal post clamps (COTS-PS-F).
188. Place the single-mode laser engine (COTS-ICHROME-MLE) on its heat dissipating plate at a suitable location and avoid moving it from this position for the remainder of the protocol. Ensure that the single-mode fiber is long enough to reach the FC/APC fiber terminator (COTS-S1FCA) of the single-mode beam launch without tension or tight turns (radius of curvature > 10 cm). Plug the fiber into the fiber in port on the laser engine.
189. Optimize the alignment of the single-mode lasers into the fiber using the COOL^{AC} auto-calibration function of the TOPAS iChrome software.
190. Install the fiber in the FC/APC fiber terminator (COTS-S1FCA) of the single-mode beam launch assembly, ensuring the key is properly aligned to the slotted recess. Adjust the fiber kinematic mount (COTS-KC1-T-M) to center the diverging beam through the cage system using drop-in cage alignment targets (COTS-CPA1). Use bronze locking nuts (COTS-LN2580) to lock the actuator positions.
191. Install the collimating lenses (COTS-AC254-075-A-ML) with correct orientation but arbitrary spacing. Set up the shear plate assembly (3D-SMLM-EMBL-005) downstream of the beam launch and move the two collimating lenses to collimate the 561 nm beam to an arbitrary diameter. Note, if the laser engine was configured with alternative laser lines, select a line that is centered in the wavelength range.
192. (Optional) If the specified configuration uses an additional booster laser, it is necessary to fix the polarization orientation out of the fiber at this stage. Install the mounted polarization beam splitter (COTS-PBS251, COTS-CCM1-4ER-M, COTS-RS10M, COTS-RS2P4M) after the collimator such that the input (mixed polarization) side is placed where the laser is incident and the horizontal polarization side is opposite to it. Loosen

- the retaining ring (COTS-SMIRR) securing the FC/APC fiber terminator (COTS-SIFCA). Using a piece of paper to view the beam, rotate the fiber terminator to minimize the power reflected by the polarization beam splitter. Secure the retaining ring.
193. (Optional) Install the booster laser (3D-SMLM-COTS-IBEAM-SMART) on its mount (3D-SMLM-FAB-EMBL-000087) and position the assembly on the optical table to direct the laser into the polarization beam splitter on the intended side of incidence.
- ▲ **CAUTION** The beam path is not well defined at this time. Take extra care to intercept stray beams using a laser safety screen (COTS-TPSM1-M).
194. (Optional) Check that the booster laser is efficiently reflected down the illumination path by the polarization beam splitter. If the beam is primarily transmitted by the beam splitter then the orientation is not correct. Orient the polarization beam splitter (COTS-PBS251) appropriately in its mount (COTS-CCM1-4ER-M) to efficiently reflect the booster laser and repeat the procedure with the rotation of the FC/APC fiber terminator (COTS-SIFCA) to transmit the single-mode laser engine fiber output.
195. Check the collimated beam diameter on the camera beam profiler (COTS-LASERCAM-HR11). Adjust the spacing between the two collimating lenses (COTS-AC254-075-A-ML) to change the effective combined focal length (decreasing the spacing between the lenses will result in a longer focal length and thus a larger collimated beam diameter) and adjust the divergence/convergence by translating the lenses as a pair to produce a collimated $\varnothing 6 \pm 0.05$ mm ($1/e^2$ criterion) beam. Switch between the beam profiler and shear plate as necessary to judge beam diameter and collimation respectively.
196. Install an iris (COTS-SM1D12D) in the xy mount (COTS-CXY1) of the single-mode beam launch and stop it down to a 1–2 mm aperture diameter. Use the camera beam profiler to center the iris on the collimated beam such that the diffraction pattern has maximum radial symmetry. When performing alignment operations (aligning the beam to the optical axis of a lens), where a smaller beam is optimal, leave the iris stopped down. When assessing collimation (aligning a lens longitudinally to achieve a minimally divergent output), where a larger beam is optimal, open the iris fully. Similarly for assessment of the beam profile or for imaging, the iris should be fully open.
197. Install the objective port alignment target assembly (3D-SMLM-EMBL-006) in the objective port (FAB-EMBL-000043) with the beam profiling camera installed on the distal end (Supplementary Fig. 36). For the following alignment steps, use the camera image to center the beam on the irises.
198. Install the pair of steering mirrors (COTS-BB1-E02, COTS-POLARIS-K1, COTS-RS5M, COTS-RS2P4M) downstream of the single-mode beam launch using 2× pedestal post clamps (COTS-PS-F) as shown in Supplementary Fig. 37. Check that the beam is well centered on the mirror faces and that the second mirror is positioned with its face centered with respect to the respective line of tapped holes on the optical table surface.
199. Use a pair of 80.4 mm beam height alignment targets (3D-SMLM-EMBL-003) to ensure that the beam travels at the correct height and approximately along the respective hole pattern of the optical table.
200. (Optional) Install the polarization beam splitter assembly (COTS-PBS251, COTS-CCM1-4ER-M, COTS-RS10M, COTS-RS2P4M).
- ▲ **CAUTION** Ensure that the polarization beam splitter is oriented to correctly pass the single-mode laser engine and reflect the booster laser given its polarization and intended direction of incidence.
201. Assemble the illumination periscope and inclination control assembly (3D-SMLM-EMBL-001-003-007, Supplementary Fig. 38).
- ▲ **CAUTION** Ensure that the M6×30 mm dowel pin (3D-SMLM-COTS-91585A668) is installed to limit the stage motion. This pin provides a safety feature which, when the system is correctly aligned, prevents the illumination lasers from being inadvertently launched obliquely away from the short optical table edge closest to the microscope body. Nevertheless, follow all laser safety guidelines noted in ‘Laboratory environment’. If the illumination control prism mirror mount (FAB-EMBL-000086) contacts the pin, it may be necessary to rehome the stage (COTS-ELL17-M) using its software (Thorlabs ELLO).

202. Move the inclination control stage (COTS-ELL17-M) to the position that it just contacts the pin and record this position. Rehome the stage and move the stage to the recorded position minus 0.75 mm. This defines the nominal position required for noninclined epi-illumination. Store and save this value in the EMU configuration for two-state device 2, 3 and 6 off values such that turning off the HILO/TIRF/Multimode controls switches the microscope to the default case of epi-illumination.
203. Introduce and align the third steering mirror of the single-mode laser engine illumination path (COTS-BB1-E02, COTS-POLARIS-K1, COTS-RSSM, COTS-RS2P4M, Supplementary Fig. 39), ensuring that the laser is centered on the mirror and that the beam is reflected parallel to the hole pattern on the optical table. Use a pair of 80.4 mm beam height alignment targets (3D-SMLM-EMBL-003) aligned to the hole pattern to ensure that the beam travels at the correct height and along the table holes. Position the mirror laterally along the incoming beam direction to align to the first target and angle the mirror to align to the second target in an iterative manner. Secure the mirror in position using a pedestal post clamp (COTS-PS-F) once the beam is aligned to the two targets.
▲ CAUTION If the beam is tilted with regard to the table hole pattern, correct alignment through the subsequent mirrors will be compromised.
204. Introduce the illumination periscope and inclination control assembly (3D-SMLM-EMBL-001-003-007) in position on the optical table and lightly secure with screws through the slotted counterbores. Install an iris (COTS-SM1D12D) into the entrance aperture in the entrance plate of the assembly (FAB-EMBL-000084) and position the assembly such that the beam passes the iris and is incident close to the center of the subsequent mirror (COTS-POLARIS-K1E3, COTS-BB1-E02).
▲ CAUTION Try to position the illumination periscope and inclination control assembly such that its faces are aligned to the hole pattern on the optical table. Adding additional screws through the counterbores may assist in maintaining reasonable alignment.
205. The beam should now pass into the illumination periscope and inclination control assembly (3D-SMLM-EMBL-001-003-007) and reflect off the upper prism mirror (COTS-MRA20-E02) and into the microscope body.
206. Use the lower steering mirror (COTS-POLARIS-K1E3, COTS-BB1-E02) to align the beam to the second target of the objective port alignment target (3D-SMLM-EMBL-006). The beam should approximately pass the first target in the left/right direction (with respect to the microscope body). To correct for any left/right misalignment, adjust the position of the beam on the first target by using an equal rotation of all three adjusters of the lower steering mirror to translate the mirror face forward or backward as necessary and use the topmost adjuster alone to then realign to the second target.
207. For back/front alignment (with respect to the microscope body) adjust to the first iris by adjusting the position of the inclination control stage (COTS-ELL17-M) and correct at the second iris using the bottom/left adjuster screw of the illumination periscope and inclination control assembly steering mirror (COTS-POLARIS-K1E3, COTS-BB1-E02). If it is necessary to move the stage for alignment, ensure that the beam remains well centered on the prism mirror (COTS-MRA20-E02) face (± 3 mm) and use the final stage position as the new nominal position for non-inclined epi-illumination. Store and save this value in the EMU configuration for two-state device 2, 3 and 6 off values.
208. Remove the beam profiling camera from the objective port alignment target (3D-SMLM-EMBL-006). The laser should now be incident on the ceiling or optical table enclosure above the microscope. Mark the position of the beam using a suitable marker. This reference is useful for realignment of the illumination to the objective during routine maintenance. Replace the beam profiling camera when finished.
209. Install the illumination tube lens (COTS-AC254-400-A) approximately half way down the length of its lens tube (COTS-SM1M10) using the two retaining rings (COTS-SM1RR) to secure it in place.
▲ CAUTION The tube lens has a correct orientation with the finite conjugate side (closest to the objective lens port) facing the side of least curvature. Indicate the orientation on

the lens tube with a permanent marker with an arrow pointing away from the side of least curvature (toward the infinite conjugate).

210. Assemble the illumination tube lens (COTS-AC245-400-A) on its pedestal post (COTS-PH40E-M, COTS-TRA30-M) with the lens tube split clamp (COTS-SM1RC-M) securing the lens tube (COTS-SM1M10). Introduce the tube lens to the beam path with the arrow pointing upstream as shown in Supplementary Fig. 40.
211. Use the back reflection method to align the illumination tube lens in its nominal longitudinal position, placing one 80.4 mm beam height alignment target (3D-SMLM-EMBL-003) upstream of the lens and using one iris of the objective port alignment target (3D-SMLM-EMBL-006). Secure the illumination tube lens assembly in position with a pedestal post clamp (COTS-PS-F).
212. Remove the objective port alignment target (3D-SMLM-EMBL-006) from the objective port (FAB-EMBL-000043) and replace it with the objective lens.
▲ CAUTION A small and divergent beam will exit the objective lens and even small misalignments may result in a strong deviation from the optical axis and constitute a laser safety hazard accordingly. Wear laser safety eyewear whenever assessing alignment through the objective lens. If the laser is launched substantially off-axis, such that it is no longer incident within ± 10 mm of the mark made in Step 208 adjust the steering mirror of the illumination periscope and inclination control assembly (COTS-POLARIS-K1E3), to recenter the beam with respect to the objective lens such that the beam is well centered on the mark.
213. Loosen the split clamp (COTS-SM1RC-M) just enough to allow motion of the tube lens in its lens tube (COTS-AC254-400-A, COTS-SM1M10). Slide the lens tube to collimate the beam by minimizing the laser spot size as viewed on the ceiling or optical table enclosure. Repeat the previous step as necessary to ensure that the beam remains incident within ± 10 mm of the mark.

◆ TROUBLESHOOTING

214. The microscope is now set up for epi-fluorescence imaging with a Gaussian illumination field.

Focusing the microscope

● TIMING 1 d

▲ CRITICAL The emission path has been set up to image an object at infinity and basic epi-illumination established thus allowing the microscope to be focused to image the native focal plane of the infinity-corrected objective in fluorescence mode. A fluorescent bead sample is used to mechanically position the objective lens to a coarse focus before focusing more finely with the objective piezo flexure stage. Note that, owing to the image-splitter geometry, the two image channels are mirrored relative to each other. Next, the bead sample is used to focus the Bertrand lens and to provide an initial adjustment of the objective correction collar (if present), to check the PSF shape more generally, and to check that all color channels appear similarly focused on the camera without the need for channel-specific refocusing.

215. Place a drop of immersion oil onto the objective after checking the applicator nozzle for clearly visible bubbles. Blot away oil from the nozzle as necessary with tissue to remove bubbles. Repeat this process whenever mounting a sample on the microscope.
216. Mount a fluorescent bead sample on the microscope. Refer to Supplementary Information Note 18 for a detailed description of the sample preparation. Note, when mounting samples on the microscope, use $4 \times M2 \times 6$ mm socket head screws to secure the sample holder FAB-EMBL-000045 in position. Failing to do so can result in greater drift, errors in repositioning and small variations in focus height between a secured and unsecured holder.
217. Move the objective piezo flexure stage (COTS-P-726.1CD) to the middle of its travel range (50 μ m).
218. Select an appropriate combination of laser line and emission filter in the reflected/transmitted path filter wheels. If the shared path filter wheel has been installed, switch it to an open position. Illuminate and image the fluorescent bead sample.

219. Focus the image of the fluorescent beads on the camera using the mechanically translatable objective piezo platform (e.g., rotating the timing pulley (COTS-HTPT48S2M060_A_P6_35). Start in a downward direction (rotating anti-clockwise as viewed from above) and if the focus is not found, move upward carefully to not break the coverslip and/or damage the objective lens.

◆ **TROUBLESHOOTING**

220. Once an approximate focus has been achieved, focus more finely using the objective piezo. If the piezo position at focus is within the last 20 μm travel range from either limit, mechanically refocus to better center the focus height with regard to the objective piezo travel range.
221. Ensure the beads are sharply in focus and switch the Bertrand lens into the emission path. Installed in its nominal position, the Bertrand lens should produce an approximately focused image of the objective back focal plane on the camera (potentially on both sides of the camera chip depending on the emission filters used. Note that when using the Bertrand lens, the channels will be flipped left to right on the camera chip).
222. Translate the Bertrand lens in its piezo resonant slider (COTS-ELL6) using the threaded mount (COTS-SM1AD20) such that the periphery of the back focal plane image appears maximally sharp. Lock the lock ring (COTS-SM1NT) to secure the position of the lens. If bubbles are present in the oil, dark occlusions may also be present on the back focal plane image (for back focal plane images with and without bubbles, see Supplementary Fig. 41). If this is the case, clean the objective and remove/replace oil. Continue with the protocol only when no bubbles are present. Repeat this step whenever mounting samples on the microscope, when moving between positions of the sample and when observing any unusual lateral asymmetry in the PSF.
223. Switch the Bertrand lens out of the emission path.
224. Observe the general PSF shape when focusing through the beads above and below the focal plane. Adjust the correction collar of the objective lens (if present) to achieve the best possible symmetry above and below the focus by visual inspection. Note, adjusting the correction collar will introduce defocus, which should be corrected by focusing as usual. When the collar is incorrectly positioned, on one side of the focus, the PSF will appear as a set of concentric rings, while on the other, the PSF will quickly fade into the background signal. Rotating the collar allows the ring/fade sides to be switched from above to below the focus and vice versa. The ideal position for the collar is the transition between rings above and below focus where spherical aberrations are minimized.
225. Acquire a z-stack of the fluorescent bead sample (over a range of $\pm 1 \mu\text{m}$, 0.05 μm spacing) using the $\mu\text{Manager}$ multidimensional acquisition wizard.
226. Use ImageJ to load the image stack, set the voxel dimensions in (Image/Properties, 0.105, 0.105, 0.05 μm , height, width, depth). Reslice the stack (Image/Stacks/Reslice) with start at 'Top' selected and no other boxes checked. Make a maximum intensity projection of the resliced stack (Image/Stacks/Z Project) to view a projection of the beads as seen from the side. Check the PSF symmetry in z (now the vertical direction in the resulting image). Adjust the correction collar and repeat this process as appropriate. The correction collar position should be in the range 0.165–0.175 mm.

◆ **TROUBLESHOOTING**

227. Switch to other appropriate combinations of laser line and emission filter in the reflected/transmitted path filter wheels. Check that the beads are focused at the same axial position for all emission bands to within $\pm 100 \text{ nm}$.

◆ **TROUBLESHOOTING**

228. Remove the objective lens from the objective port (FAB-EMBL-000043).

Field-variable and homogeneous epi-illumination alignment

● **TIMING 7 d**

▲ **CRITICAL** The basic epi-illumination system established in previous steps provides the basis for the addition of field-variable and illumination homogenizing modules. Several exchangeable Keplerian telescopes are aligned to the single-mode laser path to allow the user to quickly

optimize the illumination field size for a given application. Each telescope has an equal 4f track length ensuring that various conjugates are maintained through the optical path upon exchange. An iris is installed upstream of the telescopes, providing a field aperture to allow cleanup/cropping of the illumination field independent of the telescopic magnification. Note that builders wishing to omit the exchangeable telescope system can do so either by choosing one telescope to set a fixed non-unit magnification or omitting the relay entirely and positioning the iris at the conjugate image plane one focal length upstream of the illumination tube lens. In this case, some modification of the protocol steps and parts used will be necessary. Subsequently, a refractive beam shaper is introduced to flatten the Gaussian output. It should be noted that while the beam shaper is achromatic in design, unavoidable small spectral variations ($\pm 10\%$) in the beam diameters from the single-mode laser engine, results in a homogenization efficiency that scales accordingly. Nevertheless, when correctly adjusted, the beam homogeneity for all wavelengths is better than the case of a Gaussian beam truncated at 80% peak intensity and achieves $\sim 10\times$ greater power throughput/efficiency. Subsequent alignment of the beam shaper requires careful pitch/yaw and lateral alignment to produce a homogenized output and the use of the beam profiling camera to assess the homogeneity of the output.

229. Install the shear plate assembly (3D-SMLM-EMBL-005) at the objective port (FAB-EMBL-000043) using an RMS to SMI thread adapter (COTS-SM1A4) and lens tube (COTS-SM1S10)
230. Install the kinematic magnetic bases (COTS-AKP-BF, COTS-AKP-BC, COTS-AKP-BV) with the telescopic relay breadboard (COTS-M-SA2-04 \times 12, 3 \times COTS-AKP-TF) in the nominal position on the optical table (Supplementary Fig. 42).
231. Leaving the kinematic magnetic bases (COTS-AKP-BF, COTS-AKP-BC, COTS-AKP-BV) in place, assemble additional breadboards (COTS-M-SA2-04 \times 12, 3 \times COTS-AKP-TF) to mate with the kinematic magnetic bases for each additional magnifying telescope (as specified by the builder).
232. For the 0.5, 1 and 2 \times telescopic relays, install all lenses (2 \times COTS-AC254-040-A, 2 \times COTS-AC254-060-A, 2 \times COTS-AC254-080-A) approximately halfway down the length of their lens tubes (COTS-SM1M10) using two retaining rings (COTS-SM1RR) to secure them in place. For each lens tube, use a permanent marker to add an arrow pointing toward the most curved side of the lens and the effective focal length.
233. For the 2.85 \times telescopic relay, install the lenses COTS-AC254-075-A and COTS-AC254-050-A into one lens tube (COTS-SM1M10) with the flatter surface of COTS-AC254-075-A in contact with the more curved surface of COTS-AC254-050-A. Take extra care when placing lenses in contact, first use clean compressed air (COTS-LAB16/LAB16-EU) to ensure neither contact surface nor the lens tube have any debris that may cause scratches. Use two retaining rings (COTS-SM1RR) to hold the first lens in place and install the second lens by installing it from below the lens tube with its retaining ring (COTS-SM1RR) using an SMI spanner wrench (COTS-SPW602) to thread the retaining ring carefully into the lens tube, stopping when there is resistance signifying contact of the two lenses. Use a permanent marker to add an arrow pointing toward the more curved side of the COTS-AC254-075-A lens and the effective focal length (31.2 mm for the combined lens pair). Install the lens COTS-#49-769 into a lens tube, secure it in position and mark it as described in the previous step.
234. Assemble all lens tube mounted lenses with their split clamp/pedestal post assembly (COTS-SMIRC-M, COTS-PH30E-M, COTS-TRA20-M) and secure the split clamp with the lens tube centered.
235. For the 1 \times magnification (2 \times COTS-AC254-060-A) telescopic relay, introduce the downstream lens assembly on the breadboard (COTS-M-SA2-04 \times 12) with the arrow pointing downstream and position to approximately align and collimate the beam as viewed on the shear plate. Mark the nominal longitudinal position (i.e., along the beam axis) of the pedestal post base (e.g., with colored tape).
236. Remove the shear plate assembly (3D-SMLM-EMBL-005) from the objective port (FAB-EMBL-000043) and replace it with the objective port alignment target (3D-SMLM-EMBL-006) with the beam profiling camera installed.

237. Use the back reflection method to align the lens (AC254-060-A) approximately in the longitudinal position marked, placing one 80.4 mm beam height alignment target (3D-SMLM-EMBL-003) upstream of the lens and a second placed downstream, close to the illumination tube lens (COTS-AC254-400-A). Check alignment through one iris of the objective port alignment target (3D-SMLM-EMBL-006). If the alignment has been performed correctly the beam should pass this iris on its axis to within ± 0.25 mm. Secure the pedestal post (COTS-PH30E-M) in position with a pedestal post clamp (COTS-PS-F).
238. Remove the objective port alignment target (3D-SMLM-EMBL-006) from the objective port (FAB-EMBL-000043) and replace it with the shear plate assembly (3D-SMLM-EMBL-005).
239. Loosen the split clamp (COTS-SMIRC-M) securing the lens tube (COTS-SMIM10). Translate the lens tube to achieve collimation. Secure the split clamp. Note, minimize rotation of the lens during translation to minimize beam walk-off.
240. Remove the shear plate assembly (3D-SMLM-EMBL-005) from the objective port (FAB-EMBL-000043) and replace it with the objective port alignment target (3D-SMLM-EMBL-006) with the beam profiling camera installed.
241. Install the shear plate assembly (3D-SMLM-EMBL-005) downstream of the breadboard (COTS-M-SA2-04 \times 12).
242. For the 1 \times magnification (2 \times COTS-AC254-060-A) telescopic relay, introduce the upstream lens assembly on the breadboard (COTS-M-SA2-04 \times 12) with the arrow pointing upstream and position to approximately align and collimate the beam as viewed on the shear plate. Mark the nominal longitudinal position of the pedestal post base as previous.
243. Move the shear plate assembly out of the beam path (3D-SMLM-EMBL-005).
244. Use the back reflection method to align the lens (COTS-AC254-060-A) approximately in the longitudinal position marked, placing one 80.4 mm beam height alignment target (3D-SMLM-EMBL-003) upstream of the lens and a second placed downstream, close to the lens installed previously on the breadboard (COTS-AC254-060-A). Check alignment through one iris of the objective port alignment target (3D-SMLM-EMBL-006). If the alignment has been performed correctly the beam should pass this iris on its axis to within ± 0.25 mm. Note that the beam will be divergent after passing the illumination tube lens (AC254-400-A). Secure the pedestal post (COTS-PH30E-M) in position with a pedestal post clamp (COTS-PS-F).
245. Return the shear plate assembly to the beam path (3D-SMLM-EMBL-005).
246. Loosen the split clamp (COTS-SMIRC-M) securing the lens tube (COTS-SMIM10). Translate the lens tube to achieve collimation. Secure the split clamp.
247. The 1 \times telescope is now aligned (Supplementary Fig. 43) and the lenses positioned to conjugate the front focal plane of the upstream lens with the sample plane. Repeat this process for each telescopic relay breadboard (COTS-M-SA2-04 \times 12, 3 \times COTS-AKP-TF, for a list of lens part numbers see Supplementary Table 12, which differ between telescopic relays), as above.
▲ CAUTION These alignment steps must be carried out with precision, otherwise the exchange of the platforms will result in differential misalignments of the illumination path.
248. Switch to the 1 \times telescope.
249. Assemble the beam shaper assembly (3D-SMLM-EMBL-001-003-005: FAB-EMBL-000082, COTS-KBM1-M, COTS-ULM-TILT, COTS-M-462-XZ-M, COTS-AJS100) but omit the beam shaper (COTS-PISHAPER-6_6_VIS) itself. Adjust the pitch/yaw (COTS-ULM-TILT) and xz stages (COTS-M-462-XZ-M) to neutral positions.
250. Install the beam shaper assembly on its base (COTS-KBM1-M). The assembly should appear as shown in Supplementary Fig. 44.
251. Position the beam shaper base (COTS-KBM1-M) on the optical table such that the iris (COTS-SMID12D) is positioned approximately 60 mm upstream of the upstream lens of the 1 \times telescope (COTS-AC254-060-A) and aligned to the beam (Supplementary Fig. 45).
252. Remove the objective port alignment target (3D-SMLM-EMBL-006) from the objective port (FAB-EMBL-000043) and install the objective lens in its place.
253. Mount and image a fluorescent dye sandwich sample. Refer to Supplementary Information Note 18 for a detailed description of the sample preparation. Focus on the upper side of the

- lower coverslip in brightfield mode by illuminating with the ring LED (FAB-EMBL-000037) and imaging with all filter wheels/sliders switched to an open position. It should be possible to focus on some particulate matter on the coverslip surface.
254. Image the dye sandwich in fluorescence mode. Stop down the iris (COTS-SM1D12D) to observe the effect of the blades cropping the illuminated field of view on the camera image.
 255. Longitudinally position the beam shaper mount base (COTS-KBM1-M) on the optical table such that the cropped edges of the illumination field are maximally sharp in the image while maintaining approximate alignment of the iris to the laser source.
 256. Center the iris (COTS-SM1D12D) on the beam by inspecting the image and translating the beam shaper mount (FAB-EMBL-000082) with the *xz* stage (COTS-M-462-XZ-M).
 257. Install the beam shaper (COTS-PISHAPER-6_6_VIS) in its mount (FAB-EMBL-000082) as shown in Supplementary Fig. 46.
▲ CAUTION The beam shaper has the same M27×1.0 thread at its entrance and exit apertures. Ensure that the beam shaper is threaded into the mount in the correct orientation as shown in the CAD assembly (the graduated tick marks on the housing should be outside of the pitch/yaw (COTS-ULM-TILT) stage when the beam shaper is installed in the correct orientation).
 258. Remove the 1× telescope and install the beam profiling camera to profile the beam output close to the beam shaper exit aperture.
 259. Ensure that any irises cropping the beam are fully open and observe the 561 nm beam profile. It is likely that the beam shaper is not well aligned to the beam resulting in a highly nonuniform intensity. The four alignment adjusters of the pitch/yaw (COTS-ULM-TILT) and *xz* stages (COTS-M-462-XZ-M) should be used as two pairs (yaw/*x*) and pitch/*z*) to achieve an even illumination spot. Typically, an edge or ring of slightly higher intensity may be present toward the periphery of the spot. Iteratively, use the angular adjustment to evenly distribute the brighter region up/down and left/right and the translation to provide an even intensity across the spot. The degree of homogeneity is highly dependent on the beam quality and some small variation across the field is to be expected.
 260. Remove the camera beam profiler and replace it with the shear plate (3D-SMLM-EMBL-005). Adjust the longitudinal spacing of the beam shaper elements by releasing the locking ring and screwing the two sections in/out before relocking to provide optimum collimation of the output beam. Check and adjust the alignment as above.
 261. Remove the upper plate of the beam shaper mount base (COTS-KBM1-M) with all affixed components.
 262. To aid periodic realignment of the single-mode excitation path, install two 80.4 mm beam height kinematic magnetic alignment targets (3D-SMLM-EMBL-008) as indicated in Supplementary Fig. 47 (precise longitudinal placement is not critical) and align them to the laser. Secure the targets in place using pedestal post clamps (COTS-PS-F).
 263. Remove the top plate of the magnetic mount (COTS-KB25M) with the upper section of each target. Use a permanent marker to indicate on each which is the upstream/downstream target for future use.
 264. Fully open any irises present in the illumination path.
 265. Reinstall the 1× telescope and upper plate of the beam shaper mount base (COTS-KBM1-M) with all affixed components.
 266. Install the illumination laser cleanup filter in a lens tube (COTS-SM1L03) with the intended propagation of light moving from the external to internal threaded sections. Supplementary Information Note 3. Install the lens tube into the iris (COTS-SM1D12D) of the beam shaper assembly (3D-SMLM-EMBL-001-003-005) as shown in Supplementary Fig. 48.
 267. Image the fluorescent dye sandwich sample and check that the specified change in the illumination field diameter is visible when switching between telescopes without repositioning the field of view on the camera (within an allowable error of $\pm 2\ \mu\text{m}$, ± 20 pixels) relative to the position of the illumination field without any telescope installed or a consensus position shared by two or more telescopes. Note that without a telescope installed, the beam profile at the object will not be homogeneous but it should still be

possible to determine its center. If any of the telescopes result in a center position that does not meet this criterion, return to Step 241 to realign them to the beam.

268. Check the homogeneity of the illumination spots at all wavelengths. Since the input beam diameter and divergence will vary with wavelength, the degree of homogenization will also vary accordingly. For representative beam profiles, see Supplementary Fig. 49.
269. Partially close the iris (COTS-SM1D12D) mounted to the beam shaper mount (COTS-EMBL-000082) to sharply apodize the illumination spot at its periphery such that no dimly illuminated beads are visible. Lock the iris position.

(Optional) Setting up additional laser sources and configuring HILO/TIRF illumination

● TIMING 1–7 d

▲ **CRITICAL** With the beam homogenization and variable field illumination established, the additional booster laser can be added (Supplementary Protocol 3) and the combined single-mode sources can be setup for HILO/TIRF illumination (Supplementary Protocol 4). Alternatively, or additionally, the low-cost multimode laser engine can be introduced and aligned (Supplementary Protocol 5).

Calibration of the laser power monitoring photodiode

● TIMING 2 d

▲ **CRITICAL** Having an active readout of the laser power is recommended and helpful for two primary reasons. Firstly, to monitor the proper functioning and internal alignment of the illumination lasers. For example, the Toptica iChrome MLE laser engine included as part of the single-mode illumination system features an automated scheme for internal realignment, which can boost the output power greatly depending on the degree of misalignment. Secondly, for reproducible blinking kinetics, it is helpful to be able to achieve a defined intensity (typically stated in kW/cm^2), which can be calculated for a known transmission through the objective lens and measured illumination field size. The photodiode was installed previously but with all lasers in place it is necessary to calibrate the photocurrent generated versus laser power.

270. Remove the objective lens from the objective port (FAB-EMBL-000043) and replace it with the photodiode sensor (COTS-S121C) of the laser power meter (COTS-PM100D) coupled to the port with a thread adapter (COTS-SM1A4).
271. Illuminate with each laser line in turn at full power. In the case of a single-mode booster laser, consider the combined output of it and the corresponding line of the single-mode laser engine. Since multimode and single-mode illumination is not used in tandem, do not add sources together and rather consider them separately. Check the voltage for each line on the AnalogInput3 channel in $\mu\text{Manager}$. The microFPGA will convert the voltage to an unsigned 16-bit value (0–65,535). Check that the voltage does not saturate, if it does for any line, decrease the resistance of R2_G on the microFPGA (Supplementary Protocol 1) and continue decreasing until the voltage does not saturate. Determine which laser line gives the strongest response on AnalogInput3 at full power (this will be influenced by leakage through the illumination dichroic, the responsivity of the laser power monitoring photodiode (COTS-SM1PD1A) and the laser power available).
272. For each laser line in turn, step through laser power in small steps (1–10 % of the total) starting from 0% and check that the photocurrent scales accordingly (i.e., any step of equal size should elicit the same photocurrent response regardless of the total laser power). If the photocurrent response decreases at higher laser power, the photodiode current is saturating, in which case it is necessary to install an appropriate neutral density filter between the illumination dichroic mount and photodiode to attenuate the laser. If the steps do not elicit a noticeable change in photocurrent, increase the resistance of R2_G on the microFPGA (Supplementary Protocol 1) and continue increasing until the steps are measurable above the noise level, even for the laser line delivering the weakest response on AnalogInput3. Given the possible choices of illumination dichroic mirror and laser illumination options, it is not possible to provide a generic option that will suit all cases. Moreover, it may not be possible

to find a combination of load resistance and blocking neutral density that will work for all laser lines. In such cases, it is acceptable to calibrate different laser lines under different load resistances and with different blocking neutral densities. Simply ensure that this is noted for users of the microscope.

273. For each laser line, vary the laser power stepwise between the minimum and maximum in ten steps, recording the AnalogInput3 channel and the reading on the laser power meter (COTS-PM100D).

▲ **CAUTION** Ensure that the laser power meter is configured for the calibrated laser wavelength each time and that the laser power is allowed to stabilize after step increases/decreases.

274. For each laser line, plot the 16-bit value from the AnalogInput3 channel (x) against the reading on the laser power meter (y) to determine the offset and gradient from a linear fit (Supplementary Fig. 50). Input the offsets and gradients as comma separated values in 'Powermeter – offsets' and 'Powermeter – slopes' respectively in the EMU properties in μ Manager. The four values correspond to lasers 0, 1, 2, 3, respectively.

2D imaging quality checks and pixel size calibration

● TIMING 1 d

▲ **CRITICAL** Having set up the microscope with functional emission and illumination paths, it is necessary to perform various checks and calibrations. The $2\times$ or $2.85\times$ telescopic relay is typically used to produce the largest possible field of view and thus the most thorough test of image quality. Furthermore, since the potential for crosstalk between the two channels is greatest, the large field of view provides the limiting case for setting of slits to restrict the spatial extent of the illumination source and resulting images. The image quality and slit positioning is assessed using a fluorescent bead sample, which also provides the basis for calibrating the effective pixel size of the camera.

275. Switch to the highest magnification telescope available (typically $2\times$ or $2.85\times$ depending on the system configuration).
276. Mount and image a fluorescent bead sample. Refer to 'Fluorescent bead samples' in the Supplementary Information Note 18 for a detailed description of the sample preparation and 'Focusing the microscope' for a description of setting up the microscope to image fluorescent beads. Ensure that the bead sample is immersed in water.
277. Introduce the emission path slit (COTS-SP60, COTS-RS2P4M, COTS-KB25-M, COTS-RS05P4M) in its nominal position and position it such that the image truncation arising from the slit blades appear in sharp focus in the image. Secure the slit in place using a pedestal post clamp (COTS-PS-F). The assembly should appear as shown Supplementary Fig. 58.
278. Close the slit blades from the left and right and check for the sharpness on both sides of the image to ensure that the slit is oriented perpendicular to the emission path optical axis. Adjust alignment as necessary and fully open the slit blades.
279. View the fluorescent bead sample in both channels, adjusting contrast as necessary. Close the slit with the left/right blade such that the image is truncated from the center of the camera outward in both directions (since the channels are mirror images). Close the slit only minimally until there is no crosstalk/spatial overlap between the two channels.
280. Acquire a z-stack of the fluorescent bead sample (over a range of $\pm 1\ \mu\text{m}$, $0.05\ \mu\text{m}$ spacing) using the μ Manager multidimensional acquisition wizard.
281. Use ImageJ to load the image stack, set the voxel dimensions in (Image/Properties, 0.105, 0.105, $0.05\ \mu\text{m}$, height, width, depth). Reslice the stack (Image/Stacks/Reslice) with start at Top selected and no other boxes checked. Make a maximum intensity projection of the resliced stack (Image/Stacks/Z Project) to view a projection of the beads as seen from the side. Check the PSF symmetry in z (now the vertical direction in the resulting image). Adjust the correction collar and repeat this process as appropriate. Repeat this process, with start at Left selected to produce an orthogonally oriented projection.
282. Check the two resliced/projected z-stacks for uniformity of the PSF. For oil objectives, it is possible that some nonuniformity is visible toward the field of view (FOV) periphery (particularly for the largest FOV defined by use of the $2.85\times$ telescope) but the PSF should

look uniform otherwise. For the silicone objective lens (maximum compatible telescopic magnification of 1 \times), it is likely that the PSF will show coma aberrations in one or both views (the PSF will have a curved banana-like shape).

◆ TROUBLESHOOTING

283. Position a single fluorescent bead in the center of the FOV and acquire an image, while recording the xy stage position from its controller. Move the bead to the peripheries of the FOV in x (e.g., for a $\pm 27\ \mu\text{m}$ range when using the 2 \times magnification telescope). Acquire images at these positions, again noting the xy stage position.
284. Repeat this process for steps in y .
285. Open the images in ImageJ and either manually follow the position of the bead or determine the bead center analytically (e.g., by applying a threshold to the images and determining image centroid for a bounding box including the bead). Calculate the bead displacement in each case (in pixels) and use the recorded stage position to calibrate for nm per pixel for both the x and y axes. The pixel size should be $\sim 105\ \text{nm}$ in x and y (assuming a system magnification of 61 \times and a camera pixel size of $6.5\ \mu\text{m}$).
286. Record the x and y pixel size for later input in the SMAP Camera Manager.
287. Switch back to the 1 \times magnification telescope.

3D imaging alignment

● TIMING 2 d

▲ **CRITICAL** To perform 3D imaging, the astigmatic lens must be introduced to the emission path, aligned and adjusted to provide an appropriate amount of astigmatism. The astigmatic lens consists of a pair of cylindrical lenses of equivalent power and opposite sign. Introducing a relative rotation between the zero-power axes of the lenses results in a variable amount of astigmatism being introduced, which allows the axial position of emitters to be encoded via the resulting lateral PSF asymmetry and orientation. The astigmatic lens is placed at a conjugate of the back focal plane of the objective and is thus expected to introduce minimal distortion associated with anisotropic magnification. The correct placement of the astigmatic lens is assessed by imaging an aperture target onto the camera with the help of the Bertrand lens, which has been preconfigured to image the back focal plane and its conjugates. The alignment of the astigmatic lens proceeds via use of the alignment laser. The lens placement is further assessed by measuring the magnification anisotropy and minimized by repositioning the lens as necessary.

288. Construct the astigmatic lens assembly (3D-SMLM-EMBL-001-002-001) but omit the cylindrical lenses (COTS-LJ1516RM, COTS-LK1002RM).
289. Remove the objective lens from the objective port (FAB-EMBL-000043) and replace it with the alignment laser (3D-SMLM-EMBL-007).
290. Install 2 \times irises (COTS-SM1D12D) on the rotational mount (COTS-CRM1T-M) of the astigmatic lens assembly separated by a slotted lens tube (COTS-SM1L30C).
291. Move the piezo resonant stage (COTS-ELL20-M) to 50 mm and secure the assembly in its nominal position via the base plate (FAB-EMBL-000067) as shown in Supplementary Fig. 59.
292. Use the stage position and height of the optical post assembly (COTS-PH30-M, COTS-TRA20-M) to align the beam to the downstream iris and rotate the two optical posts in their holders (COTS-TRA20-M/COTS-TRA40-M in COTS-PH30-M/COTS180-M, respectively) to align the beam to the upstream iris. Turn off the alignment laser.
293. Taking care not to reposition components, remove the 2 \times irises (COTS-SM1D12D) and slotted lens tube (COTS-SM1L30C) from the rotational mount (COTS-CRM1T-M).
294. Place a cage alignment target (COTS-CPA2) in between the two rotation mounts (COTS-CRM1T-M, COTS-CRM1PT-M) of the assembly and supported by the 2 \times cage rods (COTS-ER1).
295. Use two fixed kinematic stops (COTS-KL01L) to indicate the position of the short side of the astigmatic lens assembly base plate (FAB-EMBL-000067) closest to the optical table edge.
296. Switch the Bertrand lens into the emission path.
297. Switch the filter wheels (COTS-FW102C) to an open position for transmission imaging.

298. Back light the target with a white light source and image it on the sCMOS camera via the second relay lenses (COTS-AC254-200-A) and Bertrand lens (COTS-#32-963). Note that the magnification from the target to the camera is $0.3\times$ and the target aperture is 5 mm. As such, the image of the target should be 1.5 mm in diameter or ~230 pixels in the camera image.

◆ TROUBLESHOOTING

299. Loosen the screws securing the base plate (FAB-EMBL-000067) and translate the assembly along the path defined by the fixed kinematic stops (COTS-KL01L), such that the aperture appears as sharply defined as possible in the camera image. Secure the screws when the correct longitudinal position has been found.
300. Remove the cage alignment target (COTS-CPA2).
301. Install the cylindrical lenses (COTS-LJ1516RM, COTS-LK1002RM) in their respective rotation mounts (COTS-CRM1T-M, COTS-CRM1PT-M). Note, some disassembly of the 30 mm cage section of the astigmatic lens assembly (3D-SMLM-EMBL-001-002-001) will be required.
302. Repeat Steps 290–293 to realign the assembly to the alignment laser in the corrected longitudinal position. Record the final piezo resonant stage position. Save this value in the EMU configuration for the two-state device 1 on value. Set the two-state device 1 off value to 0, such that turning on/off the 3D control moves the astigmatic lens in and out of the beam path.
303. Remove the alignment laser (3D-SMLM-EMBL-007) from the objective port (FAB-EMBL-000043) and replace it with the objective lens.
304. Mount and image a fluorescent bead sample and set the 3D property to off, checking that the stage repositions to move the cylindrical lenses out of the emission path. Refer to Supplementary Information Note 18 for a detailed description of the sample preparation and ‘Focusing the microscope’ for a description of setting up the microscope to image fluorescent beads.
305. Set the 3D property to on and observe the PSF shape when focusing through the beads.
306. Carefully rotate the upstream rotation mount (COTS-CRM1T-M) until the PSF appears as close to the 2D case (i.e., without the astigmatic lens) as possible. This corresponds to a position where the cylindrical lens axes are aligned and the astigmatism introduced is negligible.
307. Rotate the downstream rotation mount (COTS-CRM1PT-M) using the micrometer screw to introduce mild astigmatism such that the PSF at focus appears as a faint cross. Note, it may be necessary to refocus slightly as the amount of astigmatism is adjusted.
308. Focusing up and down should result in a PSF that extends in one axis on one side of the focus and in an orthogonal axis on the opposite side. Carefully rotate the upstream rotation mount (COTS-CRM1T-M) and compensate with an equal motion of the downstream cylindrical mount (COTS-CRM1PT-M) to achieve a similarly mild astigmatism but such that the extension axes are aligned to the pixel grid of the camera. Note, for large movements of the downstream rotation mount, manually adjust via the mount itself rather than using the micrometer, which should remain close to the center of its travel range.
309. Repeat the process of calibrating and recording the x and y pixel size from Steps 283–286.

Focus lock path buildup and alignment

● TIMING 3 d

▲ **CRITICAL** To be able to perform SMLM imaging experiments and assess drift/vibrations, it is necessary that the focus lock system is installed. Setting up the focus lock system requires aligning a near-infrared (808 nm) laser to the optical axis of the objective lens, focusing it to the back focal plane and then shifting the focused spot to the periphery of the back focal plane to fulfil the condition for total internal reflection. The reflected beam is subsequently routed to the QPD where an axial drift of the objective–coverslip spacing is detected as a lateral shift of the reflected beam. When setting up the microscope with a silicone oil objective, start with $20\times$ higher resistance to provide higher detector sensitivity. In the case of a silicone oil objective lens, the refractive index contrast between the immersion oil and the sample is too small to fulfil the total internal reflection condition at the angle defined by the maximum NA of the objective



Fig. 7 | The fully assembled focus lock path. A fiber coupled NIR (808 nm) laser is connected to the fiber terminating adapter (bottom) and focused by a lens (occluded) onto the objective BFP via a pair of steering mirrors and cleanup/neutral density filters. The second steering mirror is on a manually adjustable translation stage to offset the beam at the BFP to achieve the condition for total internal reflection at the coverslip sample interface (for oil objectives) or to optimize for Fresnel reflections (for silicone oil objective lenses). The returned beam is picked off by a D-shaped mirror and captured on a quadrant photodiode (QPD). The QPD measures focal drift as a positional offset of the returned beam and sends a corrective signal to the objective lens piezo flexure stage accordingly. Mounting the QPD on a motorized stage allows refocusing during focus lock operation by translating the QPD.

lens. In this case, one can still focus lock via Fresnel reflection of the tilted beam at the interface. In this case, the reflected signal will be much dimmer than for total internal reflection. The focus lock path needs to be constructed in a stable manner with minimized beam path lengths since any drift in the beam pointing will result in focus drift. A CAD rendering of the fully assembled focus lock path is shown in Fig. 7.

310. Remove the objective lens from the objective port (FAB-EMBL-000043) and replace it with the objective port alignment target (3D-SMLM-EMBL-006) with the beam profiling camera installed on the c-mount port at the distal end.
311. Install the focus lock laser (COTS-IBEAM-SMART-PT) on its mount (FAB-EMBL-000088) and install the mounted laser on the optical table. The precise location is arbitrary but make sure that it is placed close enough to the left side of the microscope body where the focus lock system is situated to avoid strain and damage to the fiber.
312. Assemble the focus lock laser beam launch (3D-SMLM-EMBL-001-004-001) and secure it in position on the optical table using 2× pedestal post clamps (COTS-PS-F). Install the fiber from the focus lock laser in the terminating adapter (COTS-SMIFCA).
313. Use the beam viewer card (COTS-VRC2) to view the 808 nm beam and collimate the laser as best as possible by visual inspection by translating the lens (COTS-AC127-019-B-ML) relative to the fiber tip.
▲ CAUTION The 808 nm laser is not visible and so presents an acute laser safety hazard, wear appropriate laser safety eyewear when aligning the laser.
314. Assemble the focus lock beam offset mirror assembly (3D-SMLM-EMBL-001-004-002) and install it in place on the optical table. Adjust the mirror mount (COTS-POLARIS-K1) to the nominal orientation/position and the translation stage (COTS-MSIS-M) to 6 mm as readout via the micrometer screw.
315. Introduce the first steering mirror (COTS-POLARIS-K1, COTS-BB1-E03, COTS-RSIP4M) with the beam centered on its aperture such that it reflects onto the downstream mirror at a lateral position roughly aligned to the optical table holes centered on the left side of the microscope body. With the translation stage (COTS-MSIS-M) at its to 6 mm position, the beam should be incident laterally off-center on the mirror. Secure the mirror in place with a pedestal post clamp (COTS-PS-F). The assembly should appear as shown in Supplementary Fig. 60.
316. Use the steering mirrors to align the beam into the microscope body and direct it through the two irises (COTS-SMID12D) of the objective port alignment target (3D-SMLM-EMBL-006), using the beam profiling camera to assess centration of the beam at each iris. Note, it may be necessary to reorient the downstream mirror on the stage by releasing the mirror mount (COTS-POLARIS-K1) and securing it once it has been appropriately rotated.

317. Remove the objective port alignment target (3D-SMLM-EMBL-006) from the objective port (FAB-EMBL-000043) and replace it with the objective lens.
▲ CAUTION When the objective is in place and the focus lock laser is emitting, a highly divergent beam will exit the objective lens and even small misalignments may result in a strong deviation from the optical axis and constitute a laser safety hazard accordingly. Wear laser safety eyewear whenever assessing alignment through the objective lens and use the beam viewer card (COTS-VRC2) to check the path of the beam out of the objective lens.
318. Using the beam viewer card (COTS-VRC2) to view the beam out of the objective, focus the lens (COTS-AC127-019-B-ML) of the beam launch to collimate the output by minimizing the spot size as far from the front of the objective lens as practical. Note, divergence of the beam out of the objective makes it difficult to check the beam position with the beam viewer card (COTS-VRC2) far from the objective start close to the objective and move further away as collimation is approached and the divergence is minimized. Secure the cage plate (COTS-CP32-M) mounting the lens in place.
▲ CAUTION When collimated, a minimally divergent beam will exit the objective lens and even small misalignments may result in a strong deviation from the optical axis and constitute a laser safety hazard accordingly.
319. Check the path of the focus lock laser out of the objective. If the laser is launched substantially off axis, use the first steering mirror to make minor realignments of the beam (COTS-POLARIS-K1, COTS-BB1-E03, COTS-RS1P4M) such that the beam emerging from the objective is launched as close as possible on axis.
320. Mount and image a fluorescent bead sample to establish the focal position. Refer to 'Fluorescent bead samples' in the 'Reagent setup' section for a detailed description of the sample preparation and 'Focusing the microscope' for a description of setting up the microscope to image fluorescent beads. Periodically adjust the focus as necessary.
321. Ensure that the cover is correctly installed on the microscope to intercept obliquely launched beams.
322. Translate the translation stage (COTS-MS1S-M) toward the front of the microscope such that the beam travelling parallel to the objective optical axis is translated toward the front side of the objective lens back focal plane.
▲ CAUTION Avoid translating the stage toward the back of the microscope, which will result in the beam launching obliquely out of the optical table on the proximal side.
323. While translating the stage (COTS-MS1S-M), check for total internal reflection using the beam viewer card (COTS-VRC2) to see the reflected beam spatially offset by 4–5 mm from the input beam toward the back side of the microscope, ensuring that the card does not block the input beam. Translate the stage to maximize the power of the reflected beam, which will be substantially dimmer than the input (particularly for the reduced refractive index contrast present when using a silicone oil objective). Lock the stage in place when the optimal position has been found. Note that the beam viewer card will dim with repeated exposure and needs to be charged by, e.g., room lights.
◆ TROUBLESHOOTING
324. Install the pickoff mirror (COTS-PFD10-03-P01, COTS-KM100DL, COTS-RS4M, COTS-RS05P4M), such that the input beam passes into the microscope body, while steering the reflected beam parallel to the hole pattern along the long edge of the optical table. Note, the beam will be diverging. Secure the mirror in place with a pedestal post clamp (COTS-PS-F).
325. Assemble the QPD translation stage assembly (3D-SMLM-EMBL-001-004-003) but omit the QPD itself (COTS-SD197-23-21-041).
326. Center the QPD stage (COTS-2445-L) in its travel range.
327. Install the QPD translation stage assembly (3D-SMLM-EMBL-001-004-003) in place on the optical table such that the returned focus lock beam passes centrally through its aperture as judged using the beam-viewer card (COTS-VRC2).
328. Install the QPD (COTS-SD197-23-21-041) in its mount (FAB-EMBL-000091). Recenter the QPD stage (COTS-2445-L) in its travel range if necessary. The assembly should appear as shown in Supplementary Fig. 61 (QPD omitted).

Setup of the focus lock amplifier

● TIMING 2 d

▲ **CRITICAL** Measuring the focus lock QPD signal on the microFPGA aids in determining a correct working voltage range for the feedback to the objective piezo flexure stage (COTS-P-726.1CD). The conversion of the photocurrent from each of the QPD quadrants to a voltage is handled by the QPD amplifier board but requires the installation of four resistors (of equal resistance) to provide an output in the range 0–10 V. The focus lock laser is attenuated by a neutral density filter (ND 1), allowing it to be operated at 30–50% of its total power, where it typically is most stable, while reducing the incident laser light on the objective and sample. Having set the resistance appropriately, the QPD is translated on its stage and two potentiometers adjusted to appropriately scale the positional output to the range 0–10 V as required by the analog conversion board of the microFPGA and the objective piezo flexure stage. The values for resistors provided below assume the use of an oil objective. When setting up the microscope with a silicone oil objective, start with 20× higher resistance.

329. Package the QPD amplifier board as desired (the following assumes that 3 SMB female connectors are provided for the *x*, *y* and ‘sum’ signals). Provide an appropriate power supply to the board and make connections to the QPD (COTS-SD197-23-21-041). The two LEDs should be on.
330. Connect the *x* signal SMB connector of the QPD amplifier to an appropriate SMB T-splitter and connect one of the T-splitter arms to the analog input BNC connector of the Physik Instrumente E-709 controller. Connect the other to the AI:QPD:X connector on the microFPGA.
331. Connect the Y and SUM SMB connectors of the QPD amplifier to AI:QPD:/Y/SUM connectors on the microFPGA.
332. Install 4× 51 kΩ resistors on the amplifier board (in the positions indicated in the board datasheet). Set the focus lock laser power to 30 mW. Check again for return of the focus lock laser using the beam viewer card (COTS-VRC2).
333. Install the focus lock laser ND 1 filter (COTS-NE10A-B, COTS-LMR1-M, COTS-RS1P4M) and secure it in place with a pedestal post clamp (COTS-PS-F). Note the filter can be unscrewed from its mount as necessary for realignment of the focus lock system (Supplementary Fig. 62).
334. Check the LEDs on the QPD amplifier board. If both LEDs are off, the incident intensity is too low and the resistors should be exchanged for those with higher values (the amplification is linearly proportional to the resistance). Conversely, if both LEDs are on, the resistance should be decreased. Establish a resistance for which only one LED remains on over a range 5–50 mW.
335. Check the SUM signal in the QPD tab of the EMU GUI. Adjust the laser power to bring the green bar to approximately half of its full height.
336. Connect the *x* channel of the QPD amplifier to an oscilloscope. Cover the QPD so that no light is incident on it. Adjust the *x* and *y* offset potentiometer to adjust the signal to 5 V.
337. Uncover the QPD and translate the QPD stage (COTS-2445-L) back and forth, using the LEDs to check that the beam is still incident on the QPD and note the change in the *x* voltage on the oscilloscope. Use the *x* gain potentiometer to scale the signal to the range 0–10 V (or as close as possible) across the range of motion. Note, if translating the stage does not elicit a change in the *x* signal, check the *y* signal as well. If the *y* signal shows a response, then the *x* and *y* channels have been switched at some point in assembling and connecting the electronics.
338. Repeat the process for the *y* voltage and *y* gain potentiometer, instead using the D-shaped steering mirror mount (COTS-KM100DL) to move between the *y* extremes. Recenter the red point on the 2D graph display in EMU.
339. Connect the *x* and *y* signals as necessary to the microFPGA front panels and again monitor the signals in EMU. Center the QPD stage (COTS-2445-L) in its travel range.
340. Use the D-shaped steering mirror mount (COTS-KM100DL) to center the red point on the 2D graph display.

Focus locking

● TIMING 1 d

▲ **CRITICAL** Having aligned the focus lock system and setup the amplifier, it is now possible to engage the focus lock and check that the microscope can be focused by moving the QPD stage.

341. Bring the fluorescent bead sample into focus in the image.
342. Ensure that the 'sum' signal from the focus lock laser is sufficient to half fill the green bar in the QPD tab of the EMU GUI. Adjust the focus lock laser power as necessary. Center the focus lock laser spot on the QPD (x axis) by translating its stage.
343. Engage the focus lock ('Lock' in the EMU htSMLM GUI). Note, that the focus lock will only work over a z-range for which the laser spot remains incident on the QPD. Engaging the focus lock with the focus lock laser spot not visible on the display, will lead to a sudden drift of focus typically away from the true focal position (as viewed from the z-stage position).

◆ TROUBLESHOOTING

344. Adjust the locked focus position by repositioning the QPD stage (10–100 μm increments) such that the beads move in and out of focus. Return the microscope to a sharp focus using the QPD stage.
345. Depending on the specific choices of spectrally discriminative optics in the system, it may be possible to see the focus lock laser spot on the camera. To check, set the focus lock laser to the highest operating power and set the sCMOS camera exposure time to 200 ms or the longest expected exposure time for operation. If the laser spot is visible above the background level of the camera (~100 counts), install the focus lock laser cleanup filter (COTS-FBH810-10) in a lens tube (COTS-SM1L03) with the arrow pointing toward the external thread and install the lens tube onto the focus lock laser neutral density filter (COTS-NE10A-B). This blocks out of band emission from the focus lock laser. Note, the cleanup filter bandwidth is narrow (10 nm full-width at half maximum) and so the edges are close to the nominal laser wavelength (808 nm). As such, small rotations of the filter with respect to the incident light may result in partial or complete extinction as the edges move to lower wavelengths. Appropriate rotation of the optic via the post mounting the neutral density filter (COTS-RS1P4M) should allow the laser line to pass while maximally blocking lower wavelengths. Once out-of-band emission has been blocked, the focus lock laser spot should no longer be visible on the sCMOS camera image.

(Optional) Minimizing mode-hopping of the focus lock laser

● TIMING 3 d

▲ **CRITICAL** If large jumps in z are observed during focus lock operation, it is likely that the focus lock laser is undergoing transient mode jumps, which are inherent to single-mode diode lasers. In this case follow Supplementary Protocol 6 to rectify the behavior.

Setup and configuration of software for analysis

● TIMING 1 d

▲ **CRITICAL** Analysis software is required to determine the positions of the single-molecule activation events in the camera frames to then reconstruct a super-resolution image. There are various complete software packages for this task^{46–48} that are compatible with this microscope. Here, we detail the installation of SMAP³⁰, developed in our group, that provides additional functionality to characterize the microscope. In the following sections, we then describe how to use SMAP for single-molecule fitting and analysis. For a more detailed description, consult the User Guide in the Help menu of the SMAP window.

346. If you have access to MATLAB (R2022a or newer) including the toolboxes: optimization, image processing, curve fitting, statistics and machine learning, we recommend installing the MATLAB version of SMAP from www.github.com/jries/SMAP, where you also find the installation instructions.
347. Alternatively, you can install the compiled stand-alone version of SMAP following the link on www.github.com/jries/SMAP.

348. Start SMAP.m in MATLAB or the SMAP application when using the standalone version. Consult 'Getting started' in the 'Help' menu to familiarize yourself with SMAP. Here you also have access to the User_Guide.
349. Install Micro-Manager 1.4.22 or later from <https://micro-manager.org>. Note that this is necessary even if you have Micro-Manager 2.x installed, as only version 1.4 is compatible with SMAP.
350. As described in the User_Guide, Chapter '2.2 Installation', add the Micro-Manager path to SMAP:Preferences:Directories.
351. Add the main camera to SMAP (see User_Guide Chapter '5.1 Camera Manager' for details). First, duplicate the file cameras_Hamamatsu.mat in the SMAP/settings directory and rename it to, e.g., cameras_local.mat. In the SMAP menu / Preferences... select the File tab and in the 'CameraManager file' field select the duplicated file. Press 'Save and Exit'. Second, open the Camera Manager from the SMAP menu. With 'load images' load any image file that you acquired with your camera. When asked if to add a new camera click 'no'. In the first list click (second line, next to the OrcaFusion name) in the ID column. A list will open with all metadata properties. Select a field that uniquely describes your camera, e.g., HamamatsuHam_DCAM-CameraID. Save and close the camera manager. Do not add your local camera file to the git repository. Third, by clicking on the camera name 'OrcaFusion' you can check if the correct parameters are set: Emon: 0; cam_pixelsize_um: 0.105, 0.105 (you can overwrite these values with the correct pixel sizes that were calibrated in Step 309); conversion: 0.24; offset: 100. These parameters are correct for the Hamamatsu Fusion BT camera for a system magnification of 61 \times provided by the optical scheme described. For other cameras and changes to the emission path optics, amend these values accordingly.

Performing PSF calibration

● TIMING 4 d

▲ **CRITICAL** Having set up the focus lock system, it is now possible to perform an accurate 3D calibration for subsequent image reconstruction using fluorescent beads. Focus locking is necessary in this case, since the calibration requires that a large number of individual bead-derived PSFs are averaged, which in turn requires imaging over a large region of the coverslip, which may vary slightly in height. An iterative process of optimizing correction collar and astigmatism settings is performed to attain the best possible 3D-imaging performance. Subsequently, we will describe how to perform a PSF calibration with SMAP and use this for 3D fitting. This procedure is used later to check for drifts and vibrations and to fit the example data for performance characterization. For a general overview of the system 2D and 3D PSF and multicolor performance, see Supplementary Fig. 63.

352. Release the NIR laser blocking filter from its mounting lens tube (COTS-SM1L03). Install the filter in the exposed SM1 port of the sCMOS camera c-mount adapter (FAB-EMBL-000073) securing it in place with a retaining ring (COTS-SM1RR). Note that to install the filter as such, it is necessary to remove the Bertrand lens stage on its pinned mount (FAB-EMBL-000074), which can be replaced once the filter is secured. Installing the blocking filter in front of the camera is necessary to prevent a NIR LED in the Bertrand lens stage (COTS-ELL6) causing an artificially high background on the camera for the localization imaging that follows in the protocol.
353. Turn on the 3D property to move the astigmatic lens into the emission path.
354. Mount a fluorescent bead sample. Refer to Supplementary Information Note 18 for a detailed description of the sample preparation.
355. Use 1% laser power to locate a region of the sample with ~5–20 beads that are well separated. Sharply focus the beads in the image. Acquire a z-stack from ~1 μ m to 1 μ m around the focus with a spacing of 0.02 μ m using the μ Manager multidimensional acquisition wizard.
356. Start SMAP and open the plugin: Analyze:sr3D:calibrate3DsplinePSF. Press run.
357. Using 'select Camera Files' load the bead stacks you just acquired.
358. Set the distance between the frames to 20 nm. All other settings can be left at default. Press 'Calculate bead calibration'. The bead calibration is saved in the folder of the bead stacks

with a file name ending in '_3Dcal.mat'. For additional quality control steps for single-color 3D calibration, see Box 1 3D Calibration and Fig. 8 for a description of the various tabs of the results window.

359. Iterate this process, adjusting the correction collar and amount of astigmatism (as previously described) between iterations to achieve optimal 3D localization precisions over the desired axial range. It should be possible to achieve localization precisions better than 5/15 nm laterally/axially over a range of ± 400 nm as judged from the Cramér–Rao lower bound (CRLB) plot from the 3D calibration output. The minima of the CRLB x and y plots should be ~ 400 nm apart in z height for both the oil and silicone oil objectives. In general, stronger astigmatism is associated with improved z localization precision but also a larger distance between the x and y minima resulting in a reduced effective operating z range. Results from a typical 3D calibration are shown in Fig. 8. Note, this procedure is only required the first time and after exchanging the objective, realigning aspects of the emission path or if the collar/astigmatism are adjusted for other reasons.
360. Once optimal settings have been determined, repeat the calibration step over five to ten ROIs (using the μ Manager Stage Position List to mark individual positions) to acquire several bead stacks for a more precise 3D PSF model. To this end, adjust the laser power to optimize between good signal-to-noise ratio and low bleaching and low flickering of the fluorescent beads. A good starting point is 0.5 kW/cm^2 . This process should be repeated for each imaging session.

BOX 1:

3D calibration

Having loaded the bead stack(s) in SMAP and run the analysis as described in Steps 358 and 368 for single- and dual-color 3D imaging respectively, the 'results' window, comprising multiple tabs is displayed (Fig. 8). The following checks should be carried out each time a 3D calibration is performed for single color (steps 1–4) and dual color (steps 1–5), respectively. Note, for dual-color imaging many of the tabs are found under 'global cal'. In general, experimental reasons for poor quality bead calibration include poor optical alignment and setting of the objective correction collar (if present) and the amount of astigmatism applied, the presence of an air bubble in the immersion oil, poor choice of bead regions such those with many overlapping beads or flickering and bleaching of beads or saturation of the camera due to high laser power. If any of the following checks fail, we recommend remounting the sample and acquiring a fresh bead stack, checking optical alignment as necessary; see Step 359 regarding adjustment of the correction collar and amount of astigmatism.

1. Under 'Files' the individual projected bead stacks are shown as numbered tabs. The individual beads should be identified assuming that multiple beads are not too closely spaced. If beads are not identified reduce the 'relative cut-off' parameter. If background is identified as beads reduce the 'relative cut-off' parameter.
2. In the PSF tabs, the cross-section through the PSF models along x ('PSFx'), y ('PSFy') and z ('PSFz') are shown. The individual bead profiles should envelop the average with minimal deviations. Should the spread between individual beads and the model be too wide, the bead calibration should be repeated and optical alignment of the system checked. The z PSF should appear

symmetrical about the z peak. Minor asymmetry is allowable and results from spherical aberrations. Check that the x , y and z PSFs generated are a close representation of the bead images.

3. In the 'validate' tab check that the z fit is linear with the frame number for all beads and that all lines are parallel to the z fit for the average model (black line). Deviations at the extreme frames are expected and result from the bead calibration spanning a larger z range than that which is useable.
4. In the 'CRLB' tab the achievable localization precision is calculated based on the averaged PSF for a hypothetical photon count of 5,000 and a background of 50 photons/pixel. An asymmetry of the z localization precision about the plot's z center ($z \sim 0$ nm assuming that the z -stack is well centered on the focus where the elongation in either axis is at a minimum) often hints at the presence of spherical aberrations. A peak in the z localization precision at or close to $z = 0$ nm suggests that the astigmatism is too weak. 'CRLB' should show a symmetric localization precision for z , which can be expected to reach ~ 10 – 15 nm. Similarly, x and y localization precision should be symmetrical, and with minima ~ 5 nm.
5. In the 'transformation' tab, the transformation of channel 1 onto channel 2 is evaluated. Check the 'transformation:pos' tab to check that most beads found in channel 1 are matched to a specific bead in channel 2. Beads for which no matching was possible are marked as '+' and should be substantially fewer than matched beads marked as 'o'. Ensure that most beads across the entire field of view are paired.

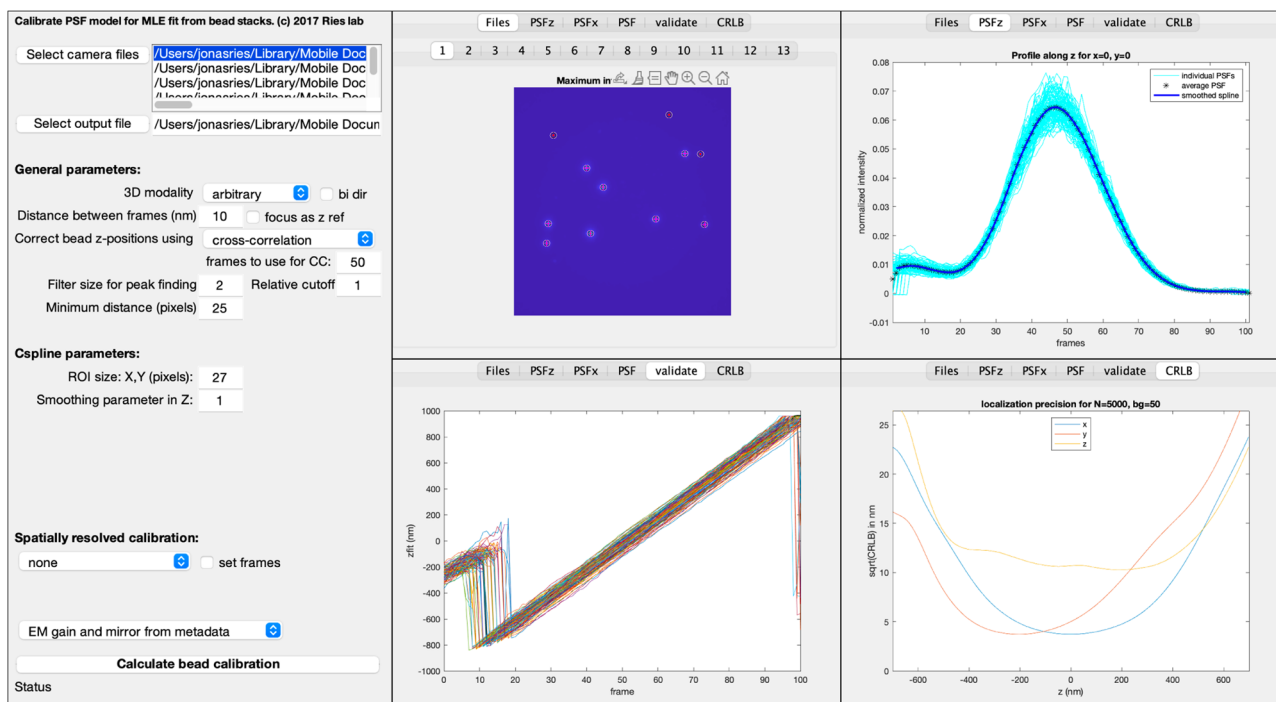


Fig. 8 | 3D calibration of the microscope based on fluorescent bead z-stacks. The SMAP GUI with default parameters and examples of the results window for a suitable bead calibration. Left: the interface for setting various fitting parameters. Top middle: a viewer for the detected beads in each z-stack. Top right: the spline fit to the averaged PSF along the z-axis. Bottom middle: the bead

calibration is validated by comparing the fitted z position to the expected one (given by the frame). Bottom right: the 3D localization precision expected for a theoretical localization with $N = 5,000$ photons and a background of 50 photons/pixel. The z range over which the x, y and z localization precisions remain acceptable defines the maximum depth of the 3D volume that can be imaged.

2D and 3D fitting with SMAP

● TIMING 2 d

▲ **CRITICAL** Here, we describe how to use SMAP to fit imaging data. In 2D, single PSFs originating from beads or a biological sample can be approximated by a 2D Gaussian function. To extract additional information such as the z-position and the color when using multiple channels, an experimental PSF model is generated and used for fitting 3D and multicolor data (see globLoc¹⁸ for more detail on generating a global PSF model for multichannel data). How to acquire these data is detailed below in the section ‘2D imaging of NPCs’ and Supplementary Protocols 7 and 8.

361. In the SMAP main window select the ‘Localize : Input Image’ tab and make sure that the ‘fast_simple’ workflow is selected (otherwise load it with the ‘Change’ button).
362. With ‘load images’ load the Micro-Manager tiff stack that you want to fit (see section ‘Performing PSF calibration’ for instructions on how to acquire this data).
363. If the camera has not been added to the camera manager or if the camera is not recognized, set the camera parameters in the dialog ‘set Cam Parameters’. Afterward check ‘lock’ to prevent this data from being overwritten.
364. In the ‘Fitter’ tab select ‘Spline’ as a PSF model and load the ‘*_3Dcal.mat’ file that you generated above with ‘Load 3D cal’.
365. Press ‘Preview’ (you can select the frame that is fitted for testing next to the ‘Preview’ button). True localizations should be marked, background noise should not. You can adjust the sensitivity of the peak finder in the ‘Peak finder’ tab by changing the value next to the ‘dynamic (factor)’ menu.
366. Once you are happy with the preview, press ‘Localize’ to start the localization process. Once the fitting is done, the results are automatically saved in the folder of the tiff files and a super-resolution image is reconstructed that can be explored.

367. For 2D fitting of data acquired without the astigmatic lens, follow the steps of this section with the following change: in the 'Fitter' tab select 'PSFxy' as PSF model, no calibration file is needed.
368. For dual-channel 3D fitting, first calibrate the dual-channel PSF as described above, but with the following modifications: as 3D modality choose 'global 2 channel'. Under 'global fit parameters' check 'make T' and select 'right-left mirror' and main Channel 'd/r'. The resulting calibration will be shown in a new window, and the MATLAB file as well as the figure are saved automatically to the imaging folder. For additional quality control steps for dual-color 3D calibration, see Box 1 3D Calibration.
369. For fitting dual-channel data navigate in SMAP to the 'Localize' tab. Check if the workflow 'fit_global_dualchannel' is selected. If not, use the 'Change' button to select the file 'fit_global_dualchannel.txt' to load this workflow.
370. Fitting is analogous to the steps described above but with the following differences: in the 'Peak Finder' tab select the PSF '*_3Dcal.mat' file you created with 'load T'. In the 'Fitter' tab select 'Spline' and load the same file again with 'Load 3D cal'. Check 'Global fit'. Make sure only *x*, *y* and *z* are checked and *N* and *bg* remain unchecked. Select 'Ch1' in 'main xy'.
371. Start the fitting process with 'Localize'.
372. After fitting assign the colors with the plugin 'Process/Assign2C/Intensity2ManyChannels' (press 'Info' for instructions). To render a specific color, you need to specify the color in the Render tab (0 is unassigned colors). You can add a layer to display the second color.
373. To fit 2D dual-channel data, you need to first generate a transformation file. For this, first fit both channels as described above for 2D data with the fast_simple workflow. Then use the plugin 'Process/Register/Register Localizations' and use as a target 'right' and 'left-right' at mirror. Press 'Run' and if the transformation is good save it with 'save T'.
374. For fitting, follow the steps above (including changing the workflow to fit_gobal_dualchannel', and in the 'Fitter' tab specify 'PSF free'. Using this setting, each detected signal is fitted with a 2D Gaussian, assuming a Gaussian-distributed PSF. In the 'Peak Finder' tab load the transformation file '*_T.mat' you just generated.

Postprocessing and rendering with SMAP

● TIMING 2 d

▲ **CRITICAL** The localization workflow discussed above extracts the coordinates of single fluorophores from the camera frames together with additional attributes, such as the localization precision or the likelihood as a measure for goodness of fit. In the following, we discuss how to merge localizations in consecutive frames, stemming from the same fluorophore, into a single localization, how to render a super-resolution image, how to filter out poor localizations and how to perform drift correction.

375. Load a fitted data set ('*_sml.mat' file) in the file tab using the 'Load' button. An overview image should appear in the SMAP window.
376. Localizations in consecutive frames stemming from the same fluorophore activation event are automatically merged ('grouped') into a single localization according to the parameters in the 'File' tab under 'Grouping'. You can change the parameters and perform the grouping again by pressing the 'Group' button. You can later select whether to display these grouped localizations or the original frame-wise localizations with the 'group' checkbox in the 'Render' tab.
377. By pressing 'Render' in the render tab you can render a super-resolution image. You can zoom into the image with the mouse wheel or track pad or the '+' and '-' buttons in the 'format' area of the SMAP window and move around by right clicking in the new position in the super-resolution window, by dragging the image to a new location or by left clicking in the overview image.
378. You can change the appearance of the super-resolution image by adjusting the parameters in the 'Render' tab and display several layers as described in the User_Guide, Chapter '7.1 The render GUI'.
379. SMAP allows for versatile filtering of localizations that are used for rendering and further analysis. To access the filtering window of SMAP press the button 'OV->filter'. In the

list, you can select any property of localizations, look at the histogram and decide on minimum and maximum values (check 'filter' to apply the filter). The following filters are used regularly and are found directly in the 'Render' tab: (a) localization precision to filter out poor localizations from dim fluorophores; (b) z position to only display a slice in z; (c) for 2D data instead the fitted size of the PSF can be used as a filter to filter out out-of-focus localizations for optical sectioning; (d) the frames to filter out the beginning where localizations might be too dense, or the end that does not contain useable localizations; and (e) LRel, a normalized log-likelihood measure that describes the goodness of fit to filter out localizations that were close to other localizations and thus poorly localized.

380. Even a stable microscope will show drift on the nanometer scale over the measurement time of minutes to hours. This drift can be corrected with the plugin: 'Process:Drift:drift correction x,y,z', which you also find in the 'Process' tab. SMAP uses an approach called 'redundant cross-correlation' that splits the data into equal windows in time and then compares super-resolution images reconstructed from each time window with those of all other time windows to estimate the displacement. From all pairwise displacements a drift trajectory is then calculated and used to correct the data. In the plugin you need to select if only to 'correct xy-drift' or also to 'correct z-drift'. The main parameter you need to choose is the number of time windows called 'timepoints'. More timepoints lead to a smoother curve, but if the data is sparse, at some point the noise increases. Press 'Run' to perform drift correction. Then check the tabs 'dxy/frame' and 'dz/frame'. Except for outliers, the colorful curves should envelope the black curve. If the noise is too large, reduce the number of time windows. As drift correction is automatically applied, you need to press 'Undo' before performing the drift correction again with altered parameters.
381. To render 3D data in 3D you can use the plugin 'Analyze:sr3D:Viewer 3D'.

Performing focus lock, drift and vibration checks

● TIMING 3 d

▲ **CRITICAL** At this juncture, the microscope is capable of focus locking and 3D imaging. Before continuing, it is first necessary to validate the focus lock performance by checking the axial drift of a fluorescent bead sample over 24 h. The measurement is then repeated to check for medium-term instability over 10 min and subsequently the presence of short-term vibrations is checked for a single bead over a few seconds. To do so, it is necessary to introduce water cooling and switch off the camera fan. The instructions provided assume the use of the base configuration Hamamatsu Fusion BT sCMOS camera.

382. Power down the sCMOS camera.
383. Install the water-cooling protection cap of the sCMOS camera to avoid ingress of water.
384. Provide suitable water cooling to the camera via the inlet/outlets and check for leaks once circulation commences.
385. Power up the sCMOS camera and turn off the fan with the DCAM API configurator.
386. Acquire camera frames continuously in the manufacturer supplied HoKaWo software and monitor the temperature of the circulating coolant and camera itself to ensure that the cooling provided is sufficient to support the thermal load of the camera. If the camera is able to maintain its -8°C operating temperature over a period of 4 h, the cooling is adequate. If the camera emits a constant tone during operation, the camera has overheated and image acquisition will cease. In this case, switch off the camera and resume with a higher load cooling system.
387. Close the HoKaWo software when the testing is complete.
388. Add the additional settings to the μ Manager presets as described in Supplementary Table 13, in order that sensor cooling is set to its maximum setting with the sensor fan set to off.
▲ **CAUTION** The sCMOS camera is now reliant on water cooling to maintain the functionality of its Peltier element. Check the sensor temperature in HoKaWo periodically.
389. Mount and image a fluorescent bead sample. Refer to 'Fluorescent bead samples' in Supplementary Information Note 18 for a detailed description of the sample preparation

- and 'Focusing the microscope' for a description of setting up the microscope to image fluorescent beads.
390. Acquire bead stacks and generate the PSF calibration as described in the section 'Performing PSF calibration', Steps 354–355 and 360.
 391. Set up for focus lock operation and engage the focus lock as described previously.
 392. Turn on the 3D property to move the astigmatic lens into the emission path.
 393. To measure long-term drift, image the bead sample once every 5 min for 24 h (289 timepoints) using the μ Manager multidimensional acquisition wizard. For this experiment, use the 'normal' imaging mode preset.
 394. Check the objective piezo flexure stage (z stage) position over the 24 h of imaging by displaying 'PIZStage-Position' using the plugin 'Process/Images/DisplayImageTagsTiff' in SMAP. Some motion of the stage will be apparent to correct for the drift between the coverslip and objective lens.
 395. Check the associated images to make sure that the focus remains stable throughout.
 396. To measure medium-term instability, repeat the drift measurement but instead image the bead sample continuously with an exposure time of 25 ms for 10 min.
 397. For the two datasets, fit the bead time-lapse data for drift analysis as described in Step 380 in the section 'Post-processing and rendering with SMAP'.
 398. Use the 'Analyze:measure:Drift_Analysis' plugin in SMAP to display the datasets over time. For the long-term drift measurements, drift values up to 200 nm/h in *x*, *y* and 50 nm/h in *z* are acceptable and can usually be corrected during post-processing. The drift observed generally results from changes in laboratory temperature, which is to be expected. However, look for sudden jumps of the position that indicate mode jumps of the focus lock laser (Supplementary Protocol 6), which are deleterious for imaging. For typical drift/instability measurement of the microscope over long (hours) and medium (minutes) timescales, see Supplementary Figs 64 and 65.
 399. For the medium-term instability measurements, peak-to-peak amplitudes up to 5 nm are acceptable. Larger instabilities often result from a failure to properly isolate the microscope from air currents. If this is the case, add additional enclosure around the microscope.
 400. Move to another field of view and locate a single isolated bead, position the bead at the vertical center of the camera chip and crop to a suitable ROI (e.g., 24 × 24 pixel) to encompass the bead and its surroundings while maintaining a small ROI size to achieve the best possible frame rate and small dataset size.
 401. Change to the 'fast' imaging mode preset and set the exposure time to 0.5 ms (thus setting a maximum frame rate of 2,000 frames per second).
 402. Increase the laser power as necessary to ensure that the bead appears as bright as possible without saturating given the much shorter exposure time.
 403. Use the μ Manager multidimensional acquisition wizard to image the single-bead field of view for 10,000 frames at the maximum frame rate of the camera (define an interval of zero between image acquisitions in μ Manager).
 404. Fit the bead time-lapse data for vibration analysis as described in Steps 361–368 in the section '2D and 3D fitting with SMAP'.
 405. Use the 'Analyze:measure:Vibrations' plugin to display the position of the bead versus time and a Fourier analysis of the position. In this frequency spectrum, you can identify the prominent vibration frequencies and by zooming in the position versus time plot one can estimate the amplitude of vibrations. Peak-to-peak amplitudes up to 5 nm indicate excellent performance. For typical vibration measurements of the microscope over short timescales, see Supplementary Fig. 66.

2D imaging of NPCs

● TIMING 7 d

▲ **CRITICAL** We note that for the following sections concerning the biological validation of the microscope's performance, the builder should refer to Supplementary Information Note 3 to aid in selection of appropriate filters and dichroics suited to the far-red ratiometric dSTORM scheme. As we are acquiring 2D data, one should follow the instructions in Steps 361–367 for

2D fitting. Fitting can be performed after the acquisition has finished. Alternatively, it can be performed 'online' to assess the reconstructed image on-the-fly during acquisition. This early evaluation offers the ability to detect any issues or artefacts during imaging and make necessary adjustments or abort the acquisition and restart with optimized settings. To investigate image quality (both during and after acquisition), visual inspection can be complemented with a statistical analysis of the image. It is important to understand the acquired data quality to identify potential points for troubleshooting. The following steps will outline a brief quality assessment. For a more in-depth analysis, refer to the SMAP documentation, which further covers the calculation of Fourier ring correlation-based resolution, geometric analyses and calculation of the effective labeling efficiency.

406. Refer to 'Biological sample preparation' for a detailed description as guidance in carrying out the following sample preparations. Seed U2OS Nup96-SNAP cells that have been in culture for at least two passages onto a coverslip.
407. After incubating seeded cells for 2 d, perform fixation and permeabilization.
408. Perform NPC labeling targeting the Nup96-SNAP tag with SNAP-Surface BG-AF647.
409. Place the coverslip onto the sample holder and add imaging buffer. For prolonged imaging (up to 24 h), fill the entire chamber of the magnet ring with imaging buffer and seal it using clean Parafilm.
410. Set up single-color imaging by manually removing the image splitter dichroic from the emission path. (COTS-SB1-M, COTS-25.5x36x3MM-DICHOIC-SP, COTS-KM200S, FAB-EMBL-000068/69).
411. Turn off the 3D property to move the astigmatic lens out of the emission path.
412. Set the exposure time to 30 ms in μ Manager.
413. Place a drop of immersion oil onto the objective and then mount the sample on the microscope.
414. Set up EMU for imaging as follows: (a) monitor stage position, (b) monitor focus lock, (c) turn on focus lock laser, (d) set 640 nm laser to 1% and (e) set appropriate emission filter in the transmitted path of the image splitter (typically for AlexaFluor647, this is a 676/37 bandpass filter).
415. Switch to the live imaging stream and focus on the coverslip. Typically, some residual dye or other autofluorescent particles are present on the coverslip to aid in focusing.
416. Double check the back focal plane (BFP) image using the Bertrand lens for potential air bubbles in the immersion oil, which appear as dark occlusions on the round back focal plane image.
417. Lock the focus (Steps 341–344).
418. Continue to use 1% 640 nm laser while searching for a ROI. If bleaching is still too strong, set the laser triggering to pulse the laser by selecting the Rising trigger mode in the Trigger tab of the htSMLM UI. Select an appropriate pulse length (shorter than the camera exposure time) to generate sufficient signal for focusing, while minimizing bleaching. A good starting point is a 10,000 μ s pulse length.
419. To achieve the best resolution, image NPCs located in the nuclear membrane closest to the coverslip. Ideally, select nuclear membrane areas that are flat, with most NPCs on the same focal plane. Start by slowly moving the focus up in z until most structures are in focus. Some blurring at the edge of the nucleus is expected, as the nuclear membrane bends upward and out of focus.
420. STORM imaging: decide between slow STORM (long acquisition times, high data quality)²⁹ and regular STORM regime (short acquisition times, decreased data quality)^{4,50}.
 - (A) **Slow STORM regime:**
 - (i) slowly turn off most fluorophores using ~ 0.2 kW/cm² laser power density until the overall signal intensity in the ROI is not decreasing anymore. This usually takes between 1 and 2 min and can be determined by eye.
 - (ii) Next, acquire images at 100 ms exposure time and ~ 6 kW/cm² laser power.
 - (B) **Regular STORM regime:**
 - (i) Directly acquire images at 30 ms exposure time and ~ 20 kW/cm² laser power density.

421. Image for ~80,000 frames (slow STORM regime) or 40,000 frames (regular STORM regime), until you reach the maximum 405 nm pulse length (10,000 μ s) and the density of activated fluorophores drops. Adjust the 405 nm pulse length manually during the experiment to keep the density of localizations constant. Alternatively, you can use the automatic feedback of the 405 nm pulse length. Adjust the activation parameters to ensure signals are not overlapping. Start with the following parameters: set activation density to 'Get N': 6 blinks per frame, at a 'sd coeff' of 4.0, 'Feedback' of 0.05; 'Average' at 1.0. Automatically detect background using the 'auto' button. You can also set the background manually to a level so that the measured number of activations reflect the visual impression. Figure 9 shows several frames of blinking emitters of reduced number over the imaging time course.
422. Use SMAP to fit the acquired data and reconstruct and render the localized image of 2D NPCs. See Steps 346–351 for a description on how to set up SMAP and Steps 475–481 for a description of the localization procedure.
423. Follow Steps 475–477 to set up image localization.
424. (Optional) To perform on-the-fly fitting, parallel to the image acquisition, additionally tick 'Online Analysis' in the 'Localize:Input Image' tab. Leave other settings on default.
425. Set up 'Localize:Peak Finder' according to Steps 361–365.
▲ CRITICAL STEP : Depending on the signal intensity of the detected peaks, the background cut off has to be adjusted. The 'dynamic (factor)' cut off ranges from 1 to 3. In the case of low-intensity fluorophores, visual inspection of the preview image might show that too many emitters remain undetected. In that case, it is advisable to lower the cut off until the desired emitters are included. As lowering this cut off will ultimately result in inclusion of background signal, an optimal balance between true detection and detection of background has to be established. In the case of bright fluorophores, the cut off can be increased. Double check new cut off settings in different frames using the slider next to the 'Preview' button.
426. The preview image also allows for restricting the ROI for which fitting is performed. To this end, draw the desired ROI in the preview image and press 'ROI to include' to include the selected ROI for fitting or 'ROI to exclude' to exclude the selected ROI from fitting. Double-click to confirm the selected region.
427. To perform 2D fitting, select 'PSF free' in the 'Fitter' tab as a PSF model instead of 'Spline'. Using this setting, each detected signal is fitted with a 2D Gaussian, assuming a Gaussian-distributed PSF.
428. In the 'Localize:Localization' tab, the frequency of rendering new localization data can be adjusted. According to the default setting, during 'online' fitting, new data is rendered every 60 s.
429. Run the localization of the acquired data. The localization data will automatically be saved to the imaging folder after the acquisition is finished.
430. Load a previously saved .sml file into SMAP via the 'File' tab.
431. Even in good samples there will be localizations of poor quality that need to be removed from further analysis. We recommend initial filtering based on lateral localization precision and relative log likelihood⁵¹ as described in the SMAP Documentation. Common cutoff values are localization precision (locprec) <20 nm and relative log likelihood (LLrel) > -1 and can be set in the 'Render' tab. For 2D data we also filter by the size of the PSF (PSF_{xnm} <175 nm) to remove out-of-focus fluorophores.
432. After this first filtering step, perform a drift correction in SMAP (Step 380). Go to the 'Process'/'Drift' tab in SMAP and run the drift correction with the default settings. For 3D data additionally check 'correct z drift'. Make sure that all of the curves scatter without too much error (tens of nm) around the black curve (Supplementary Fig. 67). Large scattering indicates that the redundant displacements are not compatible with each other and that the drift correction did not work correctly.
433. Next, analyze dye photophysics in the 'Analyze'/'Measure' tab and select 'Statistics'. By default, the plugin evaluates only localizations currently depicted in the field of view in SMAP that meet the current filtering criteria. Press Run and the resulting analysis will open in a separate window.

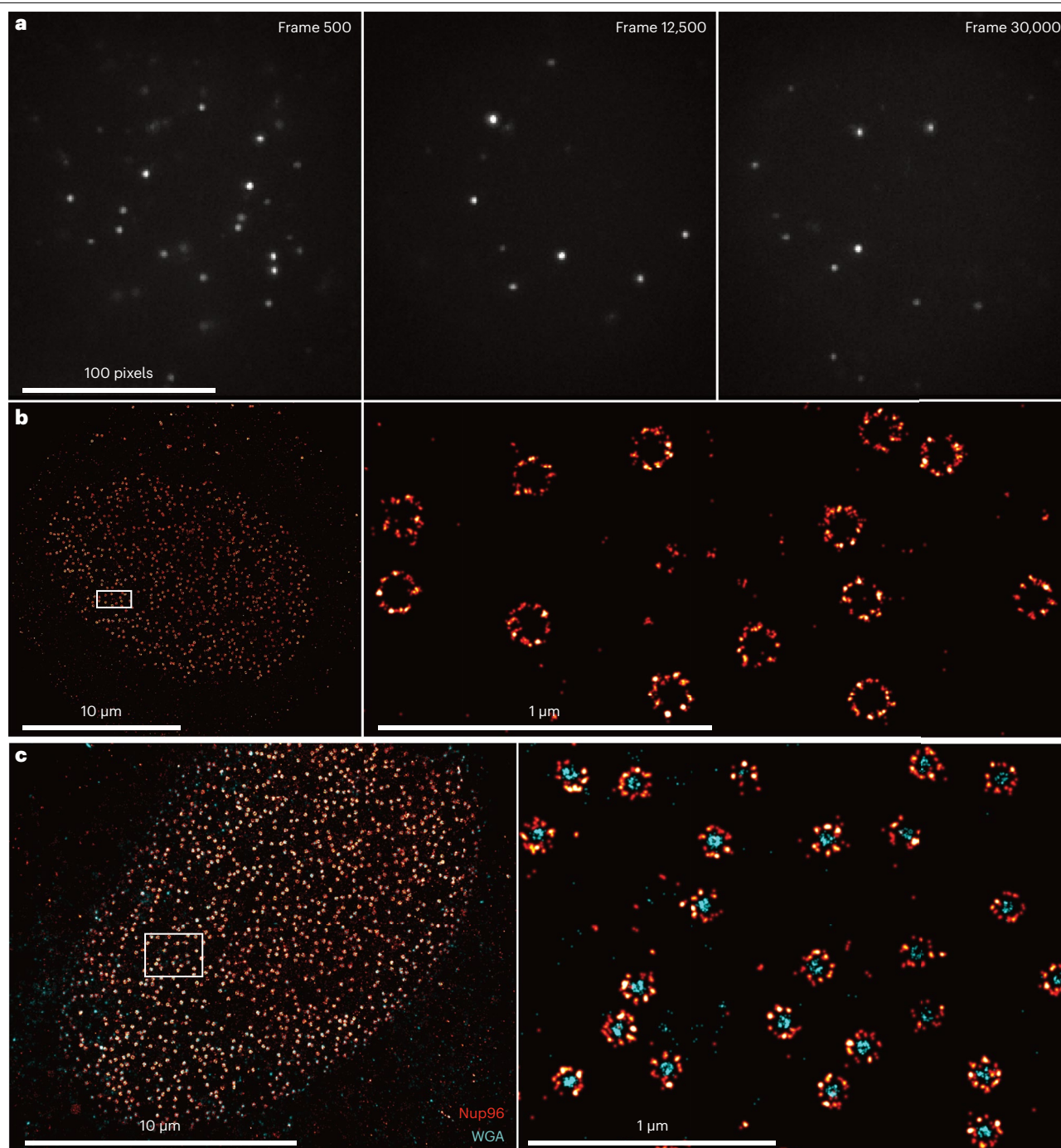


Fig. 9 | 2D imaging of the NPC. Here, Nup96-SNAP is labeled with Alexa Fluor 647 and imaged under the slow STORM regime. **a**, Raw camera frames show bright single molecules with a sufficiently low density. **b**, Single-color overview and zoom into individual NPCs. **c**, Dual-color overview and zoom, here additionally the central channel is labeled with WGA-CF680.

434. Photons: for AF647 you can expect ~6,000–8,000 photons per localization, for regular and for slow STORM regimes, respectively.
435. Localization precision can be expected to peak at 5 ± 2 nm.

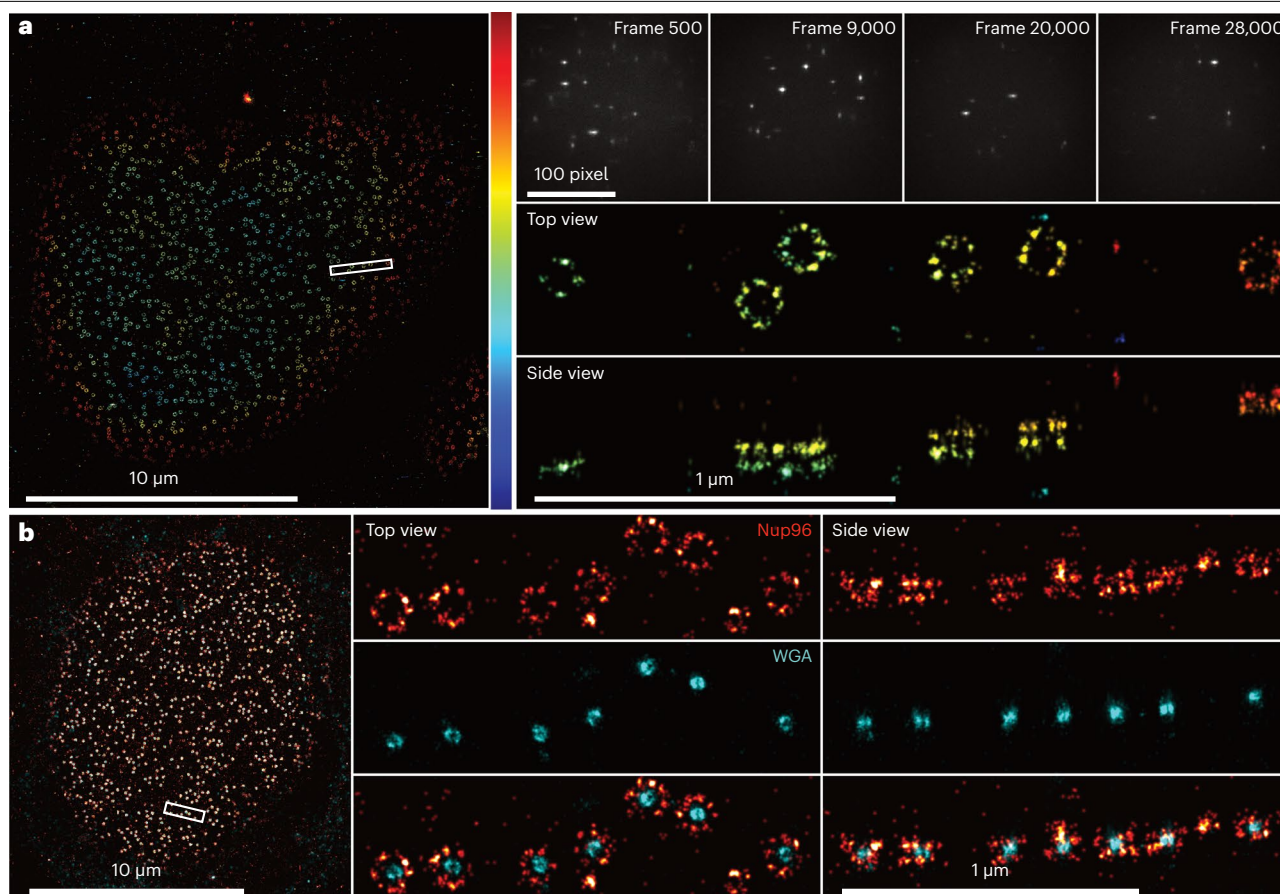


Fig. 10 | 3D imaging of the NPC. Here, Nup96-SNAP is labeled with Alexa Fluor 647 and imaged with slowSTORM. **a**, An overview, raw camera frames and single-color zoom into individual NPCs. The localizations are color coded by their z-position with blue corresponding to $z = -300$ nm and red corresponding to $z = +300$ nm. **b**, Dual-color 3D imaging.

436. The average on-time (meanall) should be kept in a range of 2–2.5 frames.
437. To assess the background, make sure to perform the analysis on ungrouped data. Background is expected to peak at 100 photons/pixel.
438. Visual inspection of individual NPCs can aid in evaluating the data qualitatively. A circular shape and noticeable corners (preferably eight) are desired traits of each NPC. Note that an average labeling efficiency of 60% (desired target) leads to most NPCs displaying six to eight corners, as each corner is occupied by four target proteins. For a quantitative approach to assess effective labeling efficiency see the SMAP documentation. Representative results are shown in Fig. 9.

◆ TROUBLESHOOTING

(Optional) 3D single- and multicolor imaging of NPCs

● TIMING 7–14 d

▲ **CRITICAL** Having performed 2D single-color imaging of the NPC, the microscope has been sufficiently benchmarked for its subsequent application to biological studies as specified by the builder or end user. For more advanced applications requiring ratiometric multicolor and 3D imaging, Supplementary Protocols 7 and 8 establish single- and multicolor 3D imaging, respectively. These workflows follow many of the features of 2D single-color imaging and their results are summarized in Figs. 9 and 10, respectively.

Troubleshooting

Achieving optimal results is contingent on correct implementation of the microscope construction as well as sample preparation, imaging and analyses, presenting a complex task with many potential pitfalls. Often, basic quality control and the repetition of preceding steps is sufficient to rectify issues. To further aid in correct implantation of the protocol, Table 1 lists several commonly encountered issues with likely causes and solutions. We encourage those following the protocol to contact us in case of other issues or if the suggested steps do not rectify the problems faced. Moreover, the corresponding authors are available to reasonable requests for information or to address technical questions.

Table 1 | Troubleshooting table

Step	Problem	Possible reason	Solution
52	Parts cannot be installed	Over-constraint due to dowel pin/hole tolerances and/or other tightly constrained mating features	Check the size and placement of dowel pin holes. Check the size of the dowel pins used. Remove dowel pins, particularly those where holes have become undersized until the parts can be installed correctly. If all dowel pin holes are undersized, have the offending parts remachined
56	Resistance to motion of the objective piezo platform is too strong to be able to rotate the actuators (FAB-EMBL-000039) using a hex key inserted through the clearance hole on the side of the actuator	Over-constraint due to dowel pin/hole tolerances and/or other tightly constrained mating features	Loosen the screws affixing the body upper plate (FAB-EMBL-000012) to the body upper standoffs (FAB-EMBL-000008/09/10/11) and retry. If this rectifies the issue, resecure the screws. If this issue persists, the FAB-EMBL-000038 platform may not be flat. Recheck the spacing between FAB-EMBL-000007 and FAB-EMBL-000038 with the 3× optical post 7 mm spacers (COTS-RS7M) as previously. Otherwise, it is acceptable to remove additional material from the section of the actuator (FAB-EMBL-000039) that mates with the bearing or remove dowel pins from the body upper standoffs/body upper plate (FAB-EMBL-000008/09/10/11/12) as necessary to relax the tolerances on fit
86	Hardware elements fail to connect in µManager	Hardware not connected to/recognized by host PC. µManager Device Configuration set incorrectly. Timeouts for connection are set too short	Try ‘Reload Hardware Configuration’ in µManager a few times. Check the hardware element in its manufacturer supplied software. Restart the device and PC to try to reconnect. Recheck communication settings set in µManager and connect to devices one by one to identify any that may not be correctly configured (e.g., wrong COM port). In the case of lasers check that interlock circuits are complete. If each device can be individually connected via µManager, but loading all devices in parallel fails, increase the length of timeouts from the default of 500 ms to 5,000 ms or however long is necessary to ensure correct loading each time
114	Beam not aligned to the proximal iris in the lateral direction	General stack up of tolerances, seating of the emission path dichroic mirror in its mount (FAB-EMBL-000025) and flatness of the leveled objective piezo platform (FAB-EMBL-000038)	Such lateral misalignment is not deleterious to system performance but makes assessment of vertical alignment more difficult. If this is the case, loosen the screws securing the image splitter platform (FAB-EMBL-000077) thus allowing the irises to be individually aligned to the beam by sliding the image splitter platform during subsequent alignment steps using the body lower plate (FAB-EMBL-000001) as a linear guide
115	Beam not aligned to both irises in the vertical direction	General stack up of tolerances, seating of the emission path dichroic mirror in its mount (FAB-EMBL-000025) and flatness of the leveled objective piezo platform (FAB-EMBL-000038)	First ensure that the actuator screws (FAB-EMBL-000077) are seated correctly in contact with the three pairs of contact pins to center the objective piezo platform (FAB-EMBL-000038) with respect to the clear aperture through the microscope body and check that the alignment laser emission is well centered on the two irises of its assembly (3D-SMLM-EMBL-007). If the issue persists, the likely cause is incorrect seating of the dichroic mirror in its mount (FAB-EMBL-000025). Depending on the adhesive used, one may reinstall the optic and check whether this improves alignment. If these steps do not rectify the issue, the dichroic mount includes features allowing for vertical realignment. Remove the mounted emission dichroic (COTS-25.5x36x3MM-DICHOIC-EM/FAB-EMBL-000025) from the optic pillar (FAB-EMBL-000023), remove the lower/center dowel pin from the emission dichroic mount (FAB-EMBL-000025) and reinstall the mount onto the optical pillar (FAB-EMBL-000023) with just one dowel pin. The rotational axis of the remaining dowel pin is centered on the reflective face of the emission dichroic and the clearance holes for the M3×35 mm socket head screws are loosely specified to allow a small range of rotation. Loosen the screws just enough to allow rotation under light force and rotate the emission dichroic mount until the beam passes as closely as possible through the center of the distal iris target (FAB-EMBL-000081/COTS-SM1D12D) on the image splitter platform (FAB-EMBL-000077). Tighten the screws once this condition is achieved. The beam should pass the proximal iris to within ±0.5 mm. If this condition is not met, repeat the procedure

Table 1 (continued) | Troubleshooting table

Step	Problem	Possible reason	Solution
131	Beam not aligned with the iris	Alignment has drifted or a component has been knocked	Return to Step 111 to check alignment out of the body and repeat subsequent alignment steps checking that components are installed correctly
135	Beam not aligned with the iris after tube lens installation (beam walk-off $>\pm 0.5$ mm)	Tube lens mount placed incorrectly or alignment tool not well centered	Realign the tube lens mount as previously. If the problem persists, secure a component with a flat side against the tube lens mount to define the angular alignment and reposition the tube lens mount along this axis such that the laser passes the target in the lateral direction. If the vertical beam walk-off is $>\pm 0.5$ mm and all previous alignment steps have been completed correctly it is possible that the tube lens is mounted at an incorrect height. Remove the tube lens mount (FAB-EMBL-000035) from the tube lens base adapter (FAB-EMBL-000034). Remove the tube lens (COTS-TTL165-A). Install a second alignment target with iris (FAB-EMBL-000081/COTS-SM1D12D) in the transmitted path of the splitter platform and check the beam height on the two irises. Return to Step 132 if the beam does not pass both irises to within ± 0.5 mm. If the beam passes the irises then the tube lens height may be at fault. Check the centration of the lens in its housing by reinstalling the tube lens on its mount (COTS-TTL165-A/FAB-EMBL-000035) and rotating the lens. If the laser spot moves noticeably between several rotational positions of the tube lens, the lens elements may not be well centered in their housing and should be exchanged with the manufacturer. Otherwise, the tube lens may not be mounted at the correct height. Check the dimensions of the tube lens mounting components (FAB-EMBL-000034/35/36) and remachine/shim as necessary
161	Position of the second relay lens is substantially shifted relative to the nominal position	Tolerances on lens focal lengths, imprecision in assembling the optical path	If the lens is placed too far upstream, it may occupy the space required to later install the filter wheel, given that there is ample room for the filter wheel this is unlikely. However, if the lens is placed too far downstream, the lens tube (COTS-SM1L10) in which it is mounted may result in vignetting of the image and/or spatial variations in PSF shape owing to blocking of the reflected light from the subsequent steering mirror. If either of these cases are apparent, it is necessary to adjust the position of the entire image splitter platform (FAB-EMBL-000077) to lie further upstream or downstream, respectively. For small adjustments (up to 25 mm), one may reposition the image splitter platform without compromising the alignment. In this case, use two fixed kinematic stops (COTS-KL01L) to indicate the position of the side of the platform running parallel to the transmitted path optical axis. The platform can then be adjusted to the correct position along the defined axis before being fixed in position. Check the alignment of the laser through the splitter platform using the various alignment targets (FAB-EMBL-000081/93 as necessary). For larger adjustments (>25 mm), it is advisable to follow the above procedure but return to Step 119 to realign the emission path more thoroughly thereafter. In the case that vignetting is observed after assembly, one may reposition the lens in the tube such that the section that protrudes toward the subsequent mirror is shorter
185	Filter wheel apertures do not approximately align (± 2 mm) with the optical pathways of the image splitter unit	The image splitter platform has been moved from its nominal longitudinal position (shown in Supplementary Fig. 34) in Step 161 to account for tolerances in lens focal lengths. As a result, the filter wheel mount bases (FAB-EMBL-000111) may not align to the optical table holes when the filter wheel aperture is aligned to the emission path when the upper part of the mount (FAB-EMBL-000076) is affixed to the base (FAB-EMBL-000111) in the nominal position	The base (FAB-EMBL-000111) and upper part of the mount (FAB-EMBL-000076) may be repositioned relative to each other
213	Range of motion of illumination tube lens is insufficient to allow collimation	Tolerances on focal lengths, upstream collimation state of the laser	Check the input laser collimation using the shear plate assembly (3D-SMLM-EMBL-005) and rectify following Steps 191 and 195. If the range of motion is still insufficient to achieve collimation, release the pedestal post clamp (COTS-PS-F), center the lens tube in the split clamp and manually position the assembly to achieve collimation. Subsequently realign the tube lens as previous but in the new nominal upstream/downstream position for collimation
219	The two channels appear in focus at different positions of the camera	Differential spacing of the second relay lenses with respect to the camera	Return to Step 160 and ensure that the alignment laser beam is collimated in the two pathways after passing both second relay lenses (COTS-AC254-200-A) of the reflected and transmitted pathways
226	Correction collar position is outside the range 0.16–0.18 mm	Infinite conjugate camera and transmission target (3D-SMLM-EMBL-004) not set up precisely enough to provide good references to infinity	Return the collar to its nominal 0.17 mm position and then focus the camera (as in Step 174) as well as the objective (using the objective piezo) to find a piezo/camera position where the spherical aberration is minimized. Again, check the color performance of the system and return to Step 219 to check that the two image splitter channels are evenly focused

Table 1 (continued) | Troubleshooting table

Step	Problem	Possible reason	Solution
227	Different colors are focused at different focal positions ($>\pm 100$ nm)	Incorrect spacing of the lenses in the emission path resulting in failure to image the native (infinity corrected) focal plane of the objective	Place a camera (e.g., the camera used for the infinite conjugate viewing camera) at the primary image produced by the emission path tube lens (COTS-TTL-165-A) and check whether the color performance is similar and whether the spherical aberrations are similarly well corrected when focused to the same plane as the sCMOS camera (secondary image). Note, it is useful to be able to remove/replace the camera at the primary image to be able to check that the focus has not drifted using the sCMOS camera. If the color performance is substantially different between the primary and secondary images, it is likely that the relay lenses which produce the secondary images are incorrectly set up. Return to Step 160 to reconfigure the emission path, taking additional care to ensure beam collimation with the use of the shear plate
282	PSF not spatially uniform over at least a $\varnothing 50$ μ m field using an oil objective. For the silicone oil objectives, it is more difficult to make assertions regarding the expected image quality	Emission path has not been aligned correctly	Recheck that the alignment laser traverses the emission path correctly, including good centration on mirrors and lenses and return to Step 109 to realign the emission path as necessary
298	Aperture does not appear on the camera image	Backlight to bright/dim or camera otherwise overexposed	Check if the camera is overexposed and reduce the backlight intensity and remove other sources of light to ensure the camera image is not overexposed and the image is uncorrupted by other light sources (e.g., room lights/monitors). If the camera is not detecting appreciable light from the backlight, increase the intensity of the backlight. If the backlight still cannot be seen try setting the astigmatic lens to the 'Off' position. If necessary use a brighter backlight
323	Total internal reflected beam cannot be seen	Blocking the incoming beam. Total internal reflection condition not met. Bubbles in the immersion oil. Low refractive index contrast. Using the silicone immersion oil objective lens	When checking for total internal reflection make sure not to block the incoming beam with the viewer card. Use the Bertrand lens to confirm that there are no bubbles in the immersion oil and that the focus lock beam is focused at the periphery of the back focal plane. It may be necessary to remove the NIR blocking filters from the emission path to see the focus lock laser on the camera. With great care one may also remove the cover of the microscope to check the beam angle out of the objective lens. CAUTION! The focus lock laser will propagate out of the objective lens at an oblique angle. Make sure to intercept the beam with the beam viewer card. When translating the stage correctly, the laser spot should be launched at ever more oblique angles until it can no longer be seen emerging from the objective when the total internal reflection condition is met. Once the beam can no longer be seen to emerge, recheck for total internal reflection. In the case of difficulties aligning the focus lock system using a silicone objective lens, we highly recommend completing the alignment with an oil objective first. If these steps do not rectify the situation, realign the focus lock system from Step 316
343	The focus begins rapidly shifting (as viewed from the z-stage position) after engaging the focus lock	Focus lock feedback parameters have been set incorrectly or parity should be reversed	Recheck that the parameters from Supplementary Table 7 have been correctly set in PI MikroMove. If the parameters have been set correctly. Try setting: Sensor Mech. Correction 2 in Sensor Mech. 2 to -0.01 . Issues may arise if the focus lock system mirrors are arranged differently
438	Low number of photons or fluorophore on time out of the suggested time range	Lower effective laser intensity than expected. Bad imaging buffer, which can be caused either by errors in buffer preparation or due to the acidification of the imaging buffer over time. See Supplementary Information Note 17	Check that the laser power is as expected using the laser power meter (COTS-PM100D/COTS-S121C) just before the illumination lasers pass into the microscope body. Prepare fresh buffer and return to Step 409 for repeating the biological sample imaging
438	Poor localization precision	Low number of photons. Most emitters out of focus. High background, which may be caused by high intracellular and out of focus signal from unspecifically bound dye or dye in solution indicating errors in sample preparation; deteriorated imaging buffer or corruption of the camera image from ambient light sources	See above regarding a low photon count and preparing fresh buffer. If most emitters are out of focus, check the correct function of the focus lock system and repeat imaging, paying special attention to focus on the nuclear envelope and nuclear pores. Check for corruption of the camera image by acquiring images with only a coverslip present (but with all lasers including the focus lock laser set as for imaging). If the lasers are not causing the background, check any ambient sources and isolate the camera with enclosure as necessary. For example, ensure that the NIR laser blocking filter is installed in front of the camera. In the case of background resulting from the presence of residual or unselective dye, repeat the sample preparation and imaging
438	Low number of localizations	Poor data quality relating to any of the above points. Too low dye concentration or poor cell permeabilization during sample preparation	Repeat the sample preparation and imaging
438	Low labeling efficiency	Low number of localizations (see above). Cell culture related issues (e.g., prolonged culturing of cells past 3 months). Problems with reagents or labeling protocol	Repeat the sample preparation and imaging with fresh cell cultures and reagents as appropriate

Timing

The time required to complete the protocol may vary substantially depending on any problems arising with components and the level of experience of the personnel with the key tasks. Ample time should be dedicated to initial checking of components before commencing the protocol. For example, to correct mistakes in custom parts and/or identify issues with integration of electronic hardware such as the camera(s), lasers and motion control elements. Similarly, the laboratory environment should be correctly configured and cleaned before starting the protocol, which may take weeks to years depending on the renovations required. Furthermore, there are a number of optional Supplementary protocols, which naturally change the length of the overall protocol and duration accordingly. Nevertheless, we assert that the protocol may be completed in 4–8 months. The timings provided below assume that some backtracking will be necessary to achieve optimal results. However, more substantial problems may lengthen the timing. Since such problems naturally arise in the course of complex endeavors such as this, the total timing of the various steps below is shorter than the full 8 months to allow unforeseen problems to be resolved.

Steps 1–66 Microscope body buildup: 4 d

(Optional) Assembly of the microFPGA: 4 d

Steps 67–70: Configuration of the microFPGA: 2 h

Steps 71–93: Setup and configuration of software and hardware for acquisition: 7 d

(Optional) Testing of the microFPGA: 1 d

Steps 94–98: Making electrical connections to hardware: 1 d

Steps 99–108: Setup of the infinite conjugate viewing camera and infinite conjugate transmission target: 1 d

Steps 109–130: Emission path beam routing: 6 d

Steps 131–185: Emission path alignment: 7 d

Steps 186–228: Basic epi-illumination alignment: 6 d

Steps 229–269: Field variable and homogeneous epi-illumination alignment: 7 d

(Optional) Setting up additional laser sources and configuring HILO/TIRF illumination: 1–7 d

Steps 270–274: Calibration of the laser power monitoring photodiode: 2 d

Steps 275–287: 2D imaging quality checks and pixel size calibration: 1 d

Steps 288–309: 3D imaging alignment: 2 d

Steps 310–328: Focus lock path buildup and alignment: 3 d

Steps 329–340: Setup of the focus lock amplifier: 2 d

Steps 341–345: Focus locking: 1 d

(Optional) Minimizing mode-hopping of the focus lock laser: 3 d

Steps 346–351: Setup and configuration of software for analysis: 1 d

Steps 352–360: Performing PSF calibration: 4 d

Steps 361–381: 2D and 3D Fitting with SMAP: 2 d

Steps 382–405: Performing focus lock, drift and vibration checks: 3 d

Steps 406–438: 2D imaging of NPCs: 7 d

(Optional) 3D single- and multicolor imaging of NPCs: 7–14 d

Anticipated results

A correct implementation of the protocols as described, including all optional aspects is expected to yield a fully functional 3D multicolor SMLM system with potential for automated high-throughput applications. Diffraction-limited resolution and 3D localization precision approaching theoretical limits will have been demonstrated across a wide field of view and used to provide exemplary 2D and 3D images of NPCs via single- and multicolor dSTORM workflows (Figs. 9 and 10). In this regard, the nuclear pore sample provides an ideal standard with which to benchmark performance and a strong basis to apply the microscope confidently to a range of biological studies.

NPC data can further allow for the correction of z-dependent image distortions. The expected ring separation for NPCs is 49.3 nm. By determining the ring separation in the data set using advance geometric model fitting, the deviance from this expected value can be calculated and the z-scaling of the data corrected accordingly^{50,52}.

Reporting summary

Further information on research design is available in the Nature Portfolio Reporting Summary linked to this article.

Data availability

All CAD parts and assemblies, mechanical drawings and electronic board files are available from the project repository: <https://github.com/ries-lab/3DSMLM>. All materials provided in the repository are licensed under a Creative Commons Attribution-NonCommercial-ShareAlike 4.0 International License (CC-BY-NC-ND-4.0). The sequences of raw images that were localized and rendered to produce Figs. 9 and 10 can be provided on request.

Code availability

The user interface, FPGA firmware and modified μ Manager device adapters are available from the project repository (<https://github.com/ries-lab/3DSMLM>). All materials provided in the repository are licensed under a Creative Commons Attribution-NonCommercial-ShareAlike 4.0 International License (CC-BY-NC-ND-4.0). The analysis software, SMAP which is used throughout the Protocol, is available at <https://github.com/jries/SMAP>.

Received: 28 June 2023; Accepted: 19 February 2024;

Published online: 3 May 2024

References

1. Betzig, E. et al. Imaging intracellular fluorescent proteins at nanometer resolution. *Science* **313**, 1642–1645 (2006).
2. Hess, S. T., Girirajan, T. P. K. & Mason, M. D. Ultra-high resolution imaging by fluorescence photoactivation localization microscopy. *Biophys. J.* **91**, 4258–4272 (2006).
3. Rust, M. J., Bates, M. & Zhuang, X. Sub-diffraction-limit imaging by stochastic optical reconstruction microscopy (STORM). *Nat. Methods* **3**, 793–795 (2006).
4. Heilemann, M., Van De Linde, S., Mukherjee, A. & Sauer, M. Super-resolution imaging with small organic fluorophores. *Angew. Chem. Int. Ed. Engl.* **48**, 6903–6908 (2009).
5. Jungmann, R. et al. Single-molecule kinetics and super-resolution microscopy by fluorescence imaging of transient binding on DNA origami. *Nano Lett.* **10**, 4756–4761 (2010).
6. Martens, K. J. A. et al. Visualisation of dCas9 target search in vivo using an open-microscopy framework. *Nat. Commun.* **10**, 3552 (2019).
7. Auer, A. et al. Nanometer-scale multiplexed super-resolution imaging with an economic 3D-DNA-PAINT microscope. *ChemPhysChem* **19**, 3024–3034 (2018).
8. Ma, H., Fu, R., Xu, J. & Liu, Y. A simple and cost-effective setup for super-resolution localization microscopy. *Sci. Rep.* **7**, 1542 (2017).
9. Diederich, B. et al. Nanoscopy on the cheal(i)p. Preprint at *bioRxiv* <https://doi.org/10.1101/2020.09.04.283085> (2020).
10. Zehrer, A. C., Martin-Villalba, A., Diederich, B. & Ewers, H. An open-source, high resolution, automated fluorescence microscope. *eLife* **12**, RP89826 (2023).
11. Alsamsam, M. N., Kopūstas, A., Jurevičiūtė, M. & Tutkus, M. The miEye: bench-top super-resolution microscope with cost-effective equipment. *HardwareX* **12**, e00368 (2022).
12. Coelho, S. et al. Ultraprecise single-molecule localization microscopy enables in situ distance measurements in intact cells. *Sci. Adv.* **6**, eaay8271 (2020).
13. Mau, A., Friedl, K., Leterrier, C., Bourg, N. & Lévêque-Fort, S. Fast widefield scan provides tunable and uniform illumination optimizing super-resolution microscopy on large fields. *Nat. Commun.* **12**, 3077 (2021).
14. Stehr, F., Stein, J., Schueder, F., Schwille, P. & Jungmann, R. Flat-top TIRF illumination boosts DNA-PAINT imaging and quantification. *Nat. Commun.* **10**, 1268 (2019).
15. Khaw, I. et al. Flat-field illumination for quantitative fluorescence imaging. *Opt. Express* **26**, 15276 (2018).
16. Niederauer, C., Seynen, M., Zomerdijk, J., Kamp, M. & Ganzinger, K. A. The K2: open-source simultaneous triple-color TIRF microscope for live-cell and single-molecule imaging. *HardwareX* **13**, e00404 (2023).
17. Jabermoradi, A., Yang, S., Gobes, M. I., Van Duynhoven, J. P. M. & Hohlbein, J. Enabling single-molecule localization microscopy in turbid food emulsions. *Philos. Trans. R. Soc. A.* **380**, 20200164 (2022).
18. Li, Y. et al. Global fitting for high-accuracy multi-channel single-molecule localization. *Nat. Commun.* **13**, 3133 (2022).
19. Roy, R., Hohng, S. & Ha, T. A practical guide to single-molecule FRET. *Nat. Methods* **5**, 507–516 (2008).
20. Ha, T. et al. Probing the interaction between two single molecules: fluorescence resonance energy transfer between a single donor and a single acceptor. *Proc. Natl Acad. Sci. USA* **93**, 6264–6268 (1996).
21. Huang, B., Wang, W., Bates, M. & Zhuang, X. Three-dimensional super-resolution imaging by stochastic optical reconstruction microscopy. *Science* **319**, 810–813 (2008).
22. Pavani, S. R. P. et al. Three-dimensional, single-molecule fluorescence imaging beyond the diffraction limit by using a double-helix point spread function. *Proc. Natl Acad. Sci. USA* **106**, 2995–2999 (2009).
23. Daniel, J. S. H. et al. Constructing a cost-efficient, high-throughput and high-quality single-molecule localization microscope for super-resolution imaging. *Nat. Protoc.* **17**, 2570–2619 (2022).
24. Carter, N., Cross, R. & Martin, D. Warwick open-source microscope. <https://wosmic.org/> (2016).
25. Edwards, J., Whitley, K., Peneti, S., Cesbron, Y. & Holden, S. LifeHack microscope. *GitHub* <https://github.com/HoldenLab/LifeHack> (2021).
26. Deschamps, J., Rowald, A. & Ries, J. Efficient homogeneous illumination and optical sectioning for quantitative single-molecule localization microscopy. *Opt. Express* **24**, 28080 (2016).
27. Li, Y. et al. Real-time 3D single-molecule localization using experimental point spread functions. *Nat. Methods* **15**, 367–369 (2018).
28. Deschamps, J. & Ries, J. EMU: reconfigurable graphical user interfaces for Micro-Manager. *BMC Bioinform.* **21**, 456 (2020).
29. Diekmann, R. et al. Optimizing imaging speed and excitation intensity for single-molecule localization microscopy. *Nat. Methods* **17**, 909–912 (2020).
30. Ries, J. SMAP: a modular super-resolution microscopy analysis platform for SMLM data. *Nat. Methods* **17**, 870–872 (2020).
31. Dasgupta, A. et al. Direct supercritical angle localization microscopy for nanometer 3D superresolution. *Nat. Commun.* **12**, 1180 (2021).

32. Diekmann, R. et al. Photon-free (s)CMOS camera characterization for artifact reduction in high- and super-resolution microscopy. *Nat. Commun.* **13**, 3362 (2022).
33. Ries, J., Kaplan, C., Platonova, E., Eghlidi, H. & Ewers, H. A simple, versatile method for GFP-based super-resolution microscopy via nanobodies. *Nat. Methods* **9**, 582–584 (2012).
34. Mund, M. et al. Systematic nanoscale analysis of endocytosis links efficient vesicle formation to patterned actin nucleation. *Cell* **174**, 884–896.e17 (2018).
35. Mund, M. et al. Clathrin coats partially preassemble and subsequently bend during endocytosis. *J. Cell Biol.* **222**, e202206038 (2023).
36. Cieslinski, K. et al. Nanoscale structural organization and stoichiometry of the budding yeast kinetochore. *J. Cell Biol.* **222**, e202209094 (2023).
37. Edelstein, A., Amodaj, N., Hoover, K., Vale, R. & Stuurman, N. Computer control of microscopes using manager. *Curr. Protoc. Mol. Biol.* <https://doi.org/10.1002/0471142727.mb1420s92> (2010).
38. Deschamps, J., Kieser, C., Hoess, P., Deguchi, T. & Ries, J. MicroFPGA: an affordable FPGA platform for microscope control. *HardwareX* **13**, e00407 (2023).
39. Schermelleh, L. et al. Super-resolution microscopy demystified. *Nat. Cell Biol.* **21**, 72–84 (2019).
40. Vangindertael, J. et al. An introduction to optical super-resolution microscopy for the adventurous biologist. *Methods Appl. Fluoresc.* **6**, 22003 (2018).
41. Jacquemet, G., Carisey, A. F., Hamidi, H., Henriques, R. & Leterrier, C. The cell biologist's guide to super-resolution microscopy. *J. Cell Sci.* **133**, jcs240713 (2020).
42. Bond, C., Santiago-Ruiz, A. N., Tang, Q. & Lakadamyali, M. Technological advances in super-resolution microscopy to study cellular processes. *Mol. Cell* **82**, 315–332 (2022).
43. Hell, S. W. & Wichmann, J. Breaking the diffraction resolution limit by stimulated emission. *Opt. Lett.* **19**, 780–782 (1994).
44. Gustafsson, M. G. Surpassing the lateral resolution limit by a factor of two using structured illumination microscopy. *J. Microsc.* **198**, 82–87 (2000).
45. Müller, C. B. & Enderlein, J. Image scanning microscopy. *Phys. Rev. Lett.* **104**, 1–4 (2010).
46. Strauss, M. T. Picasso-server: a community-based, open-source processing framework for super-resolution data. *Commun. Biol.* **5**, 1–3 (2022).
47. Ovesný, M., Křížek, P., Borkovec, J., Švindrych, Z. & Hagen, G. M. ThunderSTORM: a comprehensive ImageJ plug-in for PALM and STORM data analysis and super-resolution imaging. *Bioinformatics* **30**, 2389–2390 (2014).
48. Sage, D. et al. Super-resolution fight club: assessment of 2D and 3D single-molecule localization microscopy software. *Nat. Methods* **16**, 387–395 (2019).
49. Von Appen, A. et al. In situ structural analysis of the human nuclear pore complex. *Nature* **526**, 140–143 (2015).
50. Thevathasan, J. V. et al. Nuclear pores as versatile reference standards for quantitative superresolution microscopy. *Nat. Methods* **16**, 1045–1053 (2019).
51. Smith, C. S., Joseph, N., Rieger, B. & Lidke, K. A. Fast, single-molecule localization that achieves theoretically minimum uncertainty. *Nat. Methods* **7**, 373–375 (2010).
52. Wu, Y.-L. et al. Maximum-likelihood model fitting for quantitative analysis of SMLM data. *Nat. Methods* **20**, 139–148 (2023).

Acknowledgements

We thank C. Kieser (EMBL Electronic Workshop) for help with construction of and documentation for the microFPGA. We thank A. Milberger (EMBL Mechanical Workshop) for providing all mechanical drawings. We thank J. Deschamps (Human Technopole, Milan, Italy)

for providing the EMU htSMLM user interface and continued support in various aspects of microscope control. We thank A. Roy for assistance in testing the protocol. This work was supported by the European Research Council (CoG-724489) and the European Molecular Biology Laboratory. We acknowledge the access and services provided by the Imaging Centre at the European Molecular Biology Laboratory, generously supported by the Boehringer Ingelheim Foundation.

Author contributions

R.M.P. and J.R. designed and developed the microscope hardware. A.T. and J.R. performed sample preparation. R.M.P., A.T. and J.R. performed imaging and data analysis. T.Z. and J.R. provided project supervision. All authors wrote the manuscript and designed the protocol.

Competing interests

The authors declare no competing interests.

Additional information

Extended data is available for this paper at <https://doi.org/10.1038/s41596-024-00989-x>.

Supplementary information The online version contains supplementary material available at <https://doi.org/10.1038/s41596-024-00989-x>.

Correspondence and requests for materials should be addressed to Rory M. Power or Jonas Ries.

Peer review information *Nature Protocols* thanks Carlos Smith and the other, anonymous, reviewer(s) for their contribution to the peer review of this work.

Reprints and permissions information is available at www.nature.com/reprints.

Publisher's note Springer Nature remains neutral with regard to jurisdictional claims in published maps and institutional affiliations.

Springer Nature or its licensor (e.g. a society or other partner) holds exclusive rights to this article under a publishing agreement with the author(s) or other rightsholder(s); author self-archiving of the accepted manuscript version of this article is solely governed by the terms of such publishing agreement and applicable law.

Related links

Key references

- Li, Y. et al. *Nat. Methods* **15**, 367–369 (2018): <https://doi.org/10.1038/nmeth.4661>
 Diekmann, R. et al. *Nat. Methods* **17**, 909–912 (2020): <https://doi.org/10.1038/s41592-020-0918-5>
 Deschamps, J. et al. *HardwareX* **13**, e00407 (2023): <https://doi.org/10.1016/j.ohx.2023.e00407>
 Thevathasan, J. V. et al. *Nat. Methods* **16**, 1045–1053 (2019): <https://doi.org/10.1038/s41592-019-0574-9>
 Wu, Y.-L. et al. *Nat. Methods* **20**, 139–148 (2023): <https://doi.org/10.1038/s41592-022-01676-z>

© Springer Nature Limited 2024

Reporting Summary

Nature Portfolio wishes to improve the reproducibility of the work that we publish. This form provides structure for consistency and transparency in reporting. For further information on Nature Portfolio policies, see our Editorial Policies and the Editorial Policy Checklist.

Please do not complete any field with "not applicable" or n/a. Refer to the help text for what text to use if an item is not relevant to your study. For final submission: please carefully check your responses for accuracy; you will not be able to make changes later.

Statistics

For all statistical analyses, confirm that the following items are present in the figure legend, table legend, main text, or Methods section.

- ☒ Confirmed
 - ☒ The exact sample size (n) for each experimental group/condition, given as a discrete number and unit of measurement
 - ☒ A statement on whether measurements were taken from distinct samples or whether the same sample was measured repeatedly
 - ☒ The statistical test(s) used AND whether they are one- or two-sided
Only common tests should be described solely by name; describe more complex techniques in the Methods section.
 - ☒ A description of all covariates tested
 - ☒ A description of any assumptions or corrections, such as tests of normality and adjustment for multiple comparisons
 - ☐ n/a
 - ☒ A full description of the statistical parameters including central tendency (e.g. means) or other basic estimates (e.g. regression coefficient) AND variation (e.g. standard deviation) or associated estimates of uncertainty (e.g. confidence intervals)
 - ☒ For null hypothesis testing, the test statistic (e.g. F, t, r) with confidence intervals, effect sizes, degrees of freedom and P value noted
Give P values as exact values whenever suitable.
 - ☒ For Bayesian analysis, information on the choice of priors and Markov chain Monte Carlo settings
 - ☒ For hierarchical and complex designs, identification of the appropriate level for tests and full reporting of outcomes
 - ☒ Estimates of effect sizes (e.g. Cohen's d, Pearson's r), indicating how they were calculated
- Our web collection on statistics for biologists contains articles on many of the points above.*

Software and code

Policy information about availability of computer code

Data collection	Micro-manager 2.0.0
Data analysis	Superresolution microscopy analysis platform (SMAP)

For manuscripts utilizing custom algorithms or software that are central to the research but not yet described in published literature, software must be made available to editors and reviewers. We strongly encourage code deposition in a community repository (e.g. GitHub). See the Nature Portfolio guidelines for submitting code & software for further information.

Data

Policy information about availability of data

- All manuscripts must include a data availability statement. This statement should provide the following information, where applicable:
- Accession codes, unique identifiers, or web links for publicly available datasets
 - A description of any restrictions on data availability
 - For clinical datasets or third party data, please ensure that the statement adheres to our policy

Human research participants

Policy information about [studies involving human research participants](#) and [Sex and Gender in Research](#).

Reporting on sex and gender	
Population characteristics	
Recruitment	
Ethics oversight	

Note that full information on the approval of the study protocol must also be provided in the manuscript.

Field-specific reporting

Please select the one below that is the best fit for your research. If you are not sure, read the appropriate sections before making your selection.

☒ Life sciences ☐ Behavioural & social sciences ☐ Ecological, evolutionary & environmental sciences

Life sciences study design

All studies must disclose on these points even when the disclosure is negative.

Sample size	N/A
Data exclusions	N/A
Replication	N/A
Randomization	N/A
Blinding	N/A

Behavioural & social sciences study design

All studies must disclose on these points even when the disclosure is negative.

Study description	
Research sample	
Sampling strategy	
Data collection	
Timing	
Data exclusions	
Non-participation	
Randomization	

Ecological, evolutionary & environmental sciences study design

All studies must disclose on these points even when the disclosure is negative.

Study description	
Research sample	
Sampling strategy	
Data collection	
Timing and spatial scale	

Data exclusions	
Reproducibility	
Randomization	
Blinding	

Did the study involve field work? ☒ Yes ☐ No

Field work, collection and transport

Field conditions	
Location	
Access & import/export	
Disturbance	

Reporting for specific materials, systems and methods

We require information from authors about some types of materials, experimental systems and methods used in many studies. Here, indicate whether each material, system or method listed is relevant to your study. If you are not sure if a list item applies to your research, read the appropriate section before selecting a response.

Materials & experimental systems

n/a	Involved in the study
<input type="radio"/>	<input checked="" type="radio"/> Antibodies
<input type="radio"/>	<input checked="" type="radio"/> Eukaryotic cell lines
<input type="radio"/>	<input checked="" type="radio"/> Palaeontology and archaeology
<input type="radio"/>	<input checked="" type="radio"/> Animals and other organisms
<input type="radio"/>	<input checked="" type="radio"/> Clinical data
<input type="radio"/>	<input checked="" type="radio"/> Dual use research of concern

Methods

n/a	Involved in the study
<input type="radio"/>	<input checked="" type="radio"/> ChIP-seq
<input type="radio"/>	<input checked="" type="radio"/> Flow cytometry
<input type="radio"/>	<input checked="" type="radio"/> MRI-based neuroimaging

Antibodies

Antibodies used	
Validation	

Eukaryotic cell lines

Policy information about [cell lines](#) and [Sex and Gender in Research](#)

Cell line source(s)	RRID:CVCL_B7FL, U-2 OS-CRISPR-NUP96-SNAP clone #33, origin: Homo sapiens, sex: Female
Authentication	Cell line was not authenticated
Mycoplasma contamination	Cell line was not tested for mycoplasma
Commonly misidentified lines (See ICLAC register)	N/A

Palaeontology and Archaeology

Specimen provenance	
Specimen deposition	
Dating methods	

☐ Tick this box to confirm that the raw and calibrated dates are available in the paper or in Supplementary Information.

Ethics oversight	
------------------	--

Note that full information on the approval of the study protocol must also be provided in the manuscript.

Animals and other research organisms

Policy information about [studies involving animals](#); ARRIVE [guidelines](#) recommended for reporting animal research, and [Sex and Gender in Research](#)

Laboratory animals	
Wild animals	
Reporting on sex	
Field-collected samples	
Ethics oversight	

Note that full information on the approval of the study protocol must also be provided in the manuscript.

Clinical data

Policy information about [clinical studies](#)

All manuscripts should comply with the ICMJE [guidelines for publication of clinical research](#) and a completed [CONSORT checklist](#) must be included with all submissions.

Clinical trial registration	
Study protocol	
Data collection	
Outcomes	

Dual use research of concern

Policy information about [dual use research of concern](#)

Hazards

Could the accidental, deliberate or reckless misuse of agents or technologies generated in the work, or the application of information presented in the manuscript, pose a threat to:

No	Yes
<input type="radio"/>	<input type="radio"/> Public health
<input type="radio"/>	<input type="radio"/> National security
<input type="radio"/>	<input type="radio"/> Crops and/or livestock
<input type="radio"/>	<input type="radio"/> Ecosystems
<input type="radio"/>	<input type="radio"/> Any other significant area

Experiments of concern

Does the work involve any of these experiments of concern:

No	Yes
<input type="radio"/>	<input type="radio"/> Demonstrate how to render a vaccine ineffective
<input type="radio"/>	<input type="radio"/> Confer resistance to therapeutically useful antibiotics or antiviral agents
<input type="radio"/>	<input type="radio"/> Enhance the virulence of a pathogen or render a nonpathogen virulent
<input type="radio"/>	<input type="radio"/> Increase transmissibility of a pathogen
<input type="radio"/>	<input type="radio"/> Alter the host range of a pathogen
<input type="radio"/>	<input type="radio"/> Enable evasion of diagnostic/detection modalities
<input type="radio"/>	<input type="radio"/> Enable the weaponization of a biological agent or toxin
<input type="radio"/>	<input type="radio"/> Any other potentially harmful combination of experiments and agents

ChIP-seq

Data deposition

☐ Confirm that both raw and final processed data have been deposited in a public database such as [GEO](#).

☐ Confirm that you have deposited or provided access to graph files (e.g. BED files) for the called peaks.

Data access links

May remain private before publication

Files in database submission

Genome browser session

(e.g. [UCSC](#))

Methodology

Replicates

Sequencing depth

Antibodies

Peak calling parameters

Data quality

Software

Flow Cytometry

Plots

Confirm that:

- ☐ The axis labels state the marker and fluorochrome used (e.g. CD4-FITC).
- ☐ The axis scales are clearly visible. Include numbers along axes only for bottom left plot of group (a 'group' is an analysis of identical markers).
- ☐ All plots are contour plots with outliers or pseudocolor plots.
- ☐ A numerical value for number of cells or percentage (with statistics) is provided.

Methodology

Sample preparation

Instrument

Software

Cell population abundance

Gating strategy

- ☐ Tick this box to confirm that a figure exemplifying the gating strategy is provided in the Supplementary Information.

Magnetic resonance imaging

Experimental design

Design type

Design specifications

Behavioral performance measures

Acquisition

Imaging type(s)

Field strength

Sequence & imaging parameters

Area of acquisition

Diffusion MRI

☒ Used☐ Not used

Preprocessing

Preprocessing software

Normalization

Normalization template

Noise and artifact removal

Volume censoring

Statistical modeling & inference

Model type and settings

Effect(s) tested

Specify type of analysis:

☐ Whole brain
 ☐ ROI-based
 ☐ Both

Statistic type for inference
 (See [Eklund et al. 2016](#))

Correction

Models & analysis

n/a Involved in the study

- ☒ Functional and/or effective connectivity
- ☒ Graph analysis
- ☒ Multivariate modeling or predictive analysis

Functional and/or effective connectivity

Graph analysis

Multivariate modeling and predictive analysis

